REPORT DOCUMENTATION PAGE

The public reporting burden for this collection of information is estimated to average 1 hour per response, including the time for reviewing instructions, searching existing data sources, gathering and maintaining the data needed, and completing and reviewing the collection of information. Send comments regarding this burden estimate or any other aspect of this collection of information, including suggestions for reducing the burden, to Department of Defense, Washington Headquarters Services, Directorate for Information Operations and Reports (0704-0188), 1215 Jefferson Davis Highway, Suite 1204, Arlington, VA 22202-4302. Respondents should be aware that notwithstanding any other provision of law, no person shall be subject to any penalty for failing to comply with a collection of information if it does not display a currently valid OMB control number.
PLEASE DO NOT RETURN YOUR FORM TO THE ABOVE ADDRESS.

1. REPORT DATE *(DD-MM-YYYY)*	2. REPORT TYPE	3. DATES COVERED *(From - To)*
9/Oct/2001	THESIS	

4. TITLE AND SUBTITLE
A STATISCAL FREQUENCY ANALYSIS OF LIGHTING PRODUCING STORMS DURING STEPS 2000

5a. CONTRACT NUMBER

5b. GRANT NUMBER

5c. PROGRAM ELEMENT NUMBER

6. AUTHOR(S)
CAPT CABOSKY STEVEN R

5d. PROJECT NUMBER

5e. TASK NUMBER

5f. WORK UNIT NUMBER

7. PERFORMING ORGANIZATION NAME(S) AND ADDRESS(ES)
COLORADO STATE UNIVERSITY

8. PERFORMING ORGANIZATION REPORT NUMBER
CI01-260

9. SPONSORING/MONITORING AGENCY NAME(S) AND ADDRESS(ES)
THE DEPARTMENT OF THE AIR FORCE
AFIT/CIA, BLDG 125
2950 P STREET
WPAFB OH 45433

10. SPONSOR/MONITOR'S ACRONYM(S)

11. SPONSOR/MONITOR'S REPORT NUMBER(S)

12. DISTRIBUTION/AVAILABILITY STATEMENT
Unlimited distribution
In Accordance With AFI 35-205/AFIT Sup 1

13. SUPPLEMENTARY NOTES

14. ABSTRACT

20011016 187

15. SUBJECT TERMS

16. SECURITY CLASSIFICATION OF:			17. LIMITATION OF ABSTRACT	18. NUMBER OF PAGES	19a. NAME OF RESPONSIBLE PERSON
a. REPORT	b. ABSTRACT	c. THIS PAGE		97	19b. TELEPHONE NUMBER *(Include area code)*

THESIS

A STATISTICAL FREQUENCY ANALYSIS OF LIGHTNING

PRODUCING STORMS DURING STEPS 2000

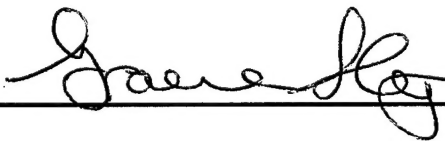Submitted by

Steven R. Cabosky

Department of Atmospheric Sciences

COLORADO STATE UNIVERSITY

Jun 11, 2001

WE HEREBY RECOMMEND THAT THE THESIS PREPARED UNDER OUR

SUPERVISION BY STEVEN R. CABOSKY ENTITLED A STATISTICAL

FREQUENCY ANALYSIS OF LIGHTNING PRODUCING STORMS DURING

STEPS 2000 BE ACCEPTED AS FULFILLING IN PART REQUIREMENTS FOR

THE DEGREE OF MASTER OF SCIENCE.

Committee on Graduate Work

_____

Richard E. Eykholt
_____

_____
Adviser

_____
Department Head

ABSTRACT OF THESIS

A STATISTICAL FREQUENCY ANALYSIS OF LIGHTNING PRODUCING

STORMS DURING STEPS 2000

Most cloud-to-ground (CG) lightning lowers negative charge to ground, but roughly 10% of flashes are reversed and transfer positive charge to ground. A small number of storms produce predominately (greater than 50%) positive CG lightning, and recent studies have associated the occurrence of tornadoes, hail, and microbursts with these "positive" storms. Much of this work has been centered on case studies. The use of case studies, however, is limited; the nature of case selection is subjective and possibly susceptible to researcher bias.

This research presents a new method for addressing how a thunderstorm "looks" from a statistical perspective, and is based on information readily available to researchers and operational forecasters alike. A statistical analysis of High Plains thunderstorms during the summer of 2000 was conducted as part of the Severe Thunderstorm Electrification and Precipitation Study (STEPS). WSR-88D NEXRAD and National Lightning Detection Network (NLDN) data sets were used to produce statistical radar reflectivity distributions based on cloud-to-ground (CG) lightning flash densities.

Comparisons were made based on flash polarity, geographical location and storm type. The main goal of this research was to better understand relationships between storm structure and microphysical processes (inferred from radar reflectivity). Consistent

with previous findings, statistical results show that for high flash densities, (above 0.1 flashes km^{-2} hr^{-1}) positive storms are five times more likely than negative storms to produce reflectivities between 55-70 dBZ. Further, these results provide evidence that low flash density storms (defined to produce less than three CGs in thirty minutes) are more likely to contain upper level reflectivity maximums if the CGs are positive. This result suggests that positive CGs are favored when a storm contains strong updrafts and contains large particles suspended aloft. These conditions are generally associated with developing convection, prior to the onset of heavy precipitation.

Steven R. Cabosky
Atmospheric Science Department
Colorado State University
Fort Collins, CO 80524
Summer 2001

ACKNOWLEDGEMENTS

TABLE OF CONTENTS

CHAPTER ONE

INTRODUCTION

1.1 Introduction

Over two centuries ago, Benjamin Franklin conducted some of the earliest experiments in atmospheric electricity. He showed the polarized nature of thunderclouds. Also, he may have been the first to recognize that while most storms contained negative charge in their lowest layers, some did not. There were a small percentage of storms that contained positive charge in their lowest layers. These "positive" storms have added a complexity to the nature of storm electrification, and have continued to puzzle researchers to this day. Lightning in general, and more specifically positive cloud-to-ground lightning, has been the focus of many studies over the years, especially in the past two decades. Now, two hundred years after Ben Franklin's initial work on lightning, the scientific community still cannot fully explain the process of lightning discharge. Over time, various hypotheses have been in and out of vogue.

In the past two decades, some progress has been made into deciphering the mystery of lightning, largely because of the installation of a national lightning detection network (NLDN) during the 1980s through the 1990s. We now know the climatology of cloud-to-ground (CG) lightning, that is, when and where lightning occurs, as well at the occurrence of positive lightning. Presently, two competing popular theories address the

1

nature of cloud electrification. The first is the convective charging theory, which does not rely on precipitation processes to induce charged layers within a cloud. The second is a charge transfer, or precipitation based theory, and is broken down into inductive and non-inductive charging mechanisms. Electrical charging may result from one of these theories or a combination of the two, or perhaps from an undiscovered process. Chapter Two presents some of the research that has specifically attempted to explain cloud charging as well as hypotheses regarding positive cloud-to-ground lightning.

Recent findings have associated severe weather with positive CG lightning; several studies have noted a higher incidence of positive cloud-to-ground lightning in severe storms. In fact, positive lightning has been associated with tornadoes, hail, microbursts, and severe weather in general, and methods have been proposed to use lightning signatures to forecast these events. The idea is that cloud-to-ground lightning information is available in (nearly) real time, whereas radar and satellite data take longer to update--between five and thirty minutes. If these theories are verified, lightning signatures may prove to be the first indication to forecasters that severe weather is imminent. These valuable minutes may be the difference in whether forecasters will be able to provide the public advance warning of impending severe weather. However, these studies are fairly recent and are yet to be verified.

One method to investigate these thunderstorms is the use of weather radars. Since the 1940's, researchers have used radar to interrogate weather phenomena. Since that time there have been numerous studies that have attempted to relate radar reflectivity with the discharge of lightning from and within thunderstorms. Indeed, as early as 1949, Workman and Reynolds speculatively concluded that thunderstorm electrification is a

"phenomena associated with precipitation and vertical convection," that the "most significant parameter (affecting electrification is) that of temperature," and "thunderstorm electrification involves the ice phase of water, and probably the ice phase in combination with supercooled water." Many studies since have attempted to expand our knowledge of the electrical nature of thunderstorms. Improvements in radar technology in the past two decades have led to greater insight into storm structure and development. Notably, the installation of Doppler Weather Radars throughout the United States in the 1980's and early 1990's allowed for wind field analysis and provided a new method for analyzing the dynamics of storms. The advent of polarimetric research radars have given us a glimpse into the microphysical workings of these storms. For example, by analyzing horizontally and vertically polarized radar waves, hydrometeor types within clouds may be identified.

Much of our work to better understand cloud electrification and its association to precipitation processes has been centered on case studies. The use of case studies, however, is limited; the nature of case selection is subjective. Cases are often selected because they are "textbook" examples and fit well into established theories. Other cases are selected because they are anomalous. Often only the "best" examples are selected, based on the researcher's interest. In all cases the research is limited in nature and subject to selection bias.

The research undertaken in this thesis is an attempt to provide a statistical profile relating the reflectivity structure of thunderstorms with various lightning signatures based on lightning frequency and polarity. This work presents a new method for addressing how a thunderstorm "looks" from a reflectivity perspective, and is based on information readily available to researchers and operational forecasters alike. We examine storms

3

over the Upper Plains during the summer of 2000, as part of the Severe Thunderstorm Electrification and Precipitation Study (STEPS) field campaign.

1.2 STEPS Project

The Severe Thunderstorm Electrification and Precipitation Study (STEPS) Project was a collaborative study funded by the National Science Foundation and the National Oceanic and Atmospheric Association. The overarching goal of STEPS was and is to achieve a better understanding of the interactions between kinematics, precipitation production, and electrification in severe thunderstorms on the High Plains.

STEPS was able to take advantage of recent advances in technologies in radar and lightning detection as well as incorporate more traditional instrumentation. The field campaign provided an unprecedented opportunity to integrate these various data platforms which included two S-Band polarimetric radars from the National Center for Atmospheric Research (S-Pol) and Colorado State University (CSU-CHILL), WSR-88D Doppler radar from the National Weather Service, an armored T-28 aircraft from the South Dakota School of Mines and Technology for in-situ storm observations, four mobile (car-mounted) mesonet observation stations from the University of Oklahoma Joint Mobile Research Facility (JMRF) and the National Severe Storms Lab, two mobile atmospheric sounders, electric field sounders for measuring charge levels within storms from the New Mexico Institute of Mining and Technology (NMIMT) and JMRF, and three separate lightning measuring systems: the National Lightning Detection Network, a lightning mapping system from the NMIMT capable of four dimensional lightning

analysis, and a CSU flat plate antenna network for quantifying intra-cloud discharges. This work focuses on two of these platforms, the NLDN and the WSR-88D radars.

STEPS had two broad goals for electrification studies: (1) to improve understanding of the electrification of severe storms, particularly understanding of how the charge generation and charge distribution depend on the microphysics and kinematics of severe storms, and (2) to better document and understand the apparently systematic variations in the types and rates of lightning relative to severe storm type and evolution. Of particular interest are ground flashes that lower positive charge to ground instead of the usual negative charge, because only in the last decade has it been discovered that they occur preferentially in a few severe storm situations (STEPS 2000).

The field phase of the program was located in Eastern Colorado and Western Kansas border area and took place between 17 May and 20 July 2000 (Fig1.1). This location is in the vicinity of the climatological position of the dry line (Fig 1.2). It is also a region well known for producing severe hailstorms (Changnon 1977), and for producing a large number of predominately positive storms (Fig. 1.3).

STEPS collected data from a variety of storm types, ranging from small airmass thunderstorms to supercell storms. Officially, STEPS observed eight weak storms, seven moderate storms, and five severe storms. Because we know so little about the electrical characteristics of many types of storms, severe or non-severe, documenting and contrasting the electrical characteristics of the various types of storms will be the focus of this study.
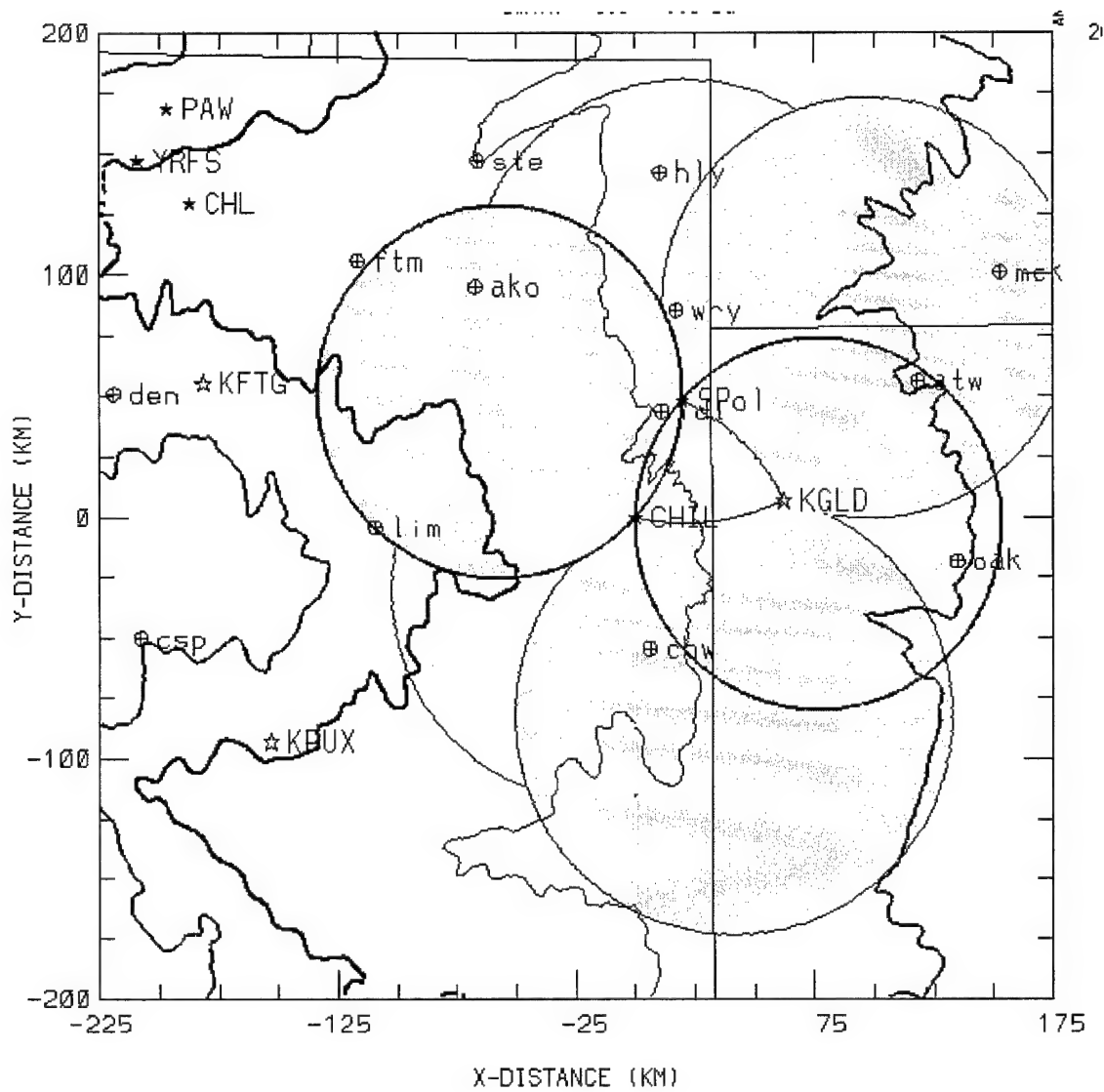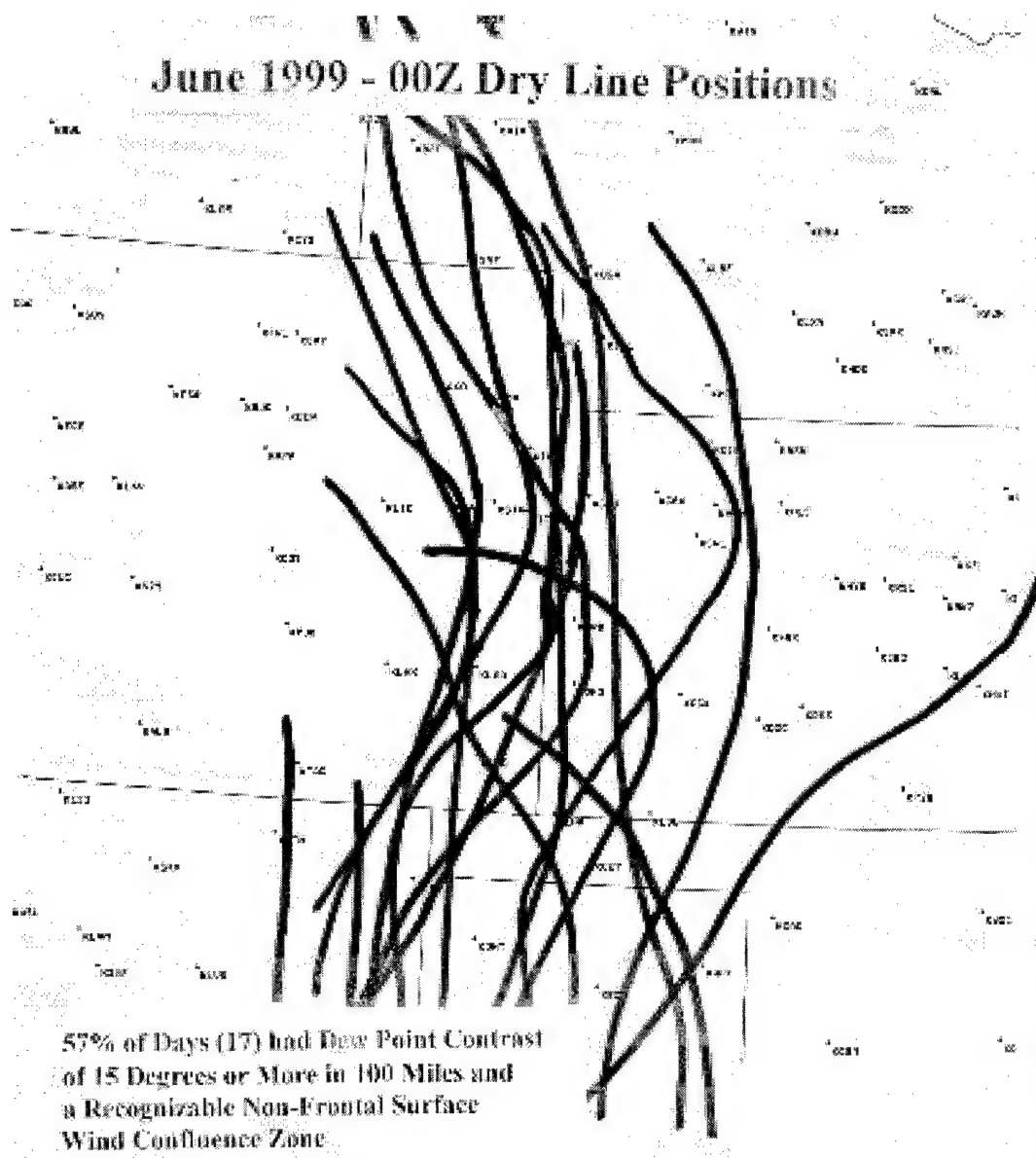
Figure 1.1: The STEPS research area (STEPS 2000).

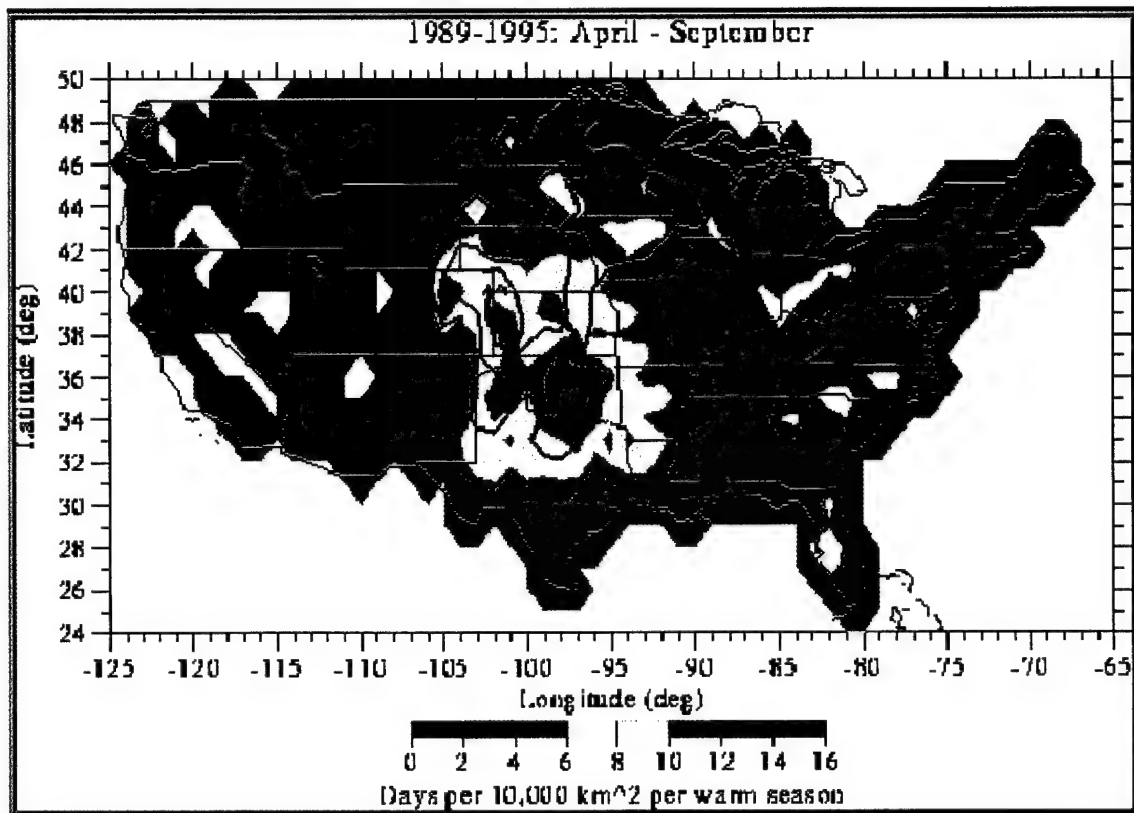Figure 1.2: Dry Line Positions, 1999 (STEPS 2000).

FIGURE 1.3: The color shading shows the number of severe storm days per 1 deg x 1 deg grid box, with overlaid contours representing the number of PPCG severe storm days per grid box. The absolute maximum in PPCG severe storm days is very close to Goodland, KS (From Carey et. al., 2001).

1.3 Objectives and Thesis Overview

This thesis uses two operational data sets, The National Lightning Detection Network and selected radars from the WSR-88D radar network. Both of these data sets are produced in near real time and are available to researchers and operational forecasters alike. These networks are discussed in detail in Chapter 3. The overall goal of this thesis is to improve our understanding of the relationship between radar reflectivity and cloud-to-ground lightning and to add to the knowledge base of reasons why some storms produce high percentages of positive CG lightning.

The specific objectives of this research are as follows:

1. Document the statistical reflectivity signature of lightning producing storms based on various CG lightning flash densities.

2. Compare and contrast these profiles based on flash polarity, electrical strength (i.e. flash density), and geographical location.

3. Provide a baseline for additional research on the STEPS data set.

This thesis is organized in five chapters. Chapter 2 reviews the state of the science and covers the background theory of thunderstorm electrification. We will also address the significance of positive cloud-to-ground lightning and briefly cover some of the recent work that has been done in the area of lightning climatology. Chapter 3 explains the data sets used and processing methods. Results are presented in Chapter 4, which begins with a description of a new analysis method. The bulk of Chapter 4 uses these frequency analyses to describe the general picture of lightning producing storms and further presents analyses based on finer distinctions between storms and ultimately

describes storm scale distributions. We also discuss geographical differences between upper plains locations. Additionally, we consider a subset of cases, those storms that produce a minimal amount of cloud-to-ground lightning yet return robust radar reflectivities. Finally, Chapter 5 summarizes the work, and recommends areas for future research.

CHAPTER TWO

BACKGROUND THEORY

2.1 Introduction to Thunderstorms and Lightning

Undoubtedly, lightning has amazed and frightened us from the beginning of mankind. No longer thought to be the wrath of an angry god, science has been able to demystify some aspects of lightning. We've been able to record when and where lightning occurs and make quantitative observations of lightning flashes. Yet lightning remains a mystery. Investigators have taken observations, conducted laboratory experiments, and remotely sensed particle electrification. Inadequate time and space sampling, inadequate instrumentation, unknown variable affects, and complex storm morphologies complicate our analyses of thunderstorm electrification. But as one of nature's most dangerous phenomena, we will continue to seek answers to questions of exactly how and why lightning forms.

Lightning is the number two weather-related killer in the United States today. Lightning owned the number one place until the last half of this century when flooding became number one. Presumably, higher population densities, especially in low-lying areas, have led to the higher death tolls from floods. Additionally, less human exposure to agricultural activity in the past fifty years has decreased the number of lightning fatalities. Still, lightning causes nearly one hundred deaths and three times as many reported injuries each year in the United States. Twenty to thirty million annual lightning

11

strikes also take their toll in property damage. Roughly 18,000 homes are destroyed or severely damaged each year. Insurance companies pay out hundreds of millions of dollars worth of claims from lightning damage. Actual damage is likely to be significantly higher since much damage, especially to small electronic appliances, may not be reported or is not covered in insurance estimates. The United States also loses hundreds of thousands of acres of forestland from lightning caused fires. Combined, annual U. S. property losses are in billions of dollars. Not surprisingly, due to the high concentration of thunderstorms, Florida sees the highest frequency of cloud-to-ground flashes, with a peak annual flash density greater than nine flashes/km^2.

Since thunder is the result of a lightning flash, a thunderstorm, by definition, is a cloud that produces lightning. So, we shall only consider thunderstorms as the source of lightning. Strictly this is not true, lightning discharges are known to have originated from sandstorms and from volcanic eruptions, but for our purposes, we will only consider cloud electrification that results from clouds made of hydrometeors, or water in its various phases. In the early 1900s, C.T.R. Wilson first proposed what we refer to as the positive dipole model of thunderstorm charge structure. He suggested that thunderstorms generally have positive charge concentrated in the upper part of the cloud, above a negative charge region in the lower portion of the storm. Since then, in the 1980s, observations confirmed the occurrence of a lower, weakly charged positive region below the main negative charge region; the result is the tripole model of thunderstorm charge (Fig 2.1). In reality, these are only conceptual models; actual charge structure in thunderstorms is much more complicated and may be similar to that proposed by

Krehbiel (1986; see Fig 2.2). In any case, observations have shown lightning discharges can occur as soon as five to ten minutes after cloud formation.

In order for a lightning flash to occur, intense charge regions must exist in a cloud. The potential difference, or voltage, must be large enough to ionize the air, which is normally a poor conductor of electricity. There are various types of lightning discharges. The first, the one we are concerned with in this work, is cloud-to-ground lightning—those that transfer charge between cloud and ground. Other lightning discharges are those that occur within cloud, from cloud-to-cloud, or extend from cloud to the surrounding air. In all cases, breakdown potential must be reached, and there are competing theories to account for this charge difference leading to breakdown

2.2 Thunderstorm Electrification

Charge separation theories can be broken down into two broad categories. The first is the convective theory of charge separation and the second are the precipitation based theories. The fundamental question is whether charge separation results from vertical transport of charge induced by the storm's convective motions or whether electrically charged hydrometeors of different phase and size transfer their charge by physically falling through, or by being carried upward in the cloud. These theories have varied in popularity throughout the years and both may contribute to cloud electrification. This section will discuss the different theories and propose the most likely mechanism, but we must keep in mind that other as yet undiscovered mechanisms may play a role in cloud electrification.

13

The convective theory begins with the "fair weather" electric field. The net charge of the earth is negative and the upper atmosphere (ionosphere) is positive. These charge regions sustain the earth's fair weather field, approximately 120 V/m near ground. These charge regions would soon equalize were it not for thunderstorms. The earth's negative charge is maintained by roughly two thousand thunderstorms occurring simultaneously around the globe, that is, they continually transfer negative charge to the earth. According to convective theory, this electric field in turn, drives the initial electrification in thunderstorms. In the initial stages of thunderstorm development, buoyant updrafts carry positive space charge from near the surface upward into the forming cloud. Negative charge aloft (produced by cosmic ray ionization) is then attracted to this newly formed, positively charged, cloud and becomes attached to the outer cloud edges. Downdrafts along the edges of the cloud carry this negative charge to lower levels, while updrafts continue to carry positive charge aloft. This results in a positive dipole, with positive charge in the upper portion of the cloud and negative charge below. This mechanism produces a positive feedback whereby, as this process continues, the respective charge centers intensify and the negative cloud base induces additional coronal discharge from the surface and results in greater charge separation. Williams (1989) investigated this theory and found that this mechanism alone cannot account for the amount of charge separation required to produce lightning on the time scales observed in typical thunderstorms. This theory also does not explain the tripole charge structure that has been observed in thunderstorms. Nor does it account for the enhanced electrical activity seen in mixed phase clouds.

14

The charge transfer or precipitation theory is divided into inductive and non-inductive mechanisms. The inductive theory (Elster and Geital 1913; Illingworth and Latham 1977) assumes an electric field that polarizes hydrometeors as they are falling. The particles are polarized with negative charge oriented on the top of the particle and positive below. Collisions between particles result because of differential fall speeds between different sized particles. A portion of the collisions between particles do not result in coalescence, they rebound. It is generally thought that negative charge is transferred from the smaller droplet, moving relatively upward, to the larger drop, moving downward (Figure 2.3). The resulting structure is one with smaller, positively charged particles carried upward with larger, negatively charged drops falling to cloud base—the positive dipole. This process also produces a positive feedback; as the cloud charge centers strengthen, then so too does the strength of the electric field, which in turn increases the rate of charge separation. We now turn to a discussion of how this strong electric field is thought to develop.

The non-inductive theory (Takahashi 1978; Jayaratne et. al. 1983; Keith and Saunders 1989; Saunders et. al. 1991) does not require the presence of an electric field to polarize hydrometeors. Laboratory experiments have shown large charge separation occurs in collisions between ice crystals and a riming ice surface—one that is growing by collecting supercooled liquid cloud droplets. That is, significant charge can be separated when relatively large graupel-type particles collide with smaller ice crystals in the presence of supercooled water. The magnitude and polarity of charge transferred have been shown to be a function of the liquid water content and temperature at temperatures below -10˚C. Above -10˚C the graupel particle became positively charged regardless of

15

liquid water content. Figure 2.4 shows the charging dependence on temperature and liquid water content. Between -10˚C and –20˚C a "charge reversal temperature" is noted where, depending on liquid water content, the charging on the riming particle changes sign. In other words, for temperatures above this reversal temperature, graupel charges positively, and at lower temperatures, graupel charges negatively. From this information, we could imagine a situation where graupel, suspended above the charge reversal temperature (at higher altitudes and colder temperatures), collides with ice particles as they are swept by. The graupel particle acquires a negative charge, and the smaller ice crystals become positively charged and are carried by the updraft to the upper portion of the cloud. This initially results in a positive dipole structure. As the particle grows, its terminal fall velocity will increase and will exceed the updraft speed. This process may be accelerated as the cloud updraft weakens. No longer suspended, it will begin to fall. As it falls and encounters warmer temperatures, the charging reverses, and the falling particle now acquires positive charge. The small ice particles will be negatively charged and may be lifted upward and contribute to the previously established negative charge center, and the positively charged graupel falls and creates a weak positive region below the main negative center. This results in a tripole structure that has been observed in thunderstorms (Williams 1989).

Though largely based on laboratory experiments, recent observational evidence has reinforced the non-inductive theory. There are still problems with the non-inductive explanation. We cannot explain why there is such a dependency on temperature and liquid water content in particle charging. Theories such as those advanced by Baker and

Dash (1994), involving the presence of a quasi-liquid layer, may help us understand this process.

2.3 Positive Lightning and Inverted Polarity Storms

Positive lightning is a rarity. Over 90% of annual cloud-to-ground (CG) lightning strikes are negative polarity strikes, that is, they transfer negative charge from cloud to earth. Positive CGs lower positive charge to ground. Positive flashes usually have only one return stroke (a multiplicity of 1), but have a longer duration and typically larger peak currents. Because of larger peak currents, they are capable of doing significant damage. Additionally, positive strikes seem to be more likely before rain begins or after it ends (on a storm-by-storm basis). Since thunderstorms typically induce positive charge directly below them on the surface, positive lightning may be attracted to negative ground away from the storm, and away from the rain shaft. These factors may lead to a higher incidence of forest fires being caused by positive lightning.

Because of its anomalous nature and its propensity to cause damage, there has been a large amount of research on the nature of positive lightning. The causative mechanisms for positive CG lightning are still unknown, but there are several hypotheses. We will cover three: the tilted dipole, the inverted dipole, and precipitation unshielding.

The tilted dipole assumes a classic positive dipole structure, with positive charge overlaying negative charge, in an environment of strong vertical shear. The shear tends to displace the upper portion of the storm such that the positive region may be directly exposed to the ground. In other words, the cloud is tilted in the vertical and the positive

charge center aloft is not "shielded" from ground by the negative charge center. This allows for a direct positive flash from the upper part of the storm to ground.

The inverted dipole hypothesis suggests that the dipole charge structure could be reversed through non-inductive charging. We could also see a tripole structure in which the lower positive charge center becomes so strong that it becomes the dominant positive region and thus "inverts" the storm. As previously mentioned, it is possible that under the right dynamic and thermodynamic conditions the non-inductive particle charging mechanism could produce and sustain this structure. Here small ice crystals would carry negative charge aloft and larger graupel particles would maintain a lower positive charge region. This lower positive region would then favor positive CG lightning.

The third hypothesis, precipitation unshielding, suggests that in intense storms, the rain rate might be so high that, the lower negative charge region is physically removed by the precipitation current, rather than by lightning discharges. Once the lower charge is removed, the upper positive charge is again unshielded in the same sense as in the tilted dipole hypothesis and positive CGs are favored.

2.4 Association of Positive Lightning with Severe Weather and "Nowcasting"

Research has shown that there is a tendency for storms which produce predominately positive cloud-to-ground (PPCG) lightning to produce severe weather though we know that positive CGs are found in non-severe weather events as well. In fact, studies have shown up to 40% of PPCG storms are severe weather producers. Nearly instantaneous readouts of lightning strikes can give a forecaster the first indication of impending weather as opposed to radar and satellite data cycles which take roughly five to thirty

18

minutes to update in a traditional operational environment. Ultimately, this may improve our ability to "nowcast" severe weather operationally or increase the lead time for issuing weather warnings. In addition, other lightning signatures may indicate or forewarn of severe weather including: very low CG flash rates (from a strong storm), transitions between predominately negative and predominately positive lightning strikes, and transitions from high to low or low to high flash densities. Research has shown examples that support this idea.

Various lightning studies have linked CGs to tornadoes, hail, and strong winds. Branick and Doswell (1992) noted an unusually high percentage of positive CG flashes were associated with tornadic thunderstorms, which were classified as low precipitation (LP) type supercells. The high precipitation (HP) supercell had lower positive CG flash rates. These findings may be significant, since LP storms often appear benign on radar despite their ability to produce tornadoes and very large hail, and thus, can be relatively difficult to identify using radar alone. Perez et. al. (1995) found significant variations in CG patterns, but decided some signatures may be related. They found peak CG flash rates preceding tornado formation in over 70% of storms and noticed a decrease in flash density coincident w/ tornado touchdown. However, he found there was no apparent correlation between relative number of CG flashes and tornadic intensity. Changnon (1992), McGorman et. al. (1993), McGorman and Burgess (1994), and Stolzenburg (1994) all associated positive CG lightning with hail. Changnon found that lightning rates increased until hail began and then diminished after the hail ended. The two McGorman studies found that hailstorms with frequent positive CG regions produced their hail during the period when positive CG flashes dominated. Buechler et. al. (1988)

suggested CG flash rates might indicate the onset of microbursts. They suggested that three to five minutes before a microburst event, the CG flash rates decreased, signaling the collapse of the storm and forewarning the event. Each of these studies provided evidence of a direct relationship between positive CG lightning and storm severity.

Carey and Rutledge (1998) found that the common characteristic of positive CG storms was storm severity. Reap and McGorman (1989) compared lightning and radar data and found a correlation between severe weather and high positive CG flash rates. They found radar reflectivity and positive flash density were directly related. Chapter 4 attempts to verify that connection, quantify the relationship between reflectivity and flash density, and discusses that relationship.
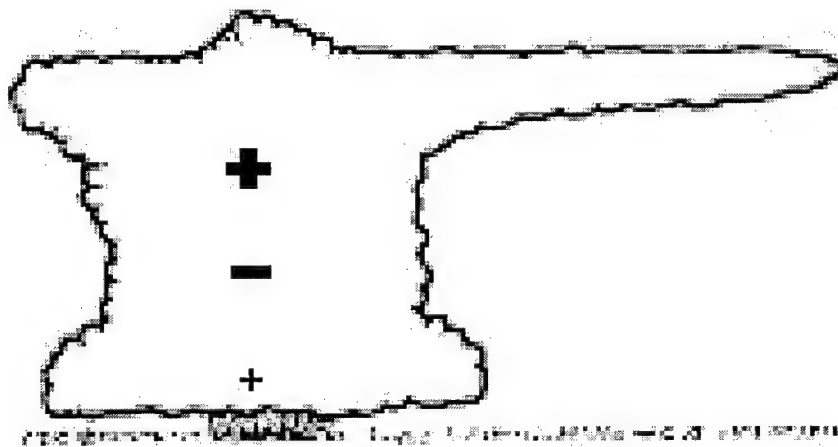

Figure 2.1: Positive dipole/tripole model of thunderstorm electrification (From McGorman and Rust, 1998).
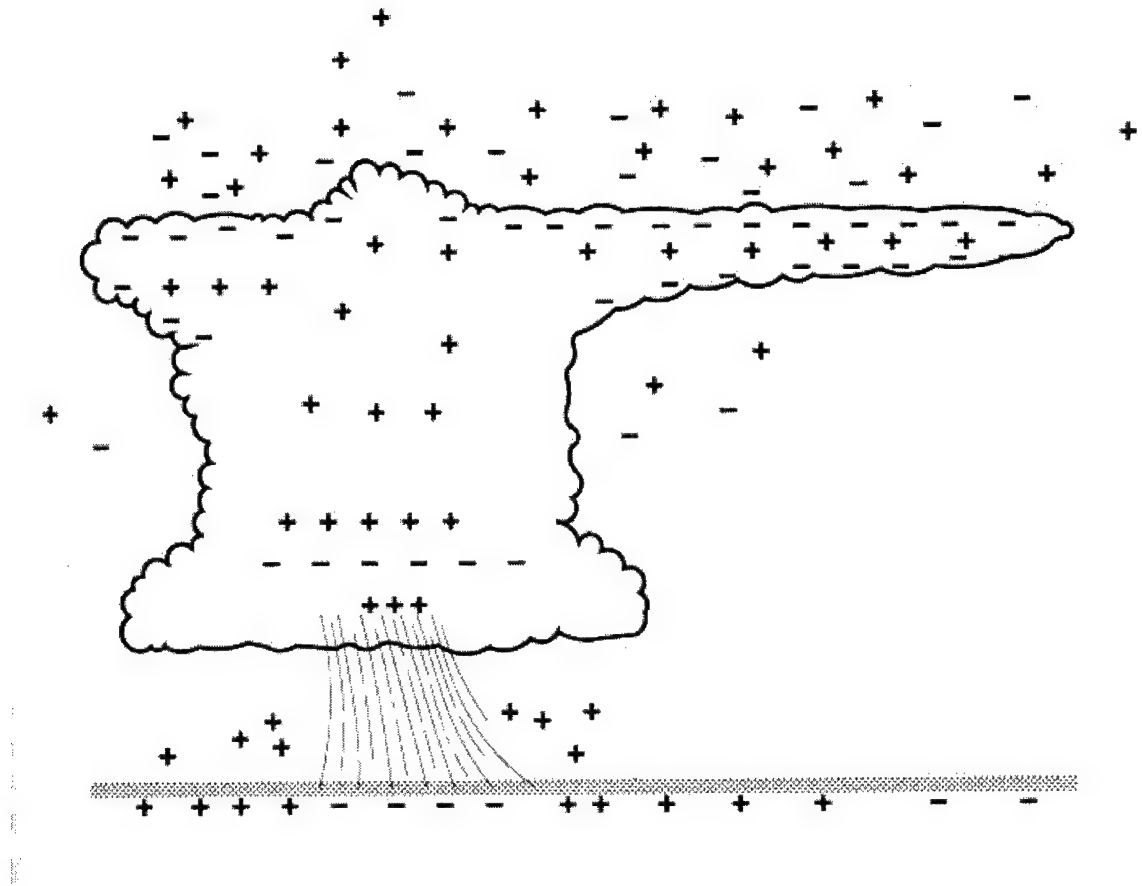
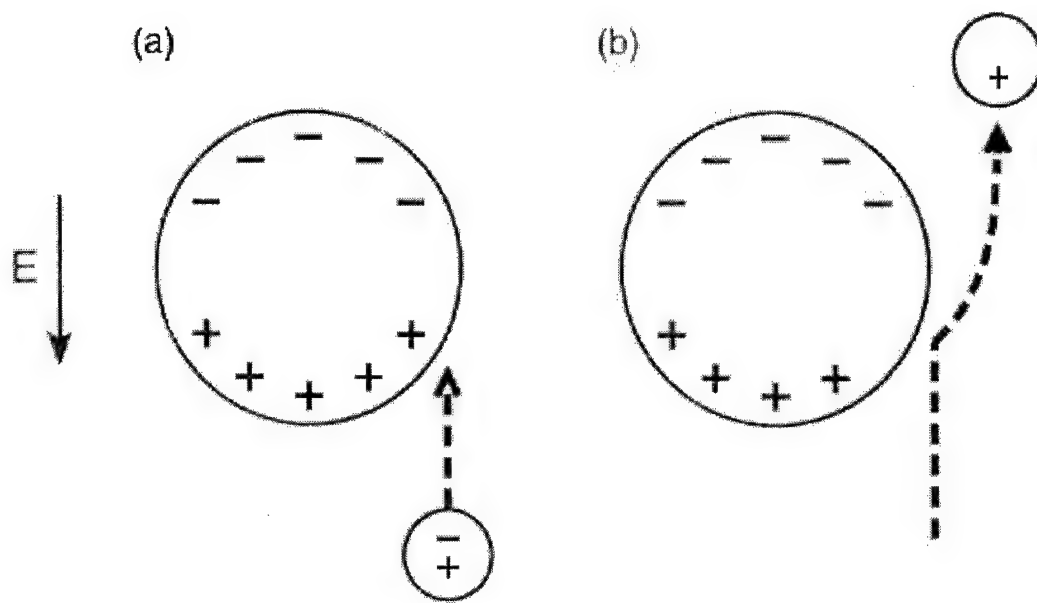Figure 2.2: Realistic thunderstorm charge distribution, (From Krehbiel, 1986).

Figure 2.3: Inductive charging mechanism. In (a) two neutrally charged particles collide. In (b) the smaller particle loses its negative charge and is carried upward. (From McGorman and Rust, 1998).
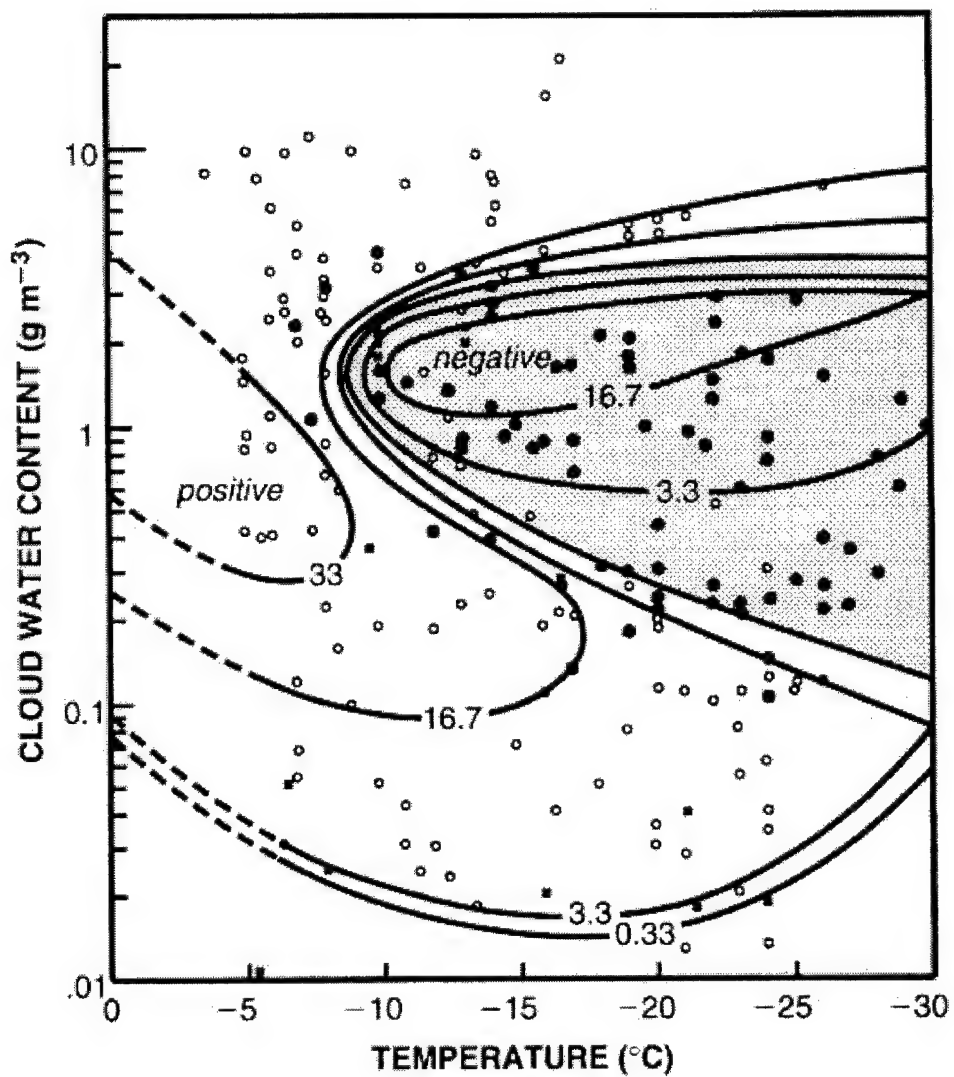
Figure 2.4: Charge in fC, on a riming graupel particle colliding with ice particles as a function of temperature and liquid water content. Open circles indicate positive charging and solid circles indicate negative charging. (From Takahashi, 1978).

CHAPTER THREE

DATA AND METHOD

3.1 National Lightning Detection Network

This thesis used observations of lightning from the National Lightning Detection Network. The National Lightning Detection Network (NLDN) was established in the 1980's beginning at the State University of New York at Albany under support from the Electric Power Research Institute. Complete coverage of the United States was completed in 1989 (Orville 2001) with a major network upgrade completed in 1995. Current operation and maintenance has been transferred to the private company, Global Atmospherics, Inc (GAI) of Tucson, AZ. The network is comprised of over 100 sensors (Figure 3.1), a satellite communication system, and a central processor (Figure 3.2). The NLDN uses a wideband magnetic direction finding antenna (Figure 3.3), where with two antennae, the network can determine the direction and range to a lightning strike. The network records time and location of cloud-to-ground lightning (using triangulation from two or more stations) as well as its polarity, peak current and multiplicity—the number of return strokes in a given flash. Detection efficiency varies by location and has improved throughout the life of the network. Current detection efficiency is above eighty percent across most of the continental United States, with efficiencies approaching 95 percent over parts of the STEPS domain (Figure 3.4; from Cummins et. al. 1998). Average

location error has also continued to improve and is currently less than one kilometer, and

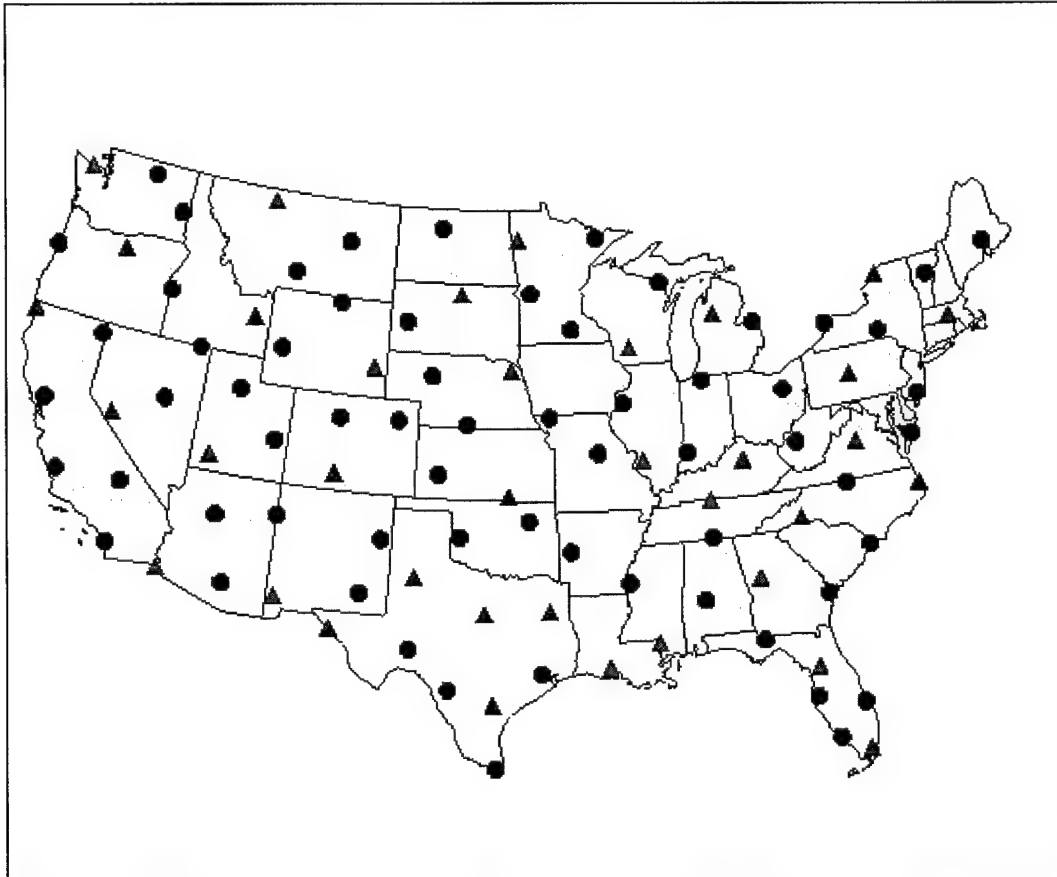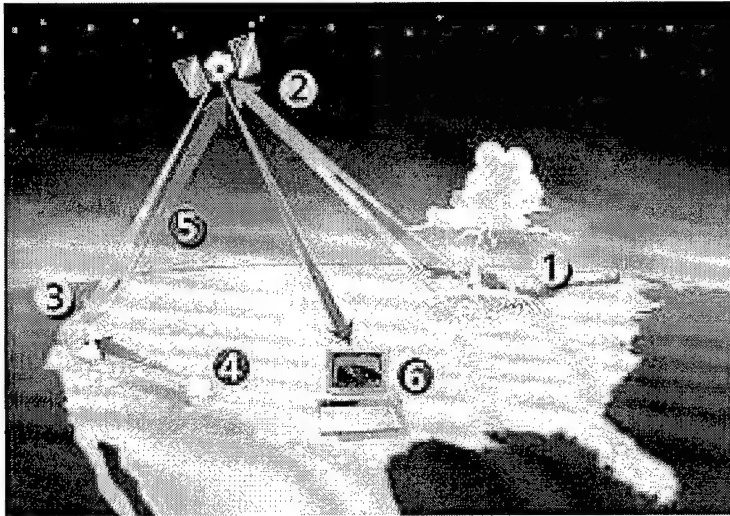average time error since 1995 is better than one millisecond.

Figure 3.1: Location of NLDN sensors. Triangles represent sensors installed during the upgrade.

1. Sensors transmit data to satellite;
2. Satellite relays information to earth station;
3. Data is transmitted to NCC via land-lines;
4. NCC processes data;
5. Processed data is relayed back to satellite;
6. Lightning data is displayed within seconds of occurrence
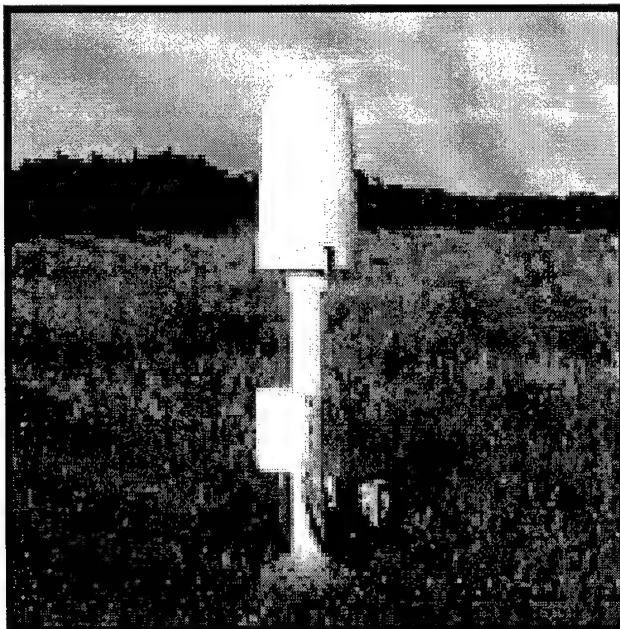
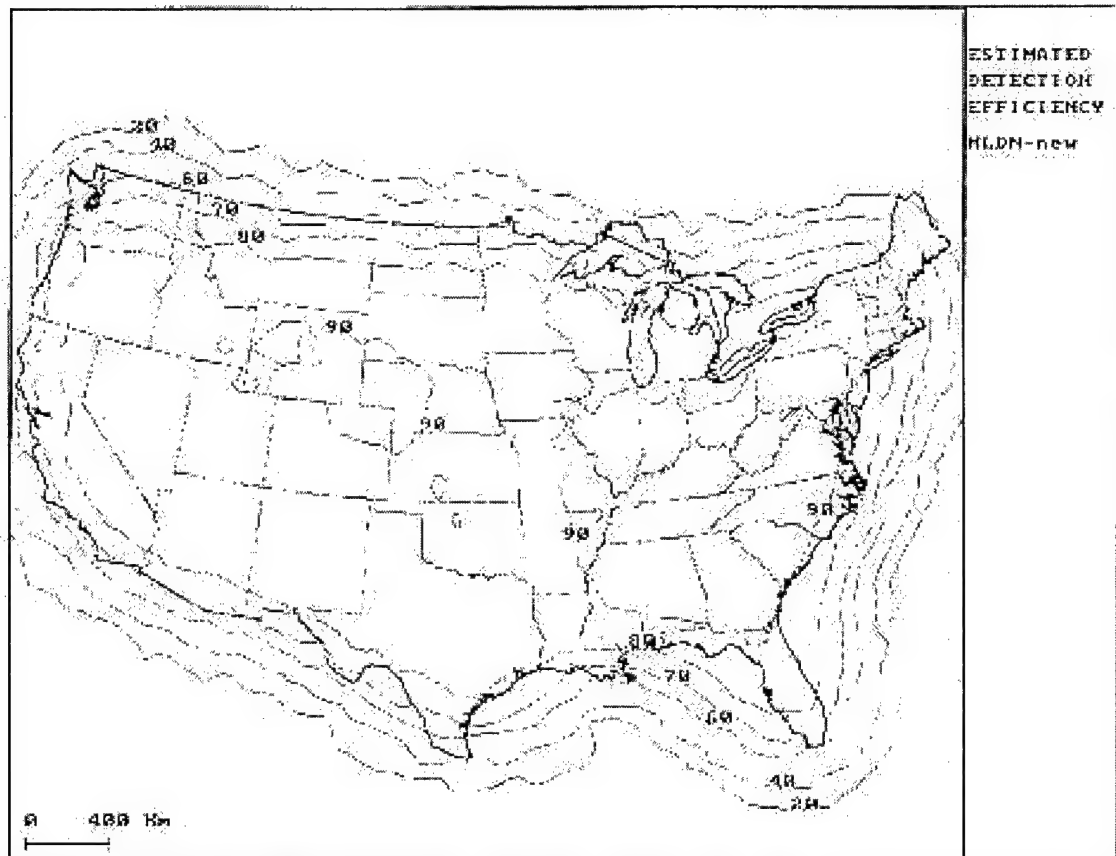Figure 3.2: Depiction of the NLDN. (GAI 2000)

Figure 3.3: NLDN sensor

Figure 3.4: NLDN detection efficiencies (From Cummins et. al., 1998)

3.2 Radar Data

3.2.1 Introduction

The radar data used in this research, the Weather Surveillance Radar 1988—Doppler (WSR-88D) or NEXt Generation Weather RADar (NEXRAD), is a tri-agency radar network. It was designed to serve the Department of Defense (USAF), the Department of Commerce (National Weather Service), and the Department of Transportation (FAA). Throughout this paper we will use WSR-88D and NEXRAD interchangeably.

The NEXRAD network consists of over 150 radar sites throughout the United States and some overseas locations. The radars are operated by the Air Force Weather Agency, the National Weather Service, and the Federal Aviation Administration. Operational forecasters from each agency use the WSR-88D in their daily forecasting, and these are the images the public see in the mass media.

3.2.2 Specifications and System Components

The WSR-88D is an S-band radar with that operates with a wavelength of approximately 10.7 centimeters. It has an operating power output of 750 kilowatts with a peak power of 1 megawatt. The WSR-88D antenna has a beam width of approximately one degree. The radar is composed of three functional parts, the Radar Data Acquisition (RDA) unit, Radar Product Generator (RPG), and the Principal User Processor (PUP).

The RDA consists of a 28 foot parabolic dish antenna capable of rotating at a maximum speed of five revolutions per minute and moves in incremental elevation steps from 0.5 to 19.5 degrees in normal operational mode. The 2,600 pound dish is mounted atop an aluminum and cast iron pedestal and enclosed in a 39 foot protective fiberglass

radome. Transmitter, receiver, and computer processors are also included in the RDA hardware. The RPG uses computer algorithms to convert base data as it is received from the RDA into meteorological products useful to the operational meteorologist. It is essentially the "brains" of the system. The PUP is the user workstation or interface between the meteorologist and the radar. It consists of a computer workstation with application terminals, graphics tablet, color printer, and communications system. From here users are able to display base products as well as derived fields

3.2.3 Scan Strategies

The WSR-88D is capable of various scan strategies or volume coverage patterns (VCPs) depending on the meteorological conditions. Each VCP denotes a number of 360 degree scans, at selected elevation angles, at a specified rate (see Figures 3.5-3.7). In precipitation mode there are two scan strategies available. VCP 11 scans 14 elevations in 5 minutes and VCP 21 scans 9 elevations in 6 minutes. VCP 21 is usually used for most non-severe precipitation events and can be used to sample distant storms. Conversely, VCP 11 has a higher sample rate and provides better coverage with less "gaps" between elevation scans. VCP 11 however, places a much higher processing workload on the RPG. In the clear air mode, VCP 31 and VCP 32 sweep 5 elevations in 10 minutes. This slower scan rate allows for increased sensitivity and is used to detect early formation of convective precipitation, boundaries, and fine lines, and to obtain wind profiles. VCP 31 uses a longer pulse length and increases sensitivity whereas VCP 32 uses a shorter pulse length and increases the velocity resolution of the radar. The WSR-88D is designed to operate in clear air mode but to automatically switch into precipitation mode when

sufficient precipitation is detected. All four scan types are included in this study, and they place restrictions on the data analysis.

From Figures 3.5-3.7, we can see that the first five to seven elevation scans are separated by one beamwidth. Above that, the spacing between sweeps progressively increases. This coarseness causes gaps in the data that cause concentric "rings" when the data is gridded. Suffice it to say for now, these data gaps limit the methods of analysis, but do not invalidate the method of analysis contained herein.
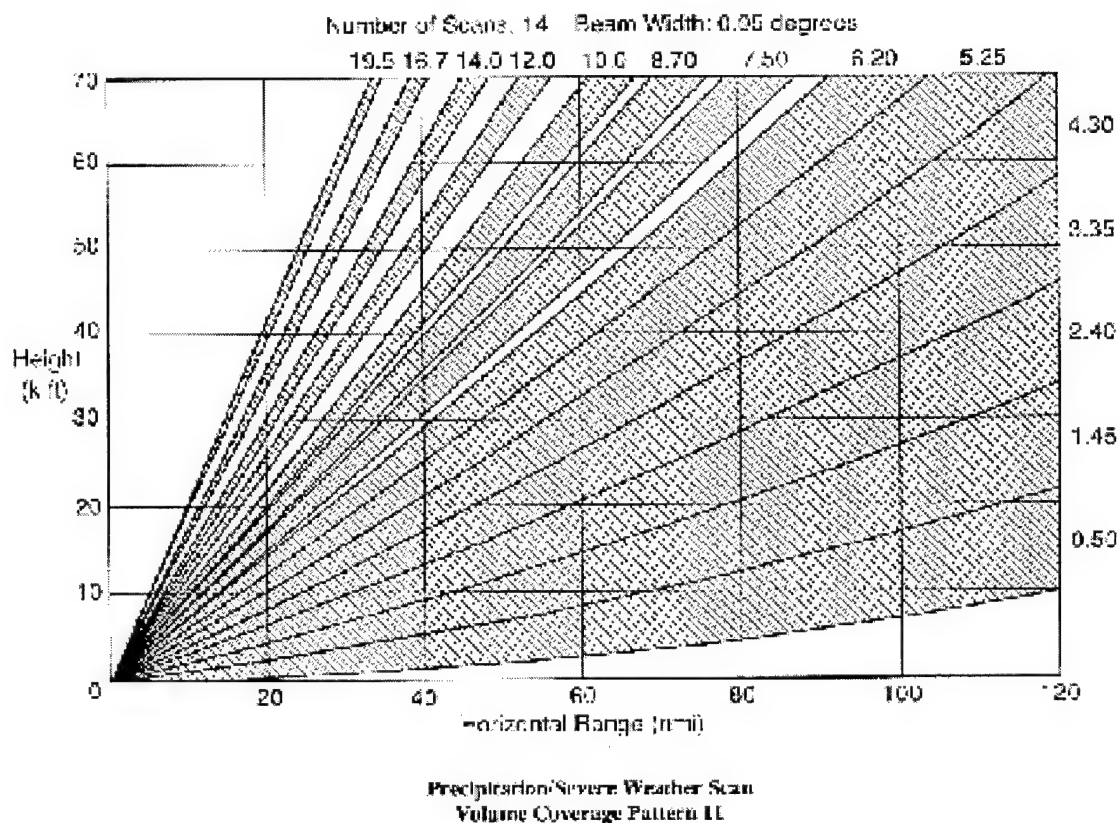

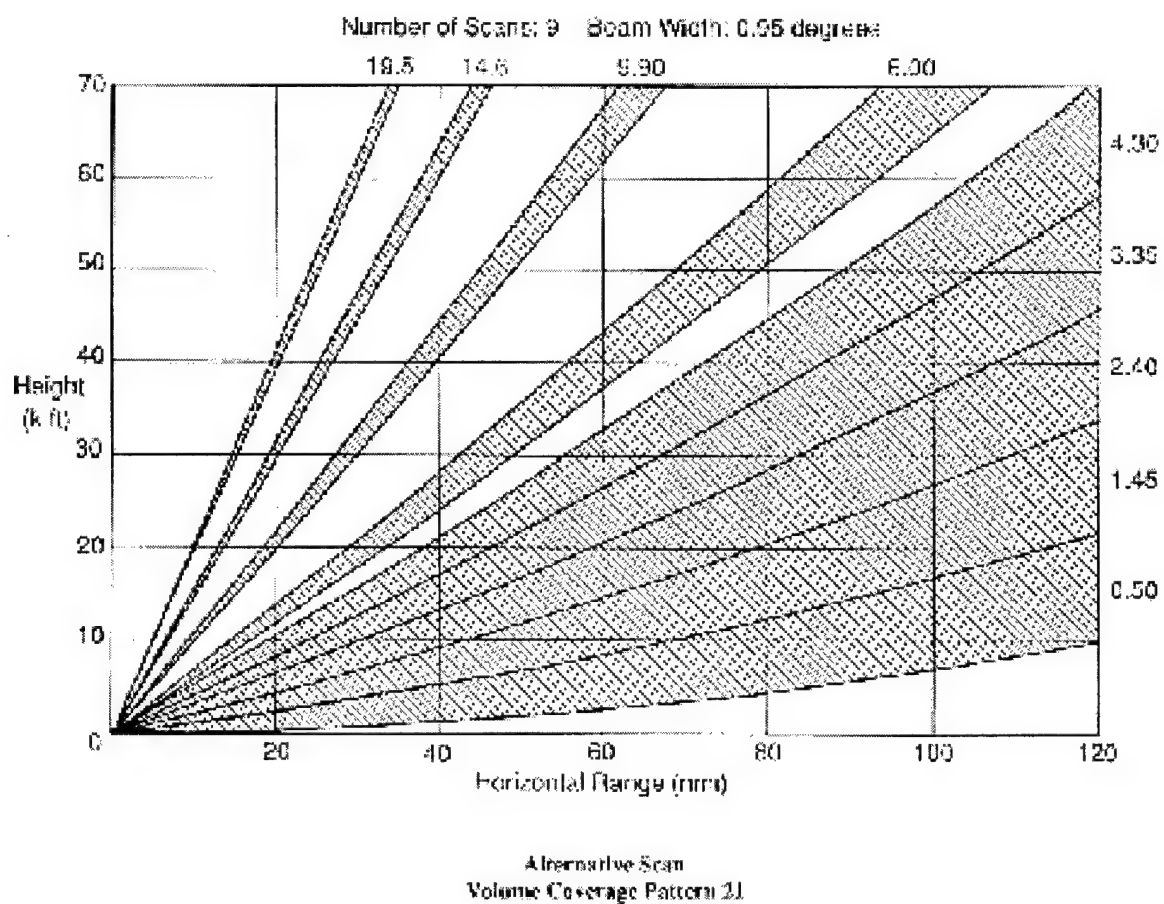Figure 3.5: VCP 11, 14 elevation scans in 5 minutes
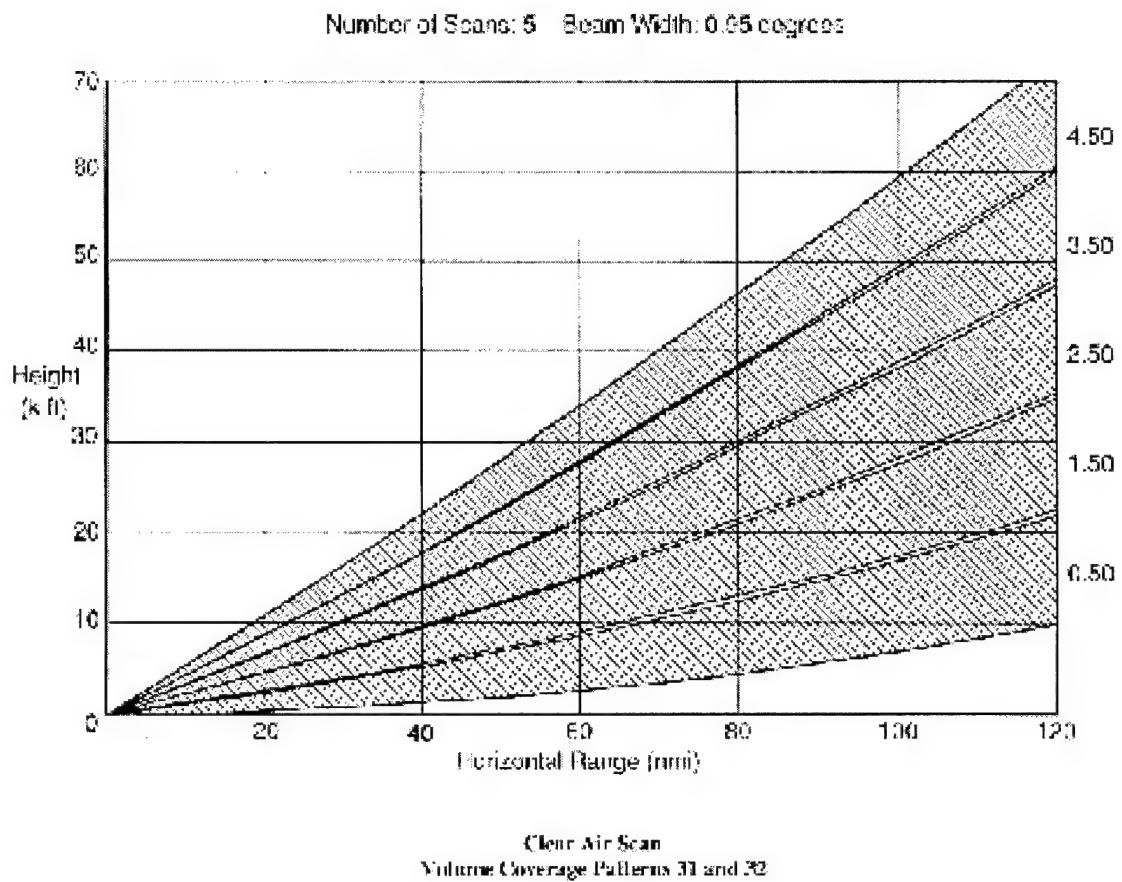
Figure 3.6: VCP 21, 9 elevation scans in 6 minutes

Number of Scans: 5   Beam Width: 0.95 degrees

Clear Air Scan
Volume Coverage Patterns 31 and 32

Figure 3.7: VCP 31 and 32, 5 elevation scans in 10 minutes

3.3 Data Collection and Analysis

The first objective of this thesis is to document reflectivity structures based on lightning signatures. The NLDN lightning data provides the basis of this analysis. Using routines developed within the CSU radar meteorology group, cloud-to-ground flashes were gridded on a 0.25 degree spatial scale (roughly 21 km by 27 km) with a 30 minute time resolution. Based on previous work, (Gauthier 1999; Stolzenburg 1994) this was a reasonable gridding scheme to determine storm scale characteristics. From the raw data, and for each grid box, we determined a total flash count, flash density, percent positive, peak current, and multiplicity for positive and negative flashes.

The radar data used in this thesis were obtained from the National Climate Data Center via the Air Force Combat Climatology Center through an interagency agreement. Archived NEXRAD data were obtained for six stations: Cheyenne, WY (KCYS), Denver, CO (KFTG), Pueblo, CO (KPUX), North Platte, NE (KLNX), Goodland, KS (KGLD), and Dodge City, KS (KDDC). These upper plains stations encompass the entire STEPS domain and provide significantly more coverage with which to expand the statistical analysis. Yet, these stations are sufficiently separated, such that regional comparisons may be made.

Level II data were received on 8mm magnetic tape cartridges, converted to and stored in Universal Format (UF). Files were then gridded on a 1 km x 1 km x 1 km Cartesian coordinate system using CEDRIC (custom editing and display of reduced information in Cartesian space) and the REORDER software developed by Dick Oye and Michele Case at the National Center for Atmospheric Research (NCAR). The software used a Cressman filter (Cressman, 1959) with a 1 km radius of influence in the horizontal and a

33

half kilometer in the vertical. The "tight" gridding was used to eliminate any overlap in the vertical grids due to the large gaps in the radar volume scans, that is, to avoid filling in the spaces between elevation scans. We also avoided smoothing or smearing the data unnecessarily, which yields a more accurate analysis. An example of a gridded reflectivity field is presented in Figure 3.8. From this figure we can plainly see that any attempt to distinguish storm tops or analyze an individual storm in a complete sense is not practical.

So, starting with the lightning grids, if a given grid box contained a non-zero flash density, it was categorized into one of eight lightning signatures. The data were then split into positive and negative storms (greater than 50% of flashes) and subdivided into four separate flash densities, 0.0-0.01 flashes per kilometer per hour, 0.01-0.03 flashes/km/hr, 0.03-0.1, flashes/km/hr, and greater than 0.1 flashes/km/hr. In a half hour and over roughly 500 km^2, these flash densities translate to 0-3 flashes, 3-9 flashes, 9-30 flashes, and more than 30 flashes, respectively. The 0.01 and 0.03 levels were determined based on the work of Stolzenburg (1994) and Gauthier (1999) defining these flash densities as "significant." Somewhat arbitrarily, 0.1 was selected as a threshold for the most electrically active storms. With this high threshold, it is assumed the storms producing these signatures are sufficiently contained in the grid box with little or no "contamination" from adjacent grids. Thus, every storm that produced cloud-to-ground lightning was considered which then initiated a second routine to access the appropriate radar files. Depending on the VCP, up to six separate radar files, each with a subsequent time, were processed for each lightning grid, i.e. five minute scans over a thirty minute period. The appropriate grid locations within those files were then accessed and simply

34

"binned" at each height. All radar echoes above 5 dBZ were counted in one of fourteen reflectivity bins, each in 5 dBZ increments. When these counts were normalized at each height, we obtain an echo structure that shows the likelihood of seeing a given reflectivity return at a given height. The overall frequency distribution will include the entire range of storm types, from ordinary air mass thunderstorms through tornado producing supercells and MCSs. However when we progressively increase the lightning flash density and isolate those storms, we might generally infer the strength of the storms is also increasing. For example, storms that only produce a couple of lightning flashes in a half hour period would usually be considered to be weaker than storms that produce several a minute. Thus there would be a much higher likelihood of seeing 50 dBZ returns at 4 km AGL from the stronger storm.

The same process was repeated using a different categorization scheme; this scheme considered strongly active storms based on the percentage of lightning strikes that were positive. These were thresholded at less than 30 percent positive, 30-50 percent, 50-70 percent, and greater than 70 percent with flash densities of 0.05, 0.07, and 0.1. After the first analysis, it had been determined the higher flash densities were more reliable for making relative comparisons.

Figure 3.8: Gridded 29 Jun 2000 radar image at a height of 8 km. Image shows the data gaps in NEXRAD scans.

CHAPTER FOUR

RESULTS AND DATA ANALYSIS

4.1 Frequency Distribution Analysis

This chapter presents a new analysis method in an attempt to better relate positive CG lightning to storm structure as observed by radar. This is the first study to relate mid-latitude thunderstorm reflectivity to specific lightning signatures using a bulk statistical approach. We have analyzed all CG producing thunderstorms, regardless of storm type, duration, or strength, and calculated a statistical frequency distribution of storm reflectivity profiles. Other researchers have used different methods to examine radar reflectivity profiles. Yuter and Houze (1995) introduced contoured frequency by altitude diagrams (CFADs) to display frequency distributions of reflectivity, mean reflectivity, differential reflectivity, and vertical velocity. Their analysis however, has been based on individual storms and akin to case studies. Peterson and Rutledge (2001) used a statistical approach and displayed a three-dimensional frequency distribution or radar reflectivities against height. Their analysis used data from the NASA TRMM satellite and focused on tropical convection. The method we present builds upon these works by applying operational data sets to mid-latitude, warm season thunderstorms using a statistical approach. We focus on storms over a portion of the Great Plains during the summer of 2000. The result is a vertical distribution of radar reflectivities. Reflectivity

is binned in 5 dBZ increments and plotted on the y-axis. Height is plotted on the x-axis and relative frequency is plotted on the z-axis. For example, Figure 4.1 shows the combined frequency distribution of all lightning producing storms in our study. The figure shows that less than one percent of all lightning producing storms had reflectivities greater than 55 dBZ above 2 km.

This method of analysis has several advantages. As stated in Chapter 1, case study selection is subject to biases. Here, we simply process all lightning and radar reflectivity data over a two month period without prejudice. We used a robust data set and processed over 1 terabyte of data using simple thresholding techniques. In doing so, we reduced noise effects. Furthermore, this is almost entirely objective. When we view these reflectivity frequency distributions we are able to glean a large amount of information from a single chart. They indicate the location of the strongest reflectivities, their vertical extent, and reflectivity distributions with height. We might infer gross hydrometeor type and location insofar as we are able based on reflectivities. Another advantage is that this method can be used to analyze and compare individual storms, once those storms have been isolated. In section 4.4 we contrast a few of these storms. On a storm scale, each binned pixel can be viewed as a volume, 1 km x 1 km x 1 km, and as such, average storm volumes can be measured and compared. Perhaps most importantly for our study, this method allows for easy comparisons between profiles.

The process of gridding the data is a source of error. As discussed in the previous chapter, we used two separate sets of grids, the NLDN lightning and the NEXRAD reflectivities. The first set, the lightning grids, pose the most significant problems. Recall that we totaled all CGs in a given grid box over a 30 minute period and used that

number to determine a flash density. Since we used a roughly 25 km grid box, large convective systems would not be "contained" by the grid box. This would not necessarily pose a problem, as adjacent grids would cover the entire system. The concern is not so much that storms are split; the concern is *where* they are divided. In fact, any storm, of any size, could be "split" by the grid boundaries. This has the effect of dividing the storm's total lightning flashes into separate grid boxes and results in a higher number of low flash density grids and a lower number of high flash density grids. Conversely, a single grid box may contain several storms. Totaling lightning counts from these separate storms would have the effect of producing a higher flash density than would be associated with any of the storms individually. These would appear as electrically active storms with relatively weak reflectivity returns. Similarly, one of these nearby storms could "contaminate" a strong storm and reverse its predominate polarity. For example, consider two storms contained within a single grid, one of which was a vigorous convective cell that was producing predominately positive CG lightning, but only by a narrow margin. It would be considered negative if the weaker storm exceeded that margin by one negative CG flash. Another potential drawback is that we do not distinguish between convective and stratiform regions of storms. Hence we are unable to differentiate between lightning strikes that occur between these two regions. While this may be a limitation in further studies, it may be considered an advantage in this first step. By isolating individual storms, the reflectivity profile structures may provide indications of whether positive storms are in predominately convective regions or if they are more frequently stratiform in nature. Similarly, this analysis is independent of storm phase; storms are sampled independent of their individual life cycles. A storm may begin as a

low flash density storm, transition to positive, and then transition again to a negative, high flash density storm. Again, while this has its drawbacks, it may also have the advantage of giving some indication of when in a storms life cycle it produces a given lightning signature. For example, a mid-level reflectivity maximum might suggest a developing storm that has not yet started to precipitate. With these considerations in mind, we have chosen our gridding scheme to minimize these impacts. Their relative contributions are assumed minor.

Some of the most important analyses we may be able to entertain are polarity and regional comparisons between "strong" storms. We define "strong" as electrically active storms, with high CG flash densities (greater than 0.1 flashes km^{-2} hr^{-1}) where strong mixed phased charging is implied. By capturing such a high flash density, we can assume that these storms are reasonably well contained within a single grid box or at least the portion of the storm producing lightning. These regions are assumed convective, as previous work (Rutledge and McGorman, 1988; Rutledge et. al. 1990) showed only in extreme cases could stratiform regions produce flash densities on this order.

It is important to remember when viewing these charts, that they are all based on their lightning signatures and the logic flows one-way. Our purpose is to determine if we can isolate differences based on lightning signature alone. Also keep in mind that the frequency distributions are normalized at each height such that the summed percentages for each height will total 100 percent. The distributions at lower heights will then have a much higher sample population than those in the upper levels. This also means that a higher frequency of low reflectivities (below 25 dBZ) implies a generally weaker storm, on average.
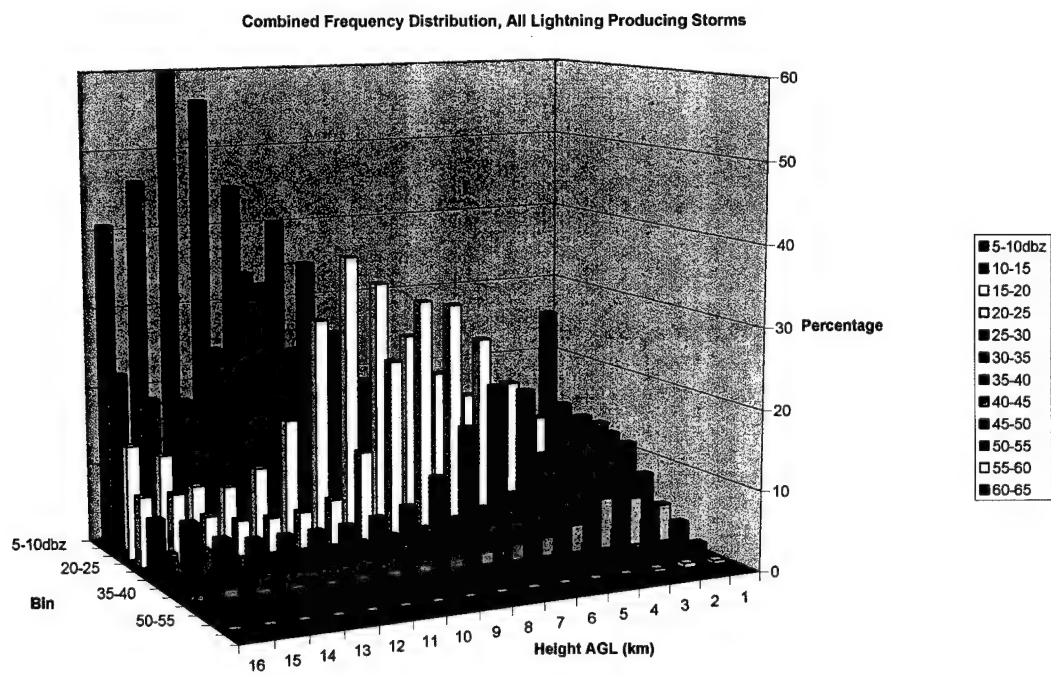
Figure 4.1: Frequency distribution of all thunderstorms that produced cloud-to-ground lightning during our study.

4.2 Polarity Comparisons

4.2.1 Discussion

For discussion in this section, we use storms that are predominately positive CG (PPCG) producers or predominately negative CG (PNCG) producers, that is, for a 30-minute portion of its life cycle, each storm produced greater than, or less than, fifty percent positive CGs, respectively. If by chance the percentage was exactly fifty percent, that grid was not considered. For our purposes we will use PPCG storm and positive storm interchangeably. Likewise, PNCG and negative storm will be used synonymously.

If there truly is a higher frequency of severe weather in positive CG storms, we should expect to see a greater incidence of higher reflectivities somewhere within the distribution. "Severe" as it is commonly used to define a storm is the occurrence of any of the following: 1) hail of at least three-quarter inch diameter, 2) wind in excess of thirty-five knots, or 3) the occurrence of a tornado. So if we accept the hypothesis posed by Carey and Rutledge (1998), that positive storms produce severe weather more often than negative storms, and that there is a corresponding association with reflectivity (Reap and McGorman, 1989); we should look for stronger reflectivities from positive storms (where the flash densities are equal).

4.2.2 Analysis

Figure 4.2 shows a comparison between all positive and all negative storms in our data set. Any thunderstorm that produced a cloud-to-ground lightning strike over the two month period was included (using data from all six radar sites). The basic structure for both of these charts is essentially the same. We can readily see from Figure 4.2 that the

distributions are, in fact, remarkably similar. Particularly at low levels in the higher reflectivity bins, above 50 dBZ, and at mid levels, from 40-50 dBZ, there is less than a 0.2 percent difference at each point. At first glance, these results are inconsistent with what we might expect from a positive to negative comparison. We might conclude that positive storms and negative storms are not dissimilar, but since these distributions are heavily weighted by ordinary thunderstorms, the results may be masked.

By selecting storms with different flash densities, we can isolate different regions along the spectrum of thunderstorm severity. An examination of Figures 4.3-4.6 shows some differences in flash polarities between storms of various strengths. These figures compare reflectivity structures based on the different flash density thresholds. They show polarity comparisons of storms with flash densities of 0.0-0.01 (Fig. 4.3), 0.01-0.03 (Fig. 4.4), 0.03-0.1 (Fig 4.5), and greater than 0.1 (Fig 4.6) flashes $km^{-2} hr^{-1}$. Recall these flash densities are for a thirty minute time period and correspond to 1-3, 4-9, 8-30, and over 30 cloud-to-ground flashes, respectively. Figures 4.3 and 4.4 show storms that were producing very little cloud-to-ground lightning at the time of radar observation. The preponderance of these are weak, short lived, air mass thunderstorms. Also included are a small number of stronger, potentially severe storms, that are simply not producing cloud-to-ground flashes. They may be producing a very high amount of intra-cloud lightning, however. In Section 4.5 we discuss these strong storms with low CG rates. The storms analyzed in Figure 4.5 represent "significant" lightning producers (Stolzenburg, 1994; Gauthier, 1998). These storms would include ordinary thunderstorms in their mature stage, moderate thunderstorms in various stages of their life cycle, as well as severe thunderstorms at various stages in their life cycle. Figure 4.6

shows frequency distributions for storms with flash densities greater than 0.1 flashes km^{-2} hr^{-1}. These storms are assumed to be robust, mature, thunderstorms.

Based on recent studies (Branick and Doswell, 1992; Perez et. al., 1995; Chagnon 1992; McGorman et. al., 1993; McGorman and Burgess, 1994; Stolzenburg, 1994; Buechler et. al., 1988; Reap and McGroman, 1989; and Carey and Rutledge, 1998) that tend to link positive CG lightning to strong storms, we might expect to see very little polarity difference in the weaker storms (Figures 4.3 and 4.4), and larger differences as the storms become stronger from a radar reflectivity perspective. Upon examination, we can see that this is generally true. Figure 4.3 shows little difference between the positive and negative reflectivity profiles. Figure 4.4 begins to show some noticeable differences. In the lower levels, below 5 km, there is a slightly higher likelihood of reflectivities above 30 dBZ for positive storms. There is also a higher frequency of 20-40 dBZ returns in the upper levels, between 9 km and 14 km. We do see one inconsistency in Figure 4.4 that contradicts what we might expect. There is a slightly higher likelihood of reflectivities between 45-55 dBZ between 11 km and 14 km from the negative polarity storms. As we focus on the stronger storms, those with flash densities between 0.03-0.1 flashes km^{-2} hr^{-1} (Fig 4.5), the differences become even more pronounced. At nearly every level, the positive storms exhibit stronger reflectivities. Though the difference at any point is less than a few percent, taken as a whole, these cumulative differences are noteworthy. Figure 4.6 depicts the strongest storms in our study, these storms are the most active electrically. Based on the references above these are the *most likely* to produce severe weather. While we might expect our trend of increasing polarity differences with increasing storm strength to hold true, it does so only partially. Fig 4.6b

generally shows a broader distribution than the positive storms in Fig 4.6a and in some cases a higher frequency; in other cases, the opposite is true. There are regions of Fig 4.6a that do seem to indicate a stronger storm structure, specifically, up to 5 km, where the positive storms have a higher frequency of reflectivities between 60-65 dBZ. These returns represent only a small portion of the storm volumes, and thus have extremely low absolute frequencies, only a few tenths of a percent; but represent the strongest, and presumably the most convectively active storms encountered. In fact, the only storms with an absolute frequency of greater than one-tenth of one percent are those positive storms with flash densities greater than 0.03 (Figs 4.3a and 4.4a). Reflectivities in this threshold should not be dismissed though their absolute frequency is very low; in fact these are precisely the storms we will want to isolate.

To better illustrate these polarity differences we have calculated a "frequency ratio." This number is simply the ratio of the positive frequency to the negative frequency. Since we have already normalized each individual distribution, this ratio can identify the relative differences between each of these storm types, especially in the higher reflectivities where absolute values are low. These storms with high reflectivities represent only a small portion of the total number of storms but are of primary interest to severe weather studies. Hence we try to isolate these storms with this particular ratio. Figures 4.7-4.8 show these ratios and illustrate very well the differences in the higher reflectivities (above 55 dBZ). Figure 4.7a shows that *statistically, for high flash densities, (above 0.1 flashes km^{-2} hr^{-1}) the relative frequency of reflectivities between 55-70 dBZ is five times higher from positive storms than from negative storms.* Figures 4.7b and 4.8 show similar results, though the average increase is smaller. More notably (see

45

Figure 4.8a), when flash densities are low, between 0.01-0.03 flashes $km^{-2} hr^{-1}$, there is nearly a factor of ten increase in the probability of reflectivities between 65-70 dBZ being associated with positive storms compared to negative storms. Another interesting point to note from Figure 4.8b is that generally there is not much difference (i.e. the ratios are near unity) between positive and negative storms in the low levels, but from 9 km to 14 km we see an increase in the positive frequency ratio. These results suggest there could be a difference between these positive and negative low flash density storms at elevated heights. Perhaps we are seeing the growth phase of developing strong storms. That is, these storms that are producing only a few CGs (less than three in thirty minutes) are more likely to contain enhanced reflectivities aloft *if the CGs are positive.*

a)

Combined Frequency Distribution, All Positive Storms

b)

Combined Frequency Distribution, All Negative Storms
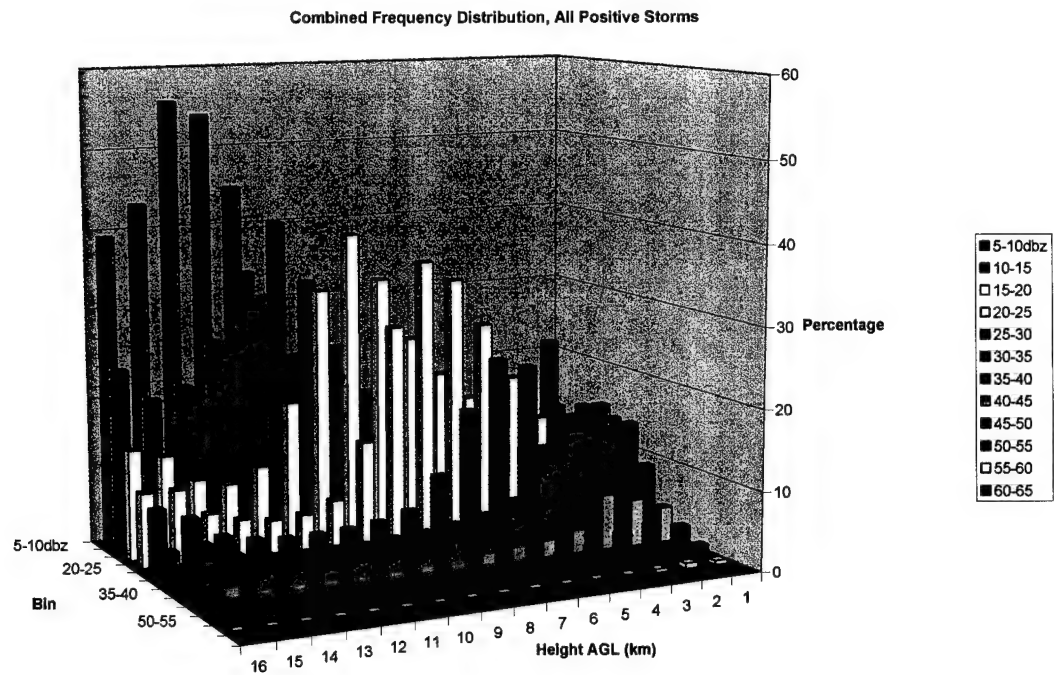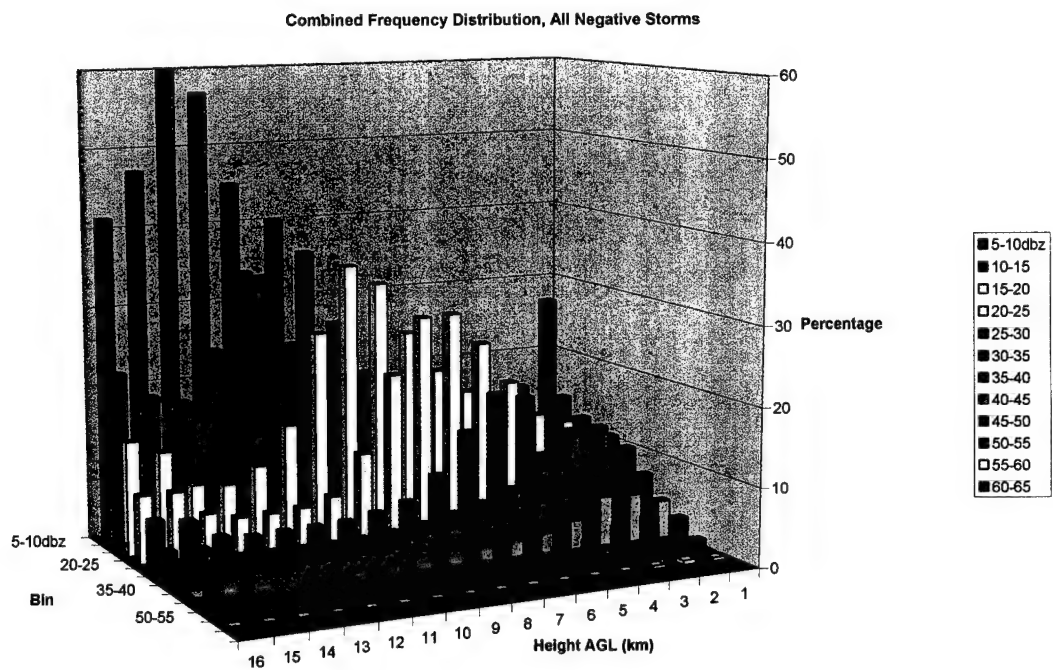
Figure 4.2: Combined Frequency Distribution for a) All positive storms, and b) All negative storms.
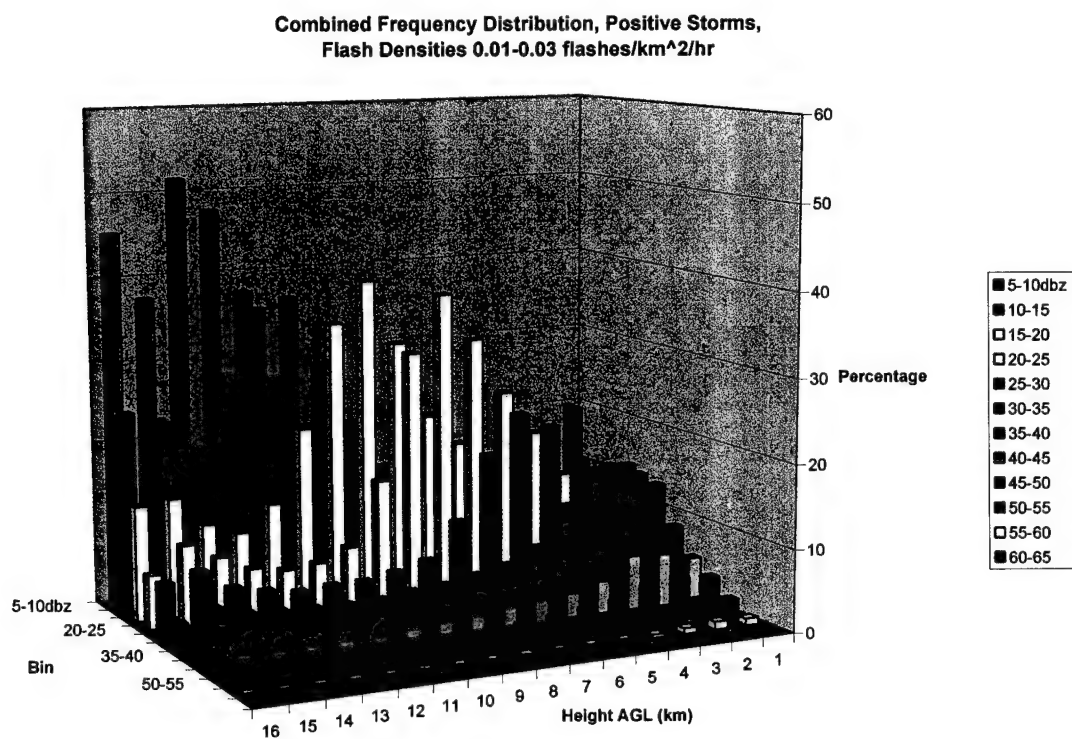
47

a)

Combined Frequency Distribution, Positive Storms,
Flash Densities 0.0-0.01 flashes/km^2/hr

b)

Combined Frequency Distribution, Negative Storms,
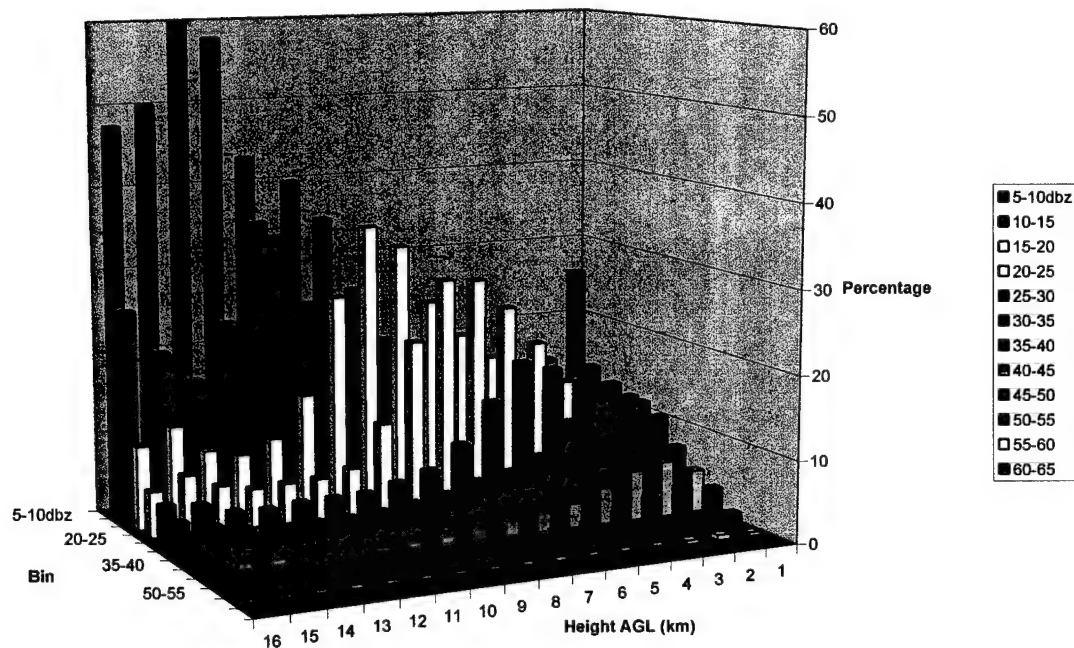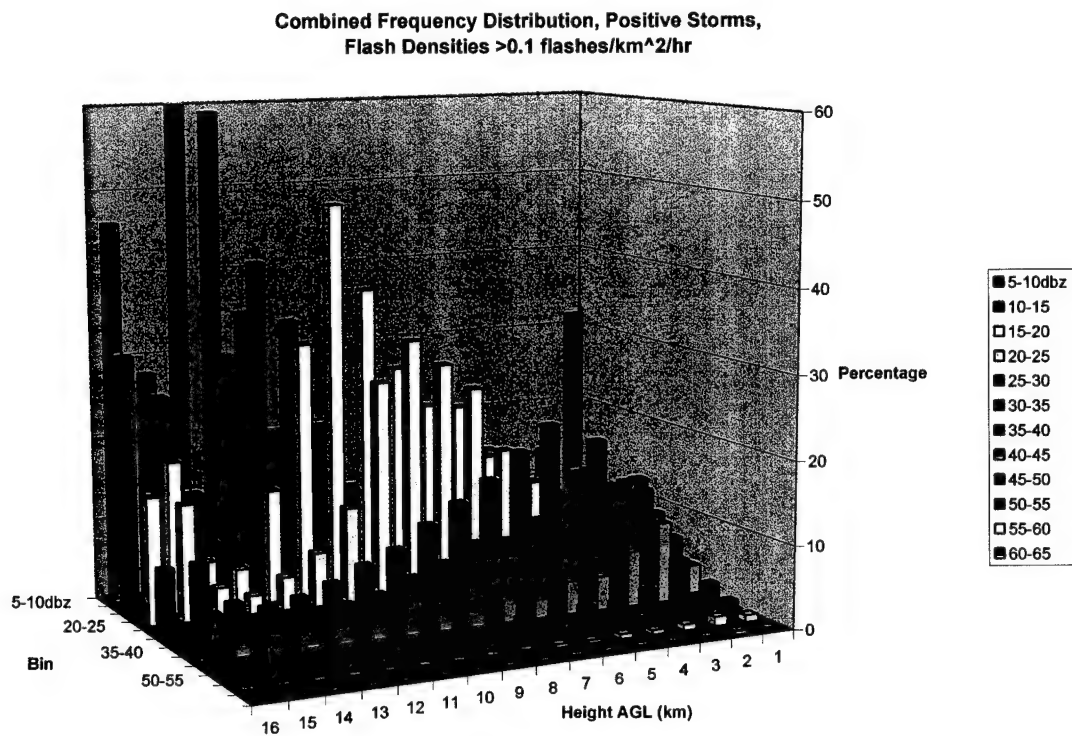**Flash Densities 0.0-0.01 flashes/km^2/hr**
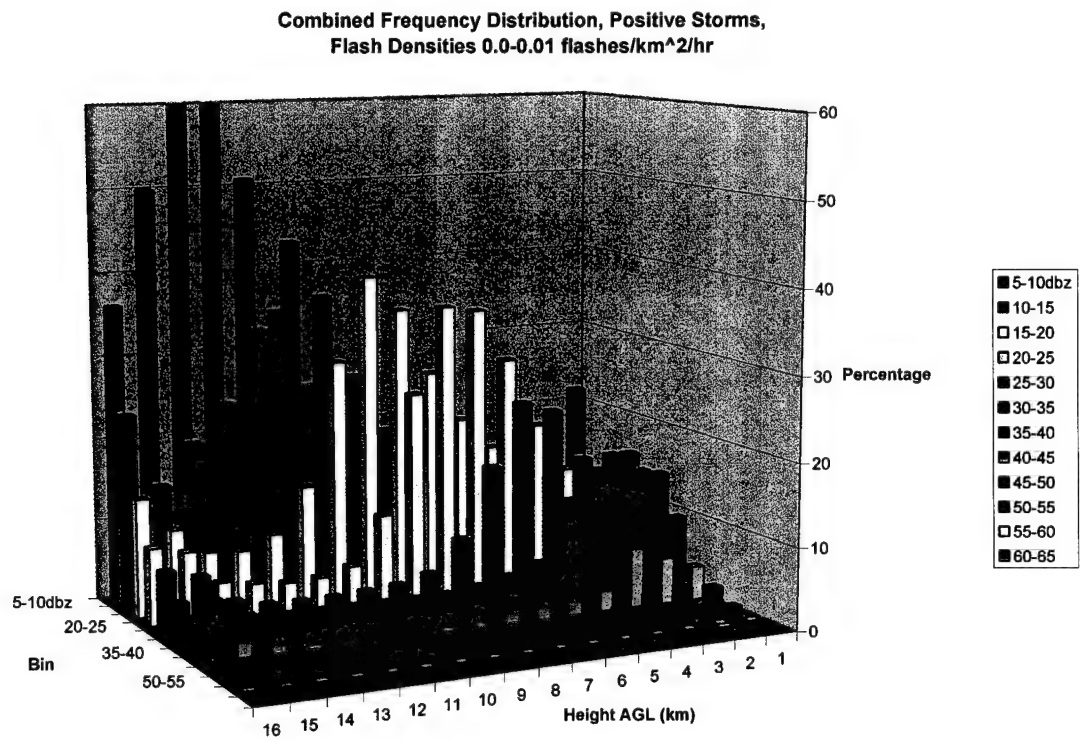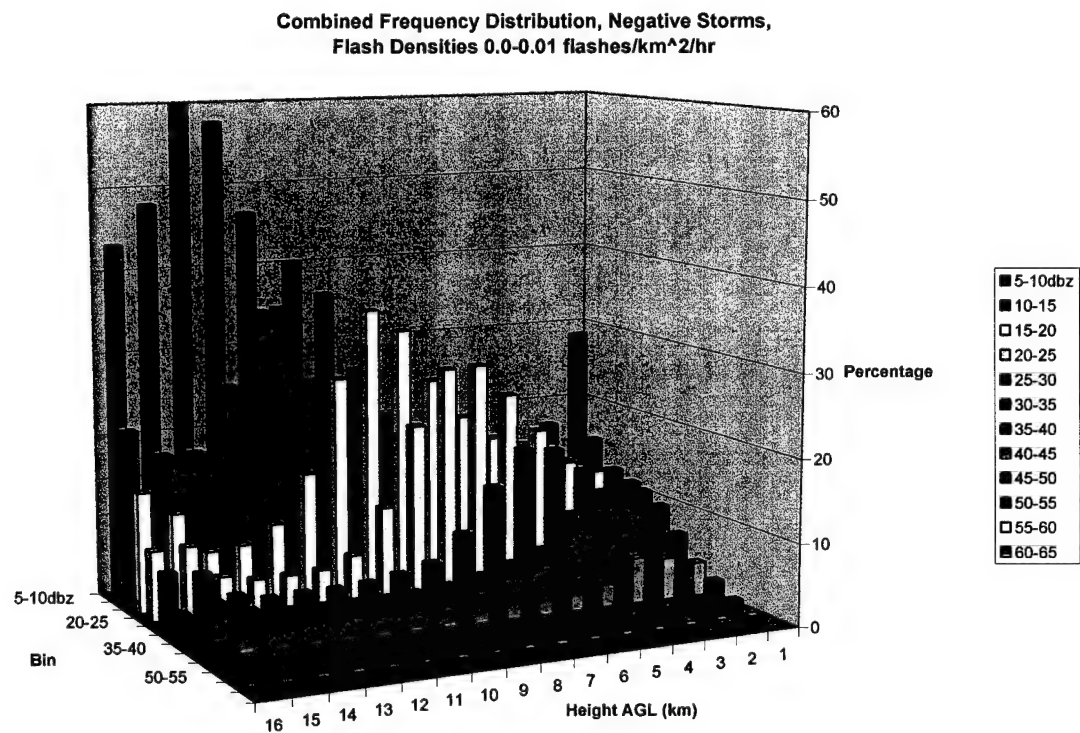
Figure 4.3: Combined Frequency Distribution with flash densities 0.0-0.01 flashes km^{-2} hr^{-1} for a) Positive storms, and b) Negative storms.

a)

Combined Frequency Distribution, Positive Storms,
Flash Densities 0.01-0.03 flashes/km^2/hr

b)

Combined Frequency Distribution, Negative Storms,
Flash Densities 0.01-0.03 flashes/km^2/hr
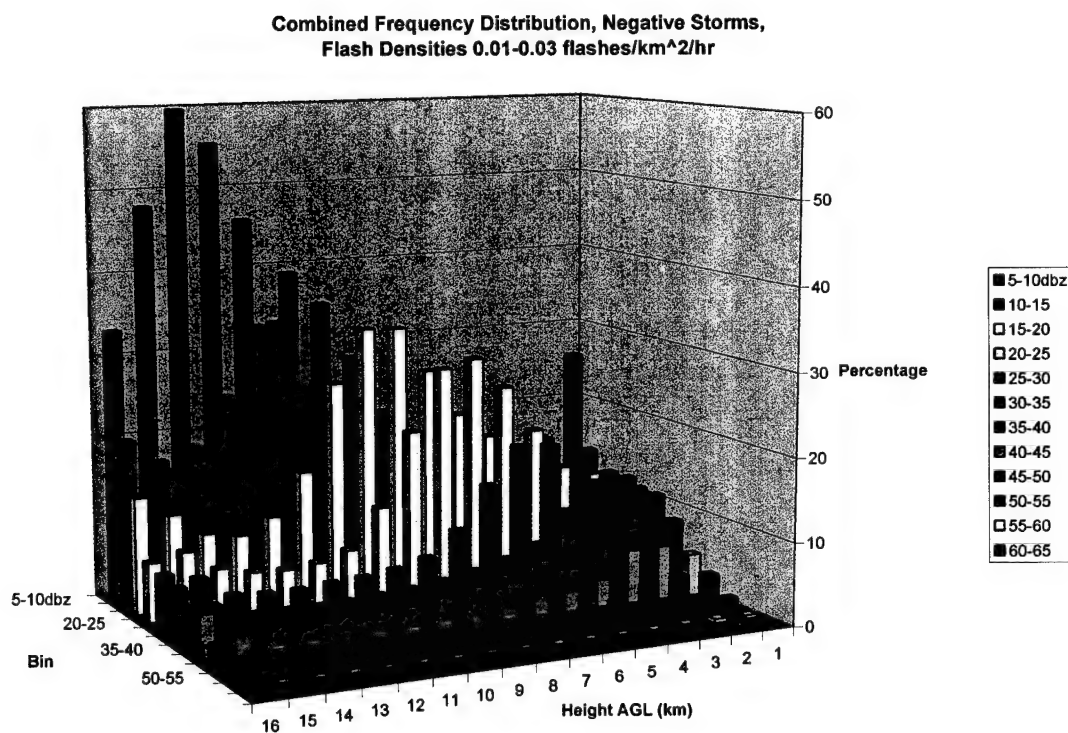
Figure 4.4: Combined Frequency Distribution with flash densities 0.01-0.03 flashes km^{-2} hr^{-1} for a) Positive storms, and b) Negative storms.
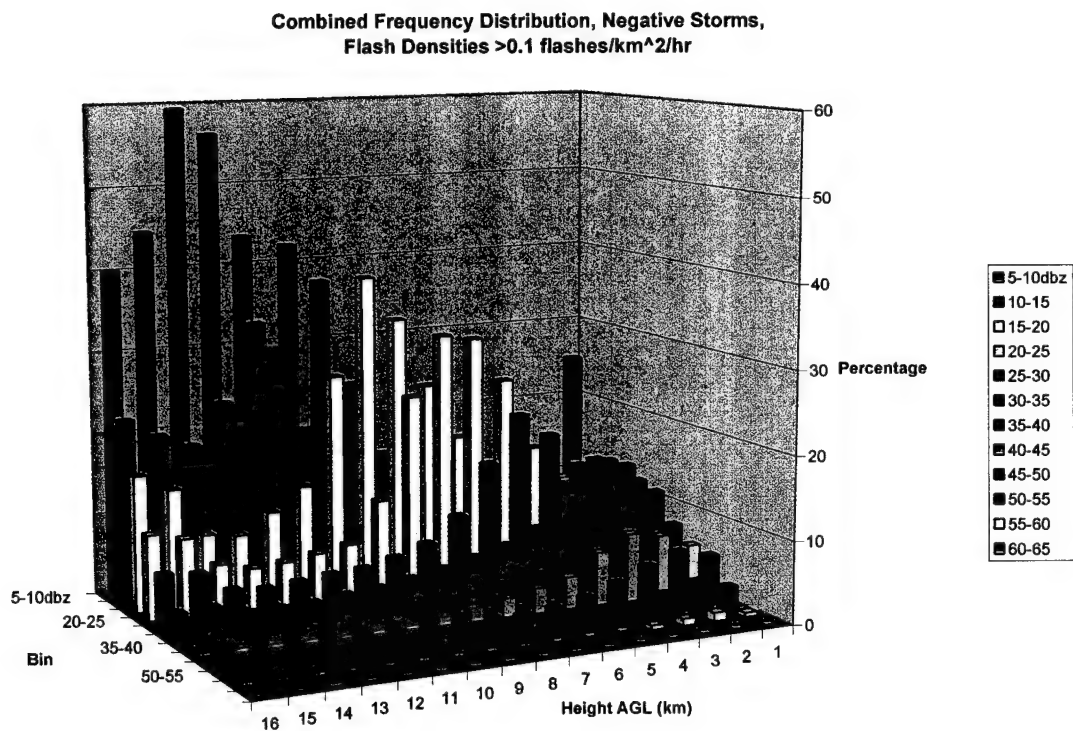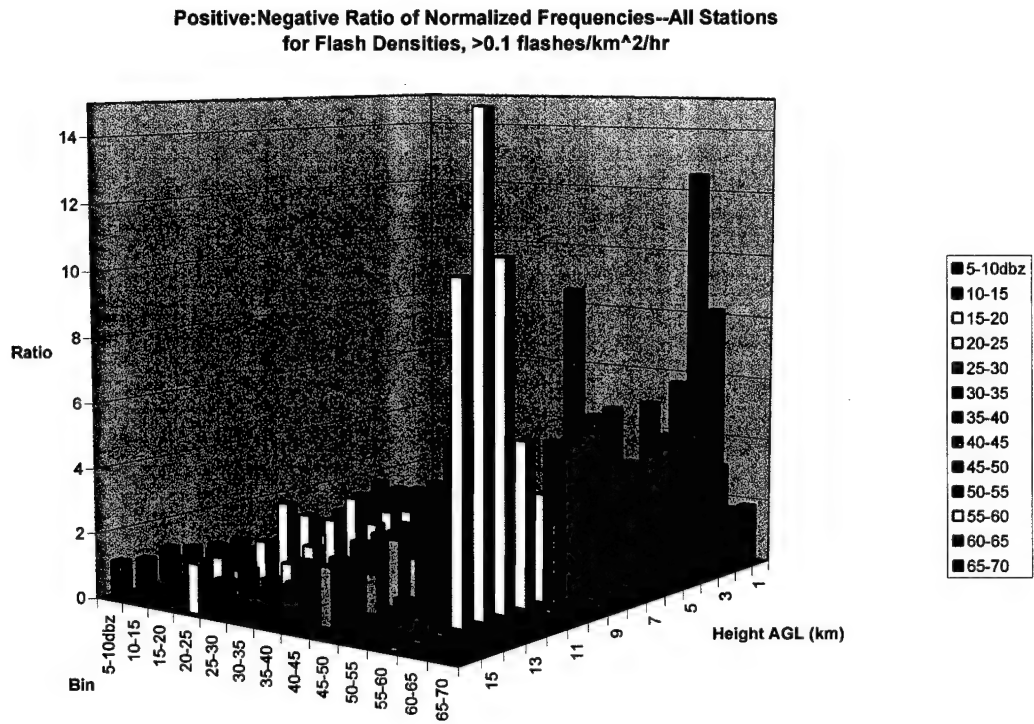
49

a)

Combined Frequency Distribution, Positive Storms,
Flash Densities 0.03-0.1 flashes/km^2/hr

b)
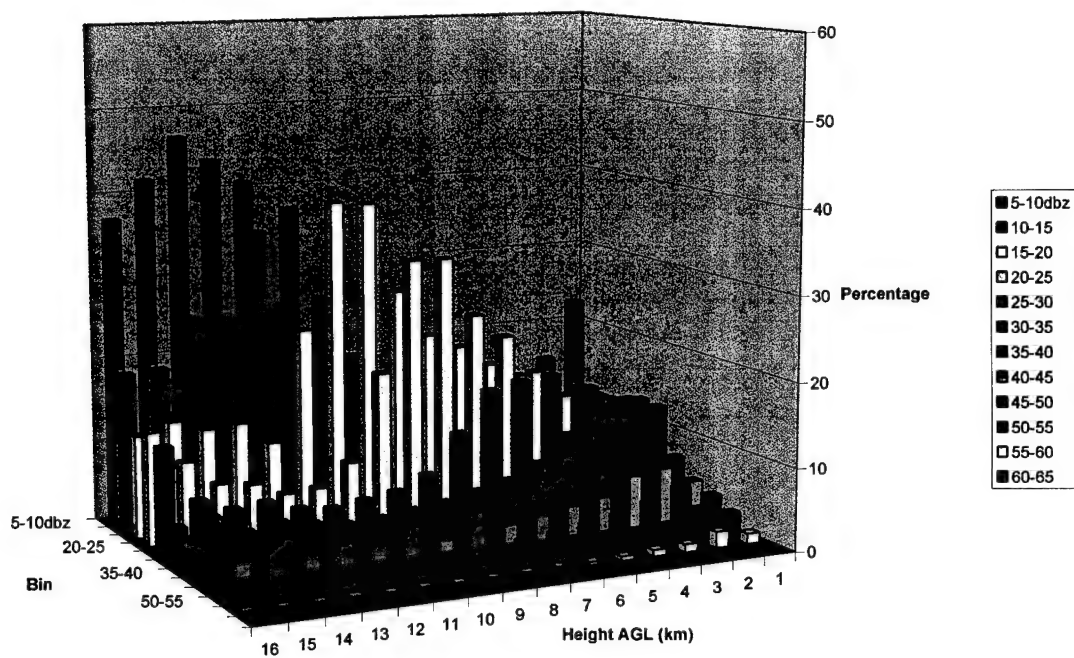
Combined Frequency Distribution, Negative Storms,
Flash Densities 0.03-0.1 flashes/km^2/hr

Figure 4.5: Combined Frequency Distribution with flash densities 0.03-0.1 flashes km^{-2} hr^{-1} for a) Positive storms, and b) Negative storms.
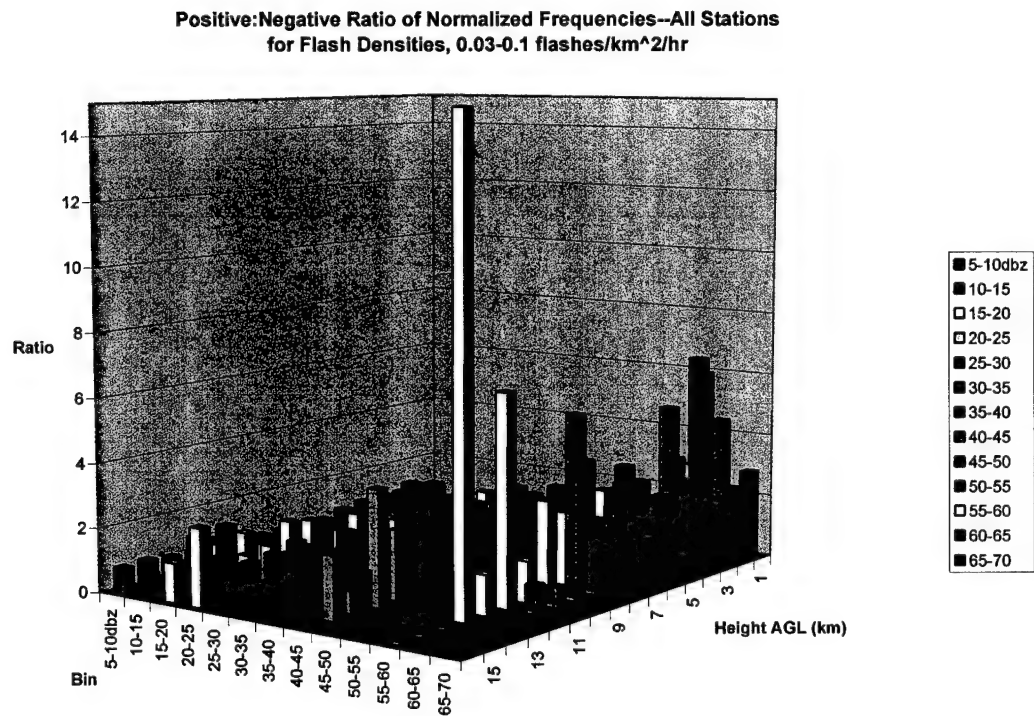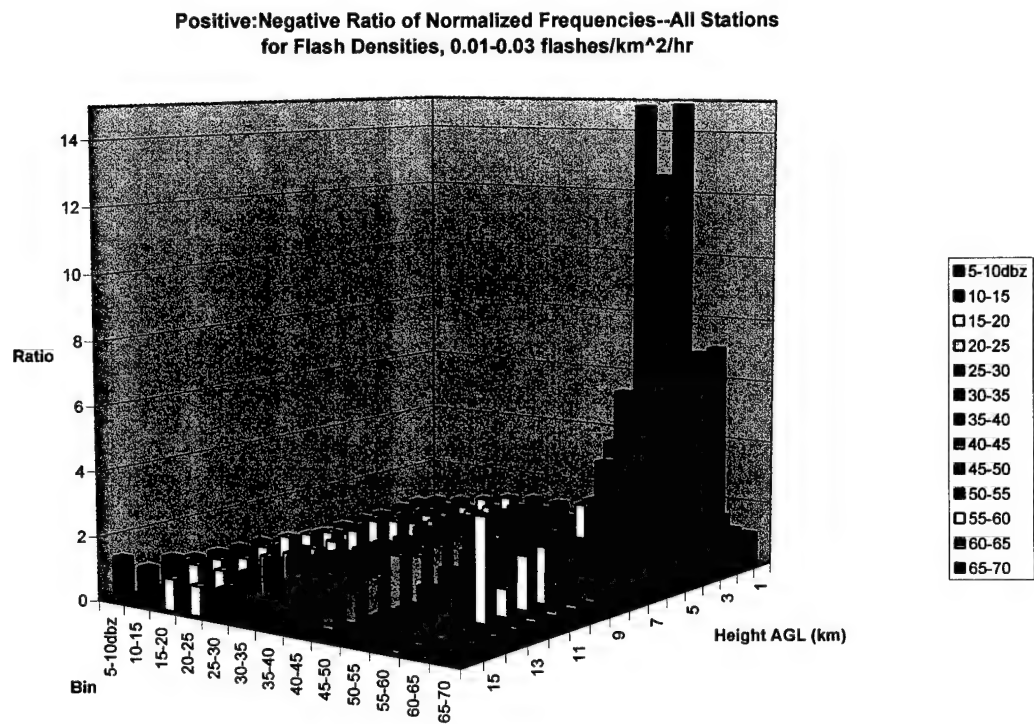
a)

Combined Frequency Distribution, Positive Storms,
Flash Densities >0.1 flashes/km^2/hr

b)

Combined Frequency Distribution, Negative Storms,
Flash Densities >0.1 flashes/km^2/hr

Figure 4.6: Combined Frequency Distribution with flash densities >0.1 flashes km^{-2} hr^{-1} for a) Positive storms, and b) Negative storms.

a)

**Positive:Negative Ratio of Normalized Frequencies--All Stations
for Flash Densities, >0.1 flashes/km^2/hr**

b)

**Positive:Negative Ratio of Normalized Frequencies--All Stations
for Flash Densities, 0.03-0.1 flashes/km^2/hr**

Figure 4.7: Positive to negative frequency ratios for storms with flash densities from
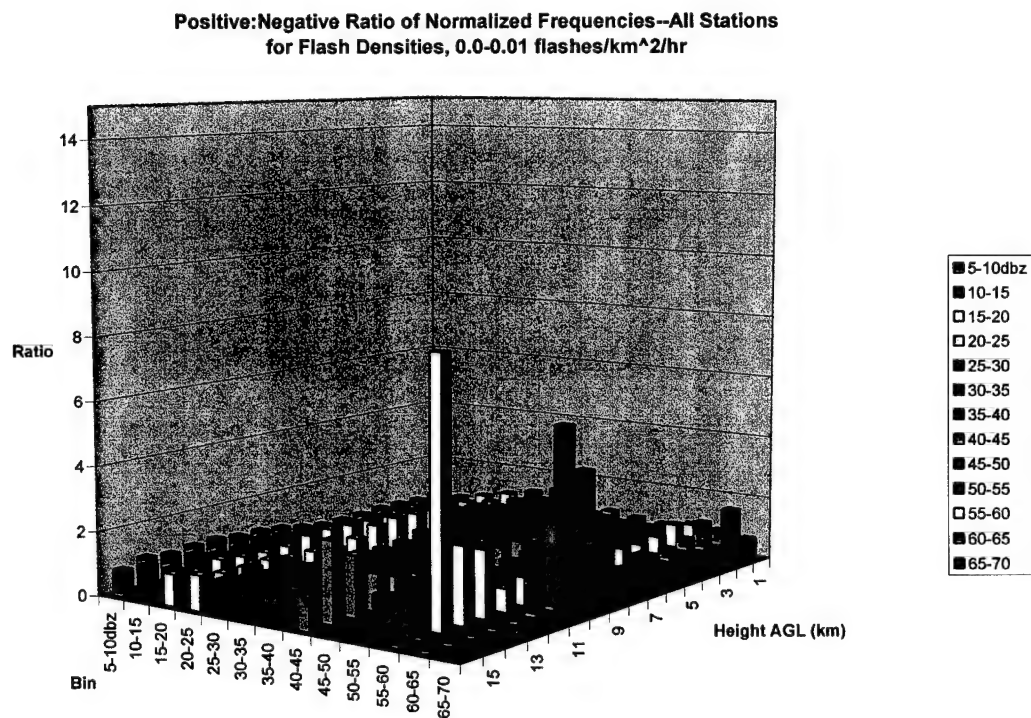a) >0.1 flashes km^{-2} hr^{-1} and b) 0.03-0.1 flashes km^{-2} hr^{-1}.

a)

Positive:Negative Ratio of Normalized Frequencies--All Stations
for Flash Densities, 0.01-0.03 flashes/km^2/hr

b)

Positive:Negative Ratio of Normalized Frequencies--All Stations
for Flash Densities, 0.0-0.01 flashes/km^2/hr

Figure 4.8: Positive to negative frequency ratios for storms with flash densities from
a) 0.01-0.03 flashes $km^{-2} hr^{-1}$ and b) 0.0-0.01 flashes $km^{-2} hr^{-1}$.

4.3 Regional Comparisons

In this section we continue our analysis by further dividing our data based on location, in an attempt to discover if the results hold true on a smaller scale. In other words, are individual station results consistent with Section 4.2 that indicated reflectivity profiles associated with positive storms were consistently stronger than for negative storms, or are there systematic latitudinal, longitudinal or individual variations in storm profiles? We compare the Rocky Mountain Front Range stations, Cheyenne, WY (KCYS), Denver, CO (KFTG), and Pueblo, CO (KPUX), with the three plains stations, North Platte, NE (KLNX), Goodland KS (KGLD), and Dodge City, KS (KDDC). We should expect differences between the Front Range stations versus those on the plains. Their proximity to the mountains affects wind flow, heating, and moisture availability. We see deeper moisture, higher shear, and higher CAPE to the east, each of which tends to produce more vigorous convection. We might also expect differences in the occurrence of positive cloud-to-ground flashes; Orville and Huffines (2000) and Zajac and Rutledge (2001) showed a higher frequency of positive flashes over the plains than over the Front Range region.

Figures 4.9-4.14 show the total positive and negative frequency distributions for each of the six radar sites. We can make a longitudinal comparison between KCYS (Fig 4.9) and KLNX (Fig. 4.12) since they are similar in latitude. In both the positive and negative cases, North Platte shows a stronger reflectivity profile. In the same sense, we can make comparisons between Denver (Fig 4.10) and Goodland (Fig 4.13), and between Pueblo (Fig 4.11) and Dodge City (Fig 4.14). These figures show the plains stations to have stronger reflectivity distributions. That is, we see higher reflectivities occurring more

54

frequently, and deeper in the storm column. It should not be surprising that storms near the eastern plains stations are more developed than those along the Front Range. The Cheyenne Ridge, the Palmer Divide and the Raton Mesa roughly coincide with the locations of Cheyenne, Denver, and Pueblo, respectively, and are formation regions for thunderstorms. Newly formed thunderstorms then advect east over the high plains by general westerly flow. The availability of moisture and CAPE causes them to grow and mature during their eastward drift resulting in deeper, more energetic storms, more capable of producing large precipitation particles. These are manifested as relatively higher reflectivities and are evident in the plains stations (Figs. 4.12-4.14).

The results of our polarity analysis from Section 4.2 do not hold true when we analyze each station individually. Polarity comparisons are not consistent from station to station. From Section 4.2, we expect positive storms to have stronger structures than the negative storms. The profiles for Cheyenne (Fig. 4.9), Denver (Fig. 4.10), and Goodland (Fig 4.13) do agree with these results; they show stronger reflectivity profiles from the positive storms versus the negative storms. However, the profiles for Pueblo (Fig. 4.11), North Platte (Fig. 4.12), and Dodge City (Fig. 4.14) show stronger reflectivities from negative polarity storms. Reasons for this are not clear, but these results are intriguing.
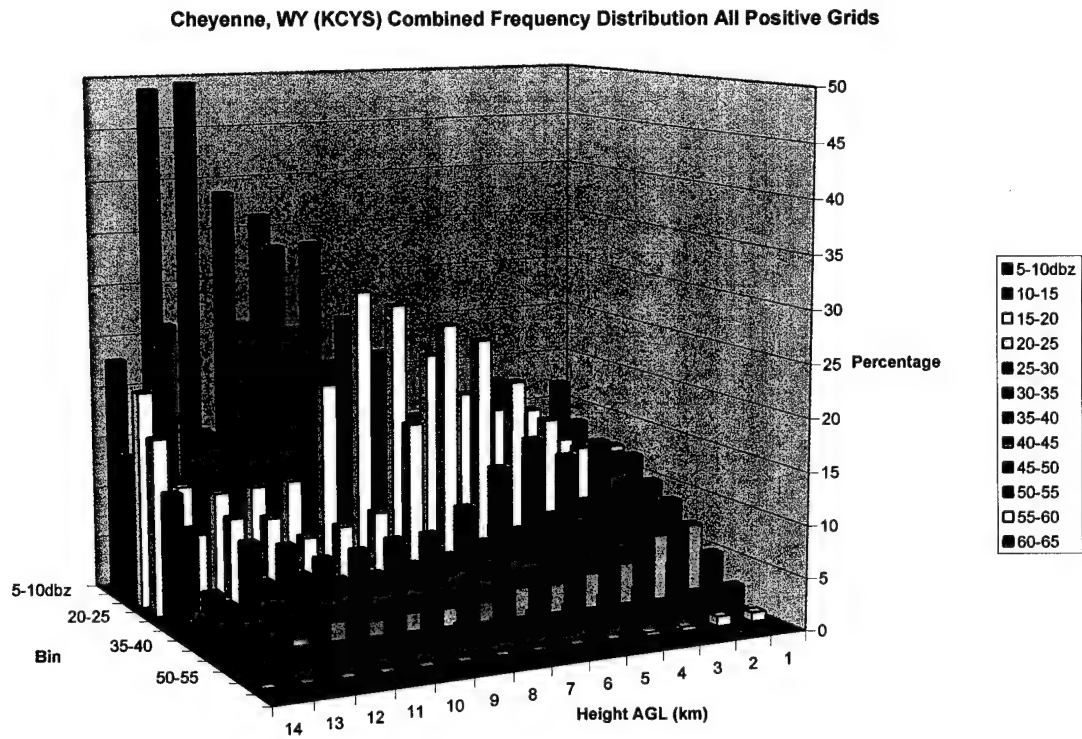
If we isolate the frequency distributions for the strongest storms, those with flash densities greater than 0.1 flashes $km^{-2} hr^{-1}$, we continue to see contradictions. We must exclude the Front Range sites, KPUX, KFTG, and KPUX from this analysis; the sample population was not large enough for positive storms in this range of flash densities to produce meaningful distributions. Hence, only considering the plains stations, we see opposite polarity relationships from these strong storms between stations. The

southernmost station, KDDC is consistent with our previous results--from Fig 4.17 it is apparent that the positive, high flash density storms produce stronger reflectivity returns at all levels than do the negative storms. Moving north to KGLD, Fig 4.16 shows a mixed relationship between positive and negative storms. In agreement with Section 4.2 and our KDDC analysis, Fig 4.16a shows a higher frequency of reflectivities in the 60-65 dBZ range from positive storms than from negative storms. But that is where the agreement ends. Reflectivities between 40-60 dBZ are more frequent at all heights in negative storms. The frequency distribution for KLNX (Fig 4.15) clearly shows a much higher frequency of reflectivities above 40 dBZ at all heights associated with the negative storms compared to the positive storms. The results from these three locations are summarized in Figure 4.18. That figure is derived from Figures 4.15-4.17. We have summed all of the frequencies above 55 dBZ at each height and plotted each of the stations. We see an apparent systematic variation with latitude, on the plains. Figure 4.18a shows that positive storms (with flash densities above 0.1 flashes km^{-2} hr^{-1}) are much stronger and deeper over Dodge City, and decrease to the north. Conversely, when we examine the high flash density negative storms, we see the northern stations are favored. We must conclude that although Section 4.2 showed positive storms are more likely to produce vigorous storms; that result does not hold everywhere in our sample.

In order to shed light on this dilemma, the first consideration is whether the sample size was large enough; small population sizes could have a statistical affect on the distributions. The sample sizes for Goodland and North Platte are actually larger than that for Dodge City and are not the source of the problem. Next we considered storm morphology as having a potential affect on the analysis. A qualitative examination of

storms occurring over our study period showed that there were a greater number of storms over KLNX than there were over KDDC. During this examination we discovered an interesting phenomena. The occurrence of Mesoscale Convective Systems, MCSs, loosely defined, was higher over KLNX than over KDDC. Upon further consideration we would expect a slightly higher climatological frequency of MCSs to the north. Though the locations are relatively close, we expect slightly less convective available potential energy (CAPE) to the north and relatively higher shear. These two factors combine to favor MCS formation over the northern portion of our study area. The occurrence of MCS or MCS-like systems may be the key to the apparent lower frequency of strong positive storms over KLNX. We pose the following hypothesis: *MCS-type systems produce cloud-to-ground lightning that statistically tends to reach ground away from the storms' convective cores.* If enough MCS generated CGs occur away form the storm's convection, the ground strikes will be distributed over a larger area. This would cause a lower flash density near the storm's core and higher flash densities away from the core. In both cases, our statistical analysis would show weaker reflectivities associated with the higher flash densities. This is a weakness with our analysis method; we cannot determine where the lightning flash originated, only where it struck ground. A possible mechanism to explain this phenomenon is the presence of a charged stratiform region. Horizontally advected charge within the cloud can provide charged channels or ducts through which a lightning flash may travel. Once drawn away from the core through these charged layers, these lightning strikes may come to ground at significant distances from the core. To examine this hypothesis more closely, we further reduce the scale of our analysis and examine individual storm structures.
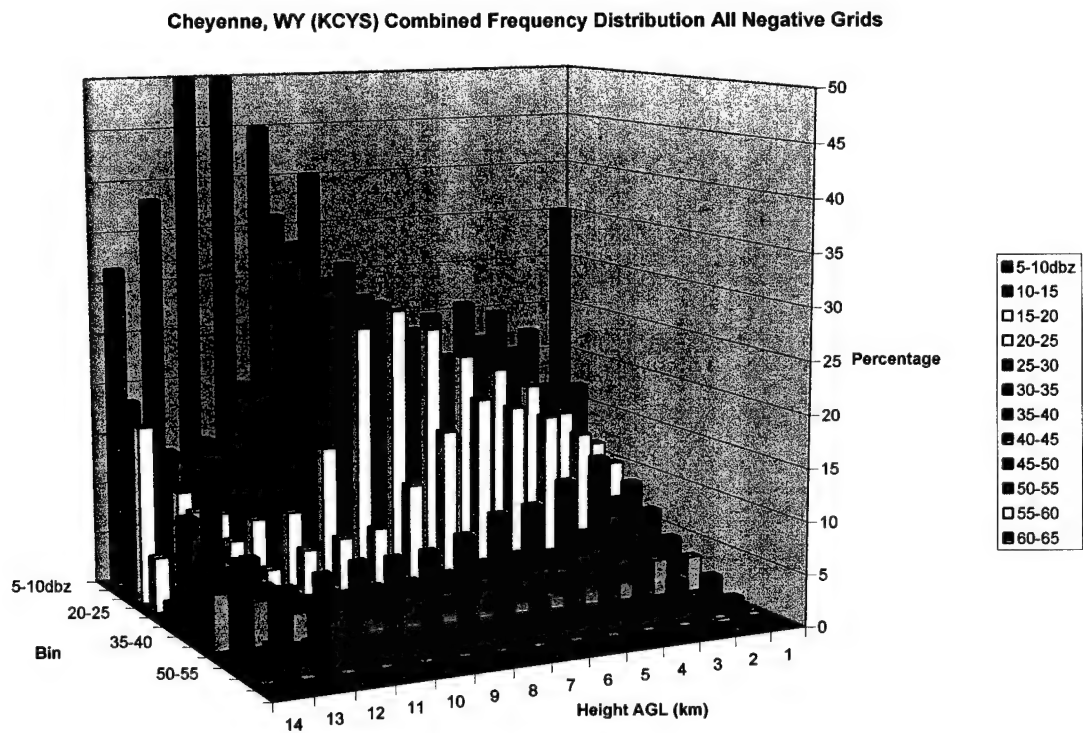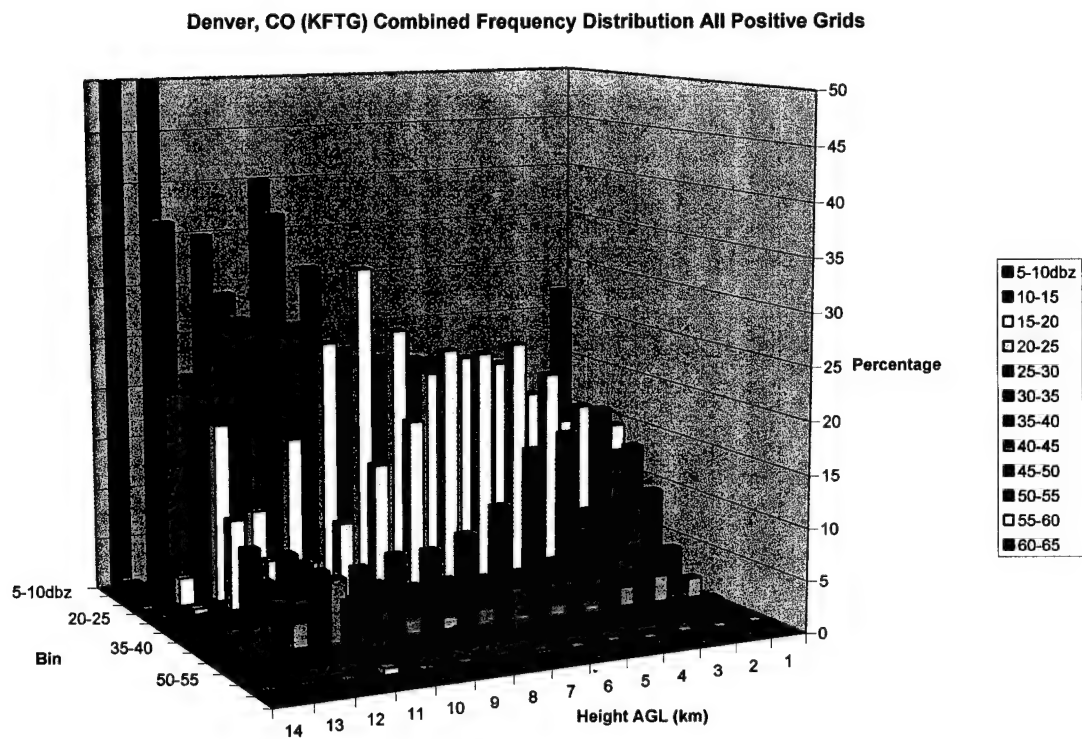
a)

Cheyenne, WY (KCYS) Combined Frequency Distribution All Positive Grids

b)

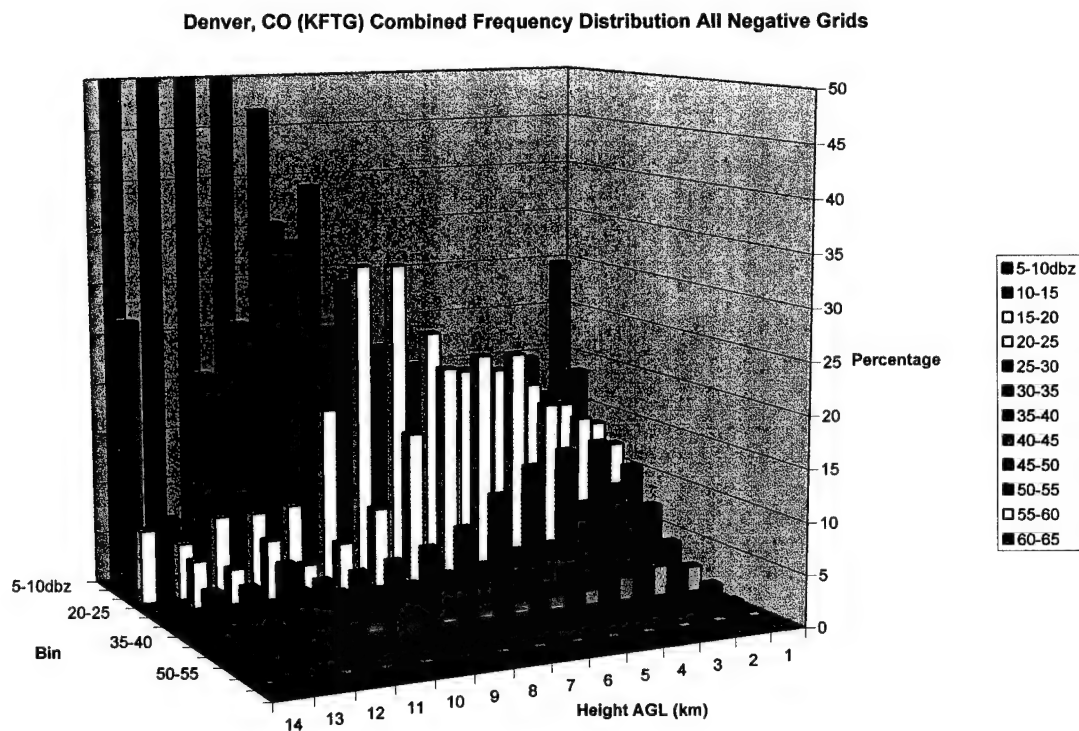Cheyenne, WY (KCYS) Combined Frequency Distribution All Negative Grids

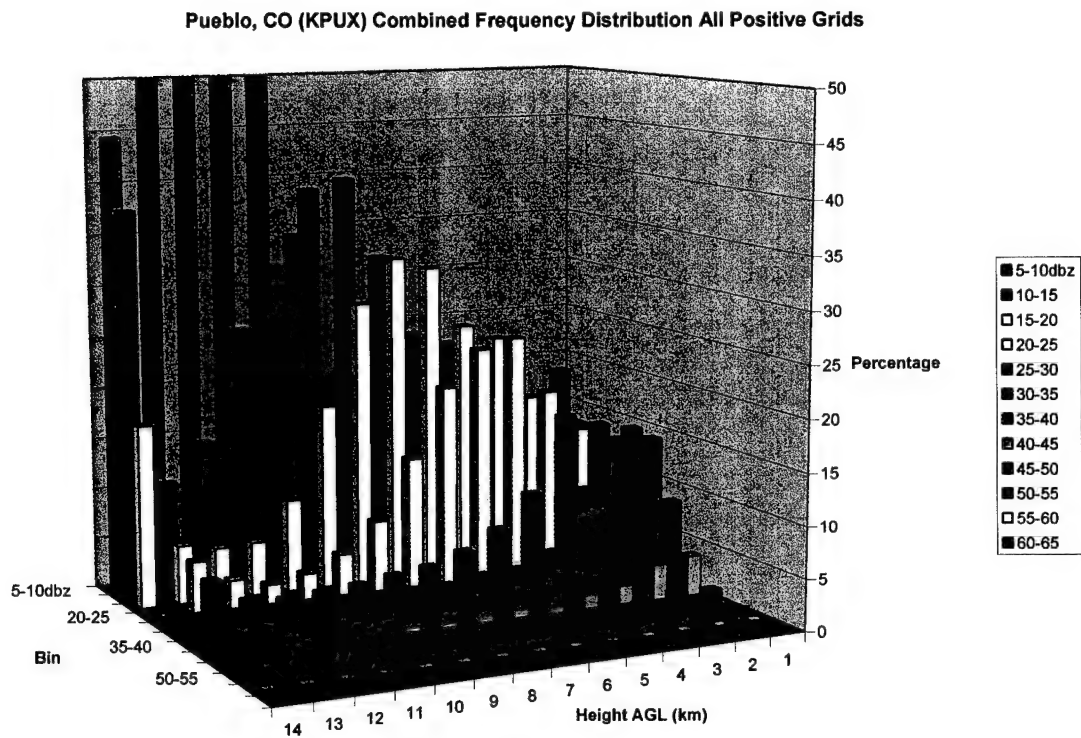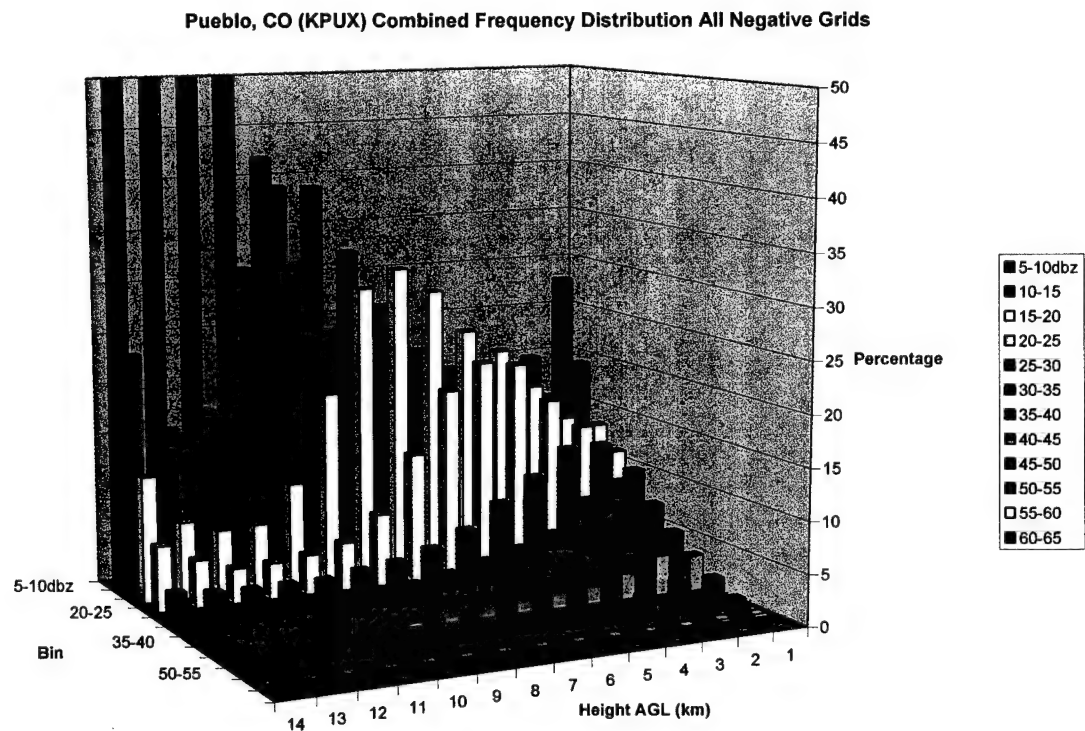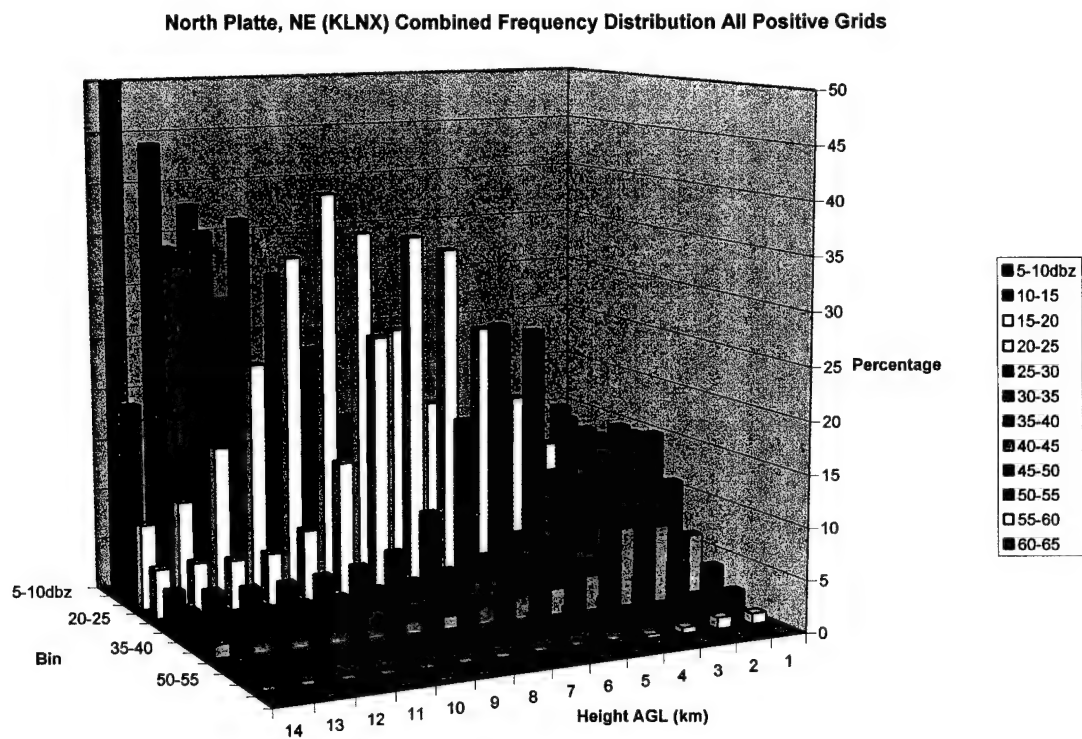Fig 4.9: Cheyenne, WY frequency distribution for a) Positive storms and b) Negative storms.
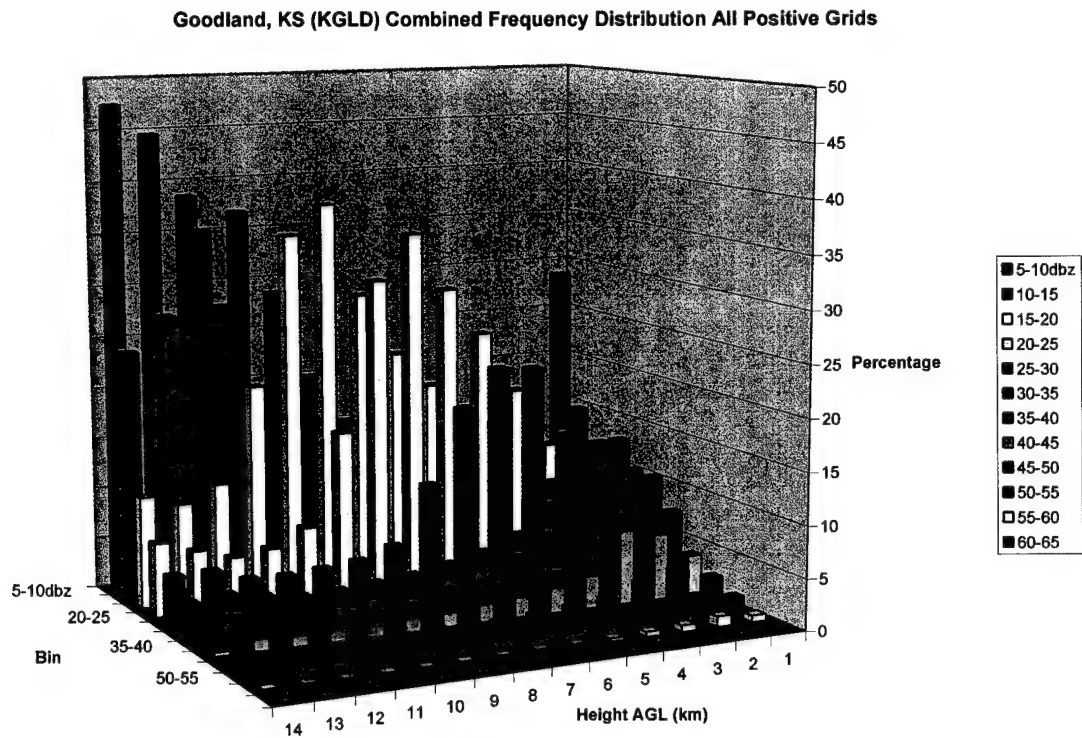
a)

Denver, CO (KFTG) Combined Frequency Distribution All Positive Grids

b)

Denver, CO (KFTG) Combined Frequency Distribution All Negative Grids

Fig 4.10: Denver, CO frequency distribution for a) Positive storms and b) Negative storms.

59

a)

Pueblo, CO (KPUX) Combined Frequency Distribution All Positive Grids

b)

Pueblo, CO (KPUX) Combined Frequency Distribution All Negative Grids

Fig 4.11: Pueblo, CO frequency distribution for a) Positive storms and b) Negative storms.

60

a)

North Platte, NE (KLNX) Combined Frequency Distribution All Positive Grids

b)

North Platte, NE (KLNX) Combined Frequency Distribution All Negative Grids
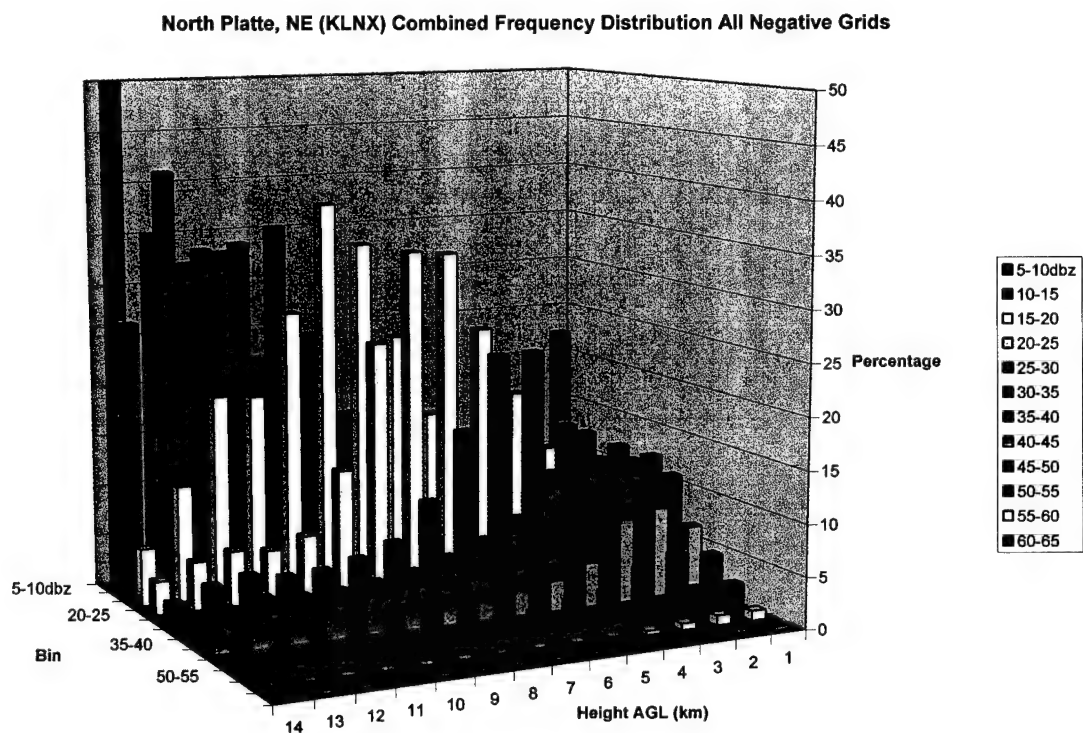
Fig 4.12: North Platte, NE frequency distribution for a) Positive storms and b) Negative storms.

61

a)

Goodland, KS (KGLD) Combined Frequency Distribution All Positive Grids

b)

Goodland, KS (KGLD) Combined Frequency Distribution All Negative Grids
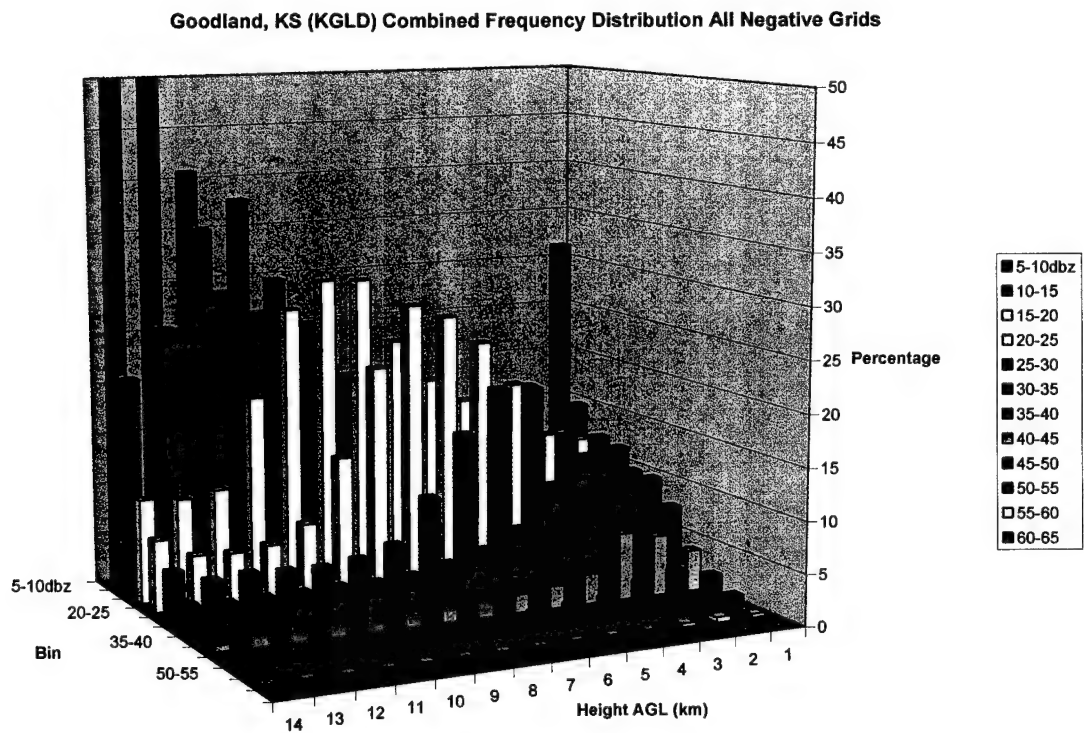
Fig 4.13: Goodland, KS frequency distribution for a) Positive storms and b) Negative storms.

a)

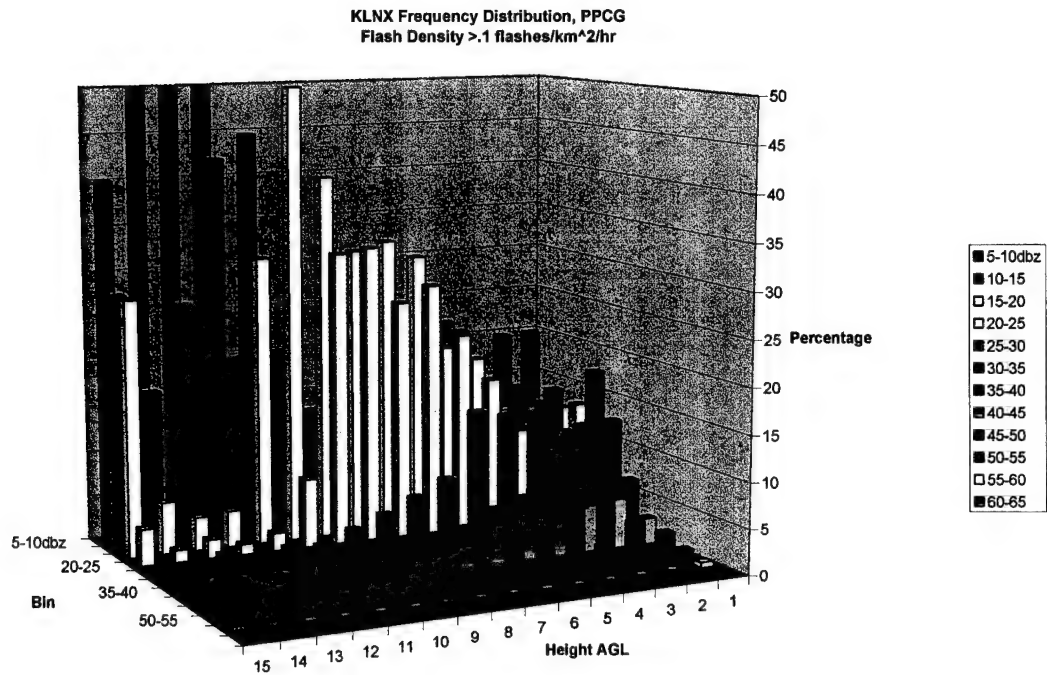**Dodge City, KS (KDDC) Combined Frequency Distribution All Positive Grids**

b)

Dodge City, KS (KDDC) Combined Frequency Distribution All Negative Grids
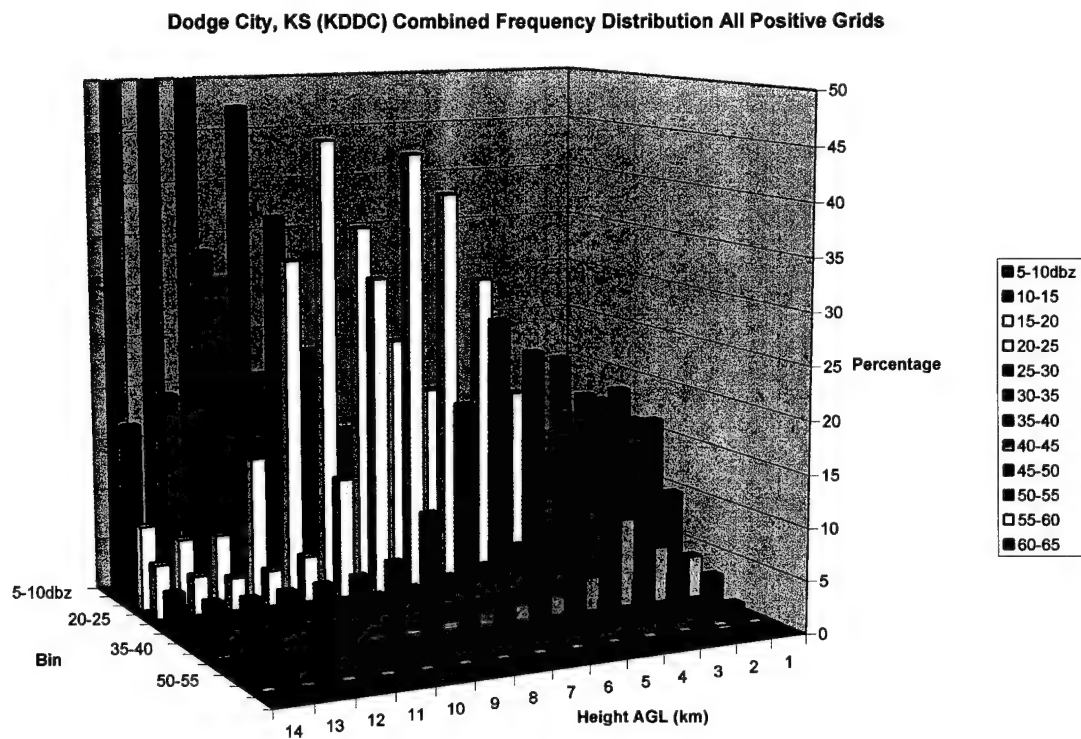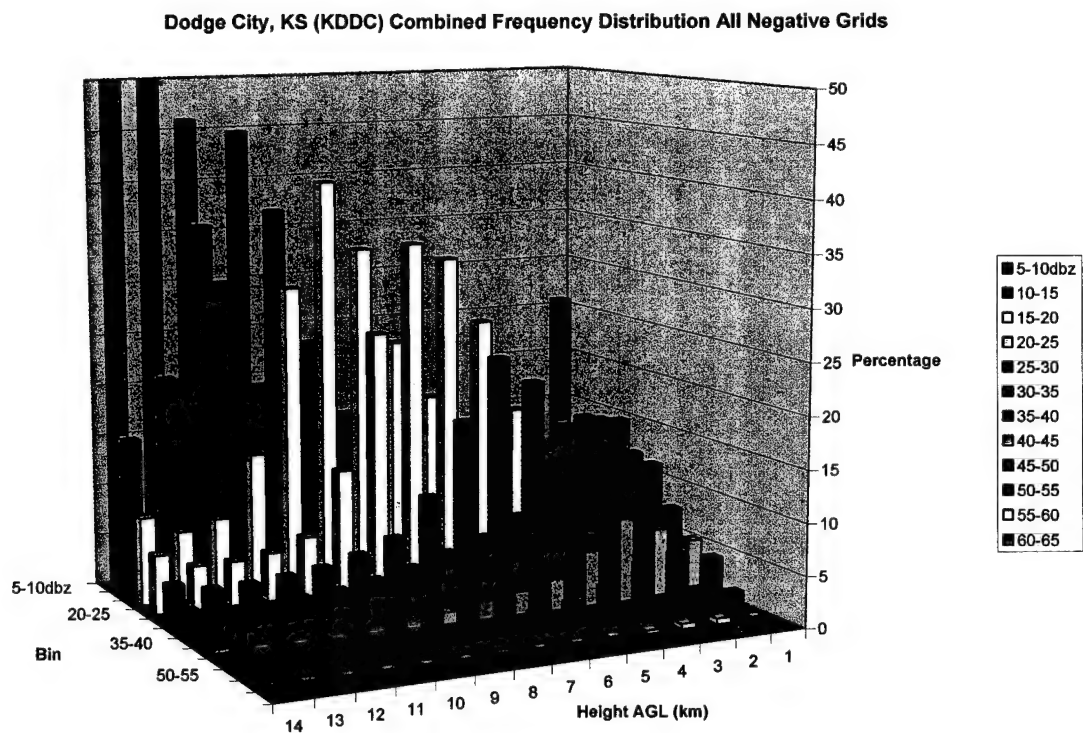
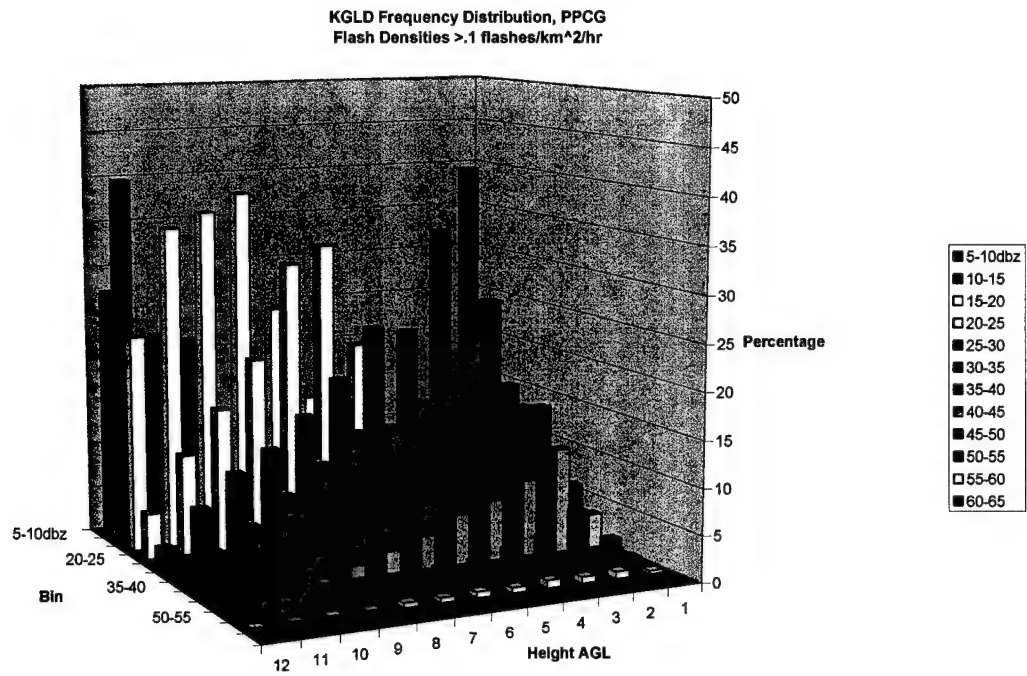Fig 4.14: Dodge City, KS frequency distribution for a) Positive storms and b) Negative storms.

63

a)

KLNX Frequency Distribution, PPCG
Flash Density >.1 flashes/km^2/hr

b)

KLNX Frequency Distribution, PNCG
Flash Density >.1 flashes/km^2/hr
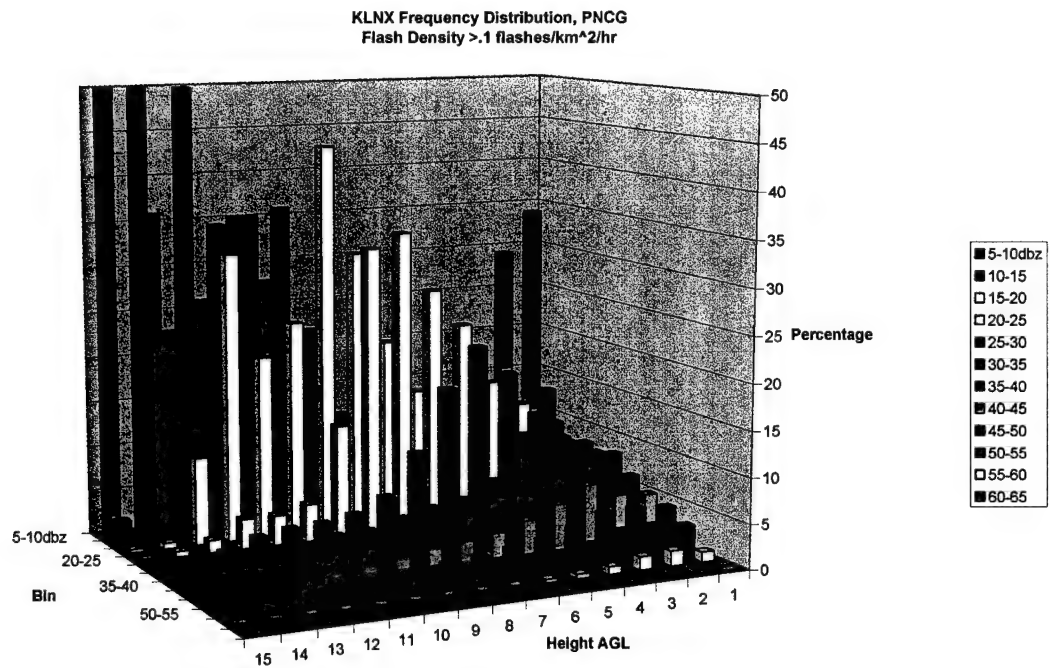
Fig 4.15: North Platte frequency distribution of storms with flash densities of
> 0.1 flashes $km^{-2} hr^{-1}$ for a) Positive storms and b) Negative storms

a)

KGLD Frequency Distribution, PPCG
Flash Densities >.1 flashes/km^2/hr

b)

KGLD Frequency Distribution, PNCG
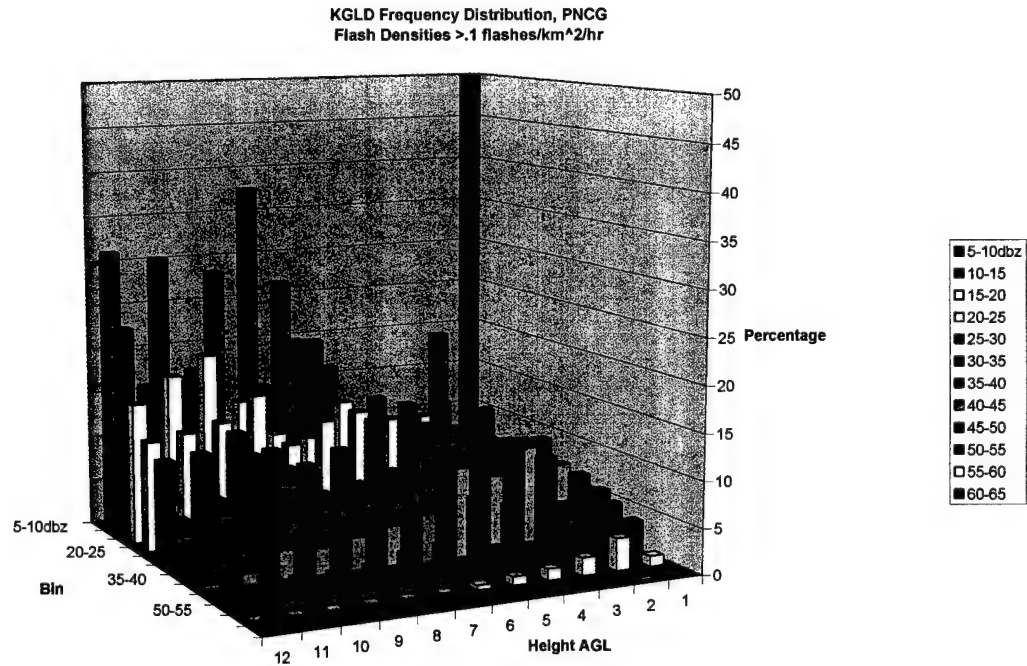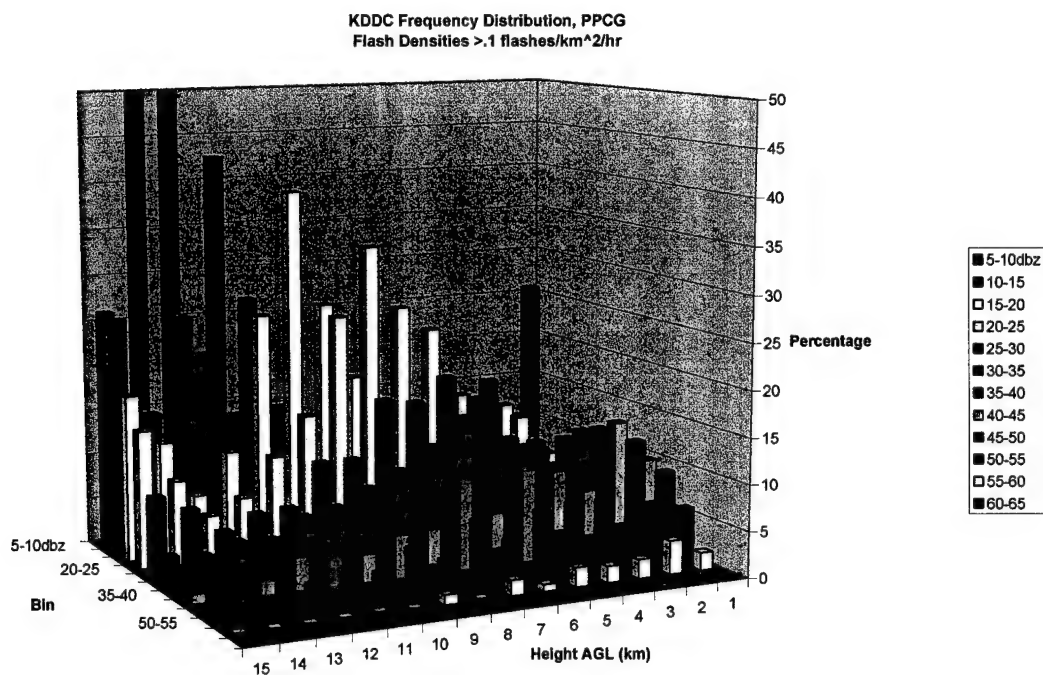**Flash Densities >.1 flashes/km^2/hr**

Figure 4.16: Goodland frequency distribution of storms with flash densities of > 0.1 flashes $km^{-2} hr^{-1}$ for a) Positive storms and b) Negative storms
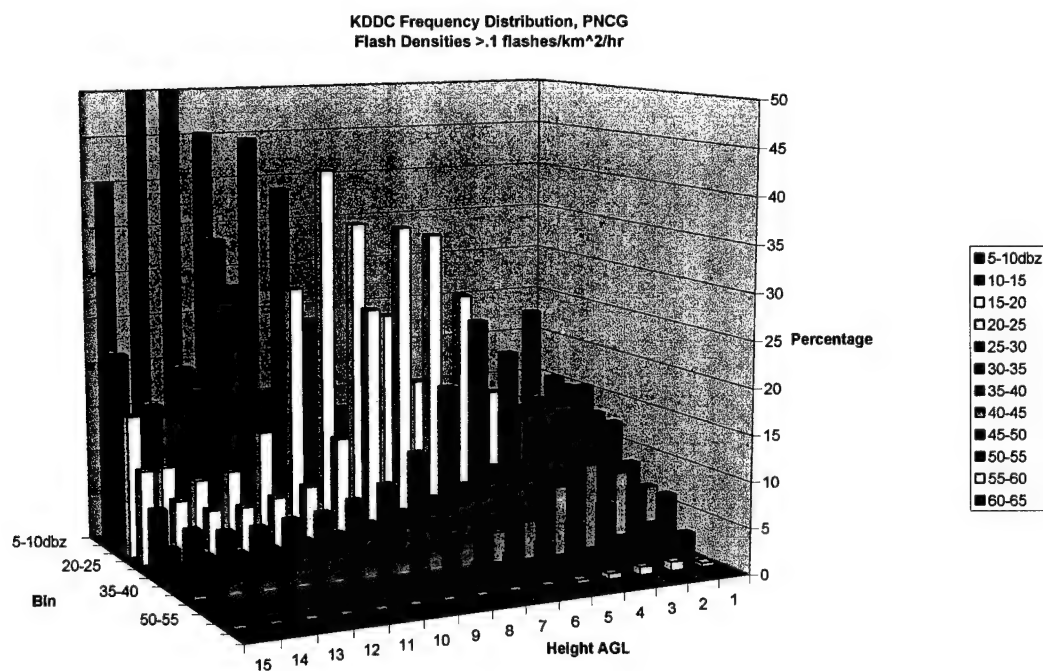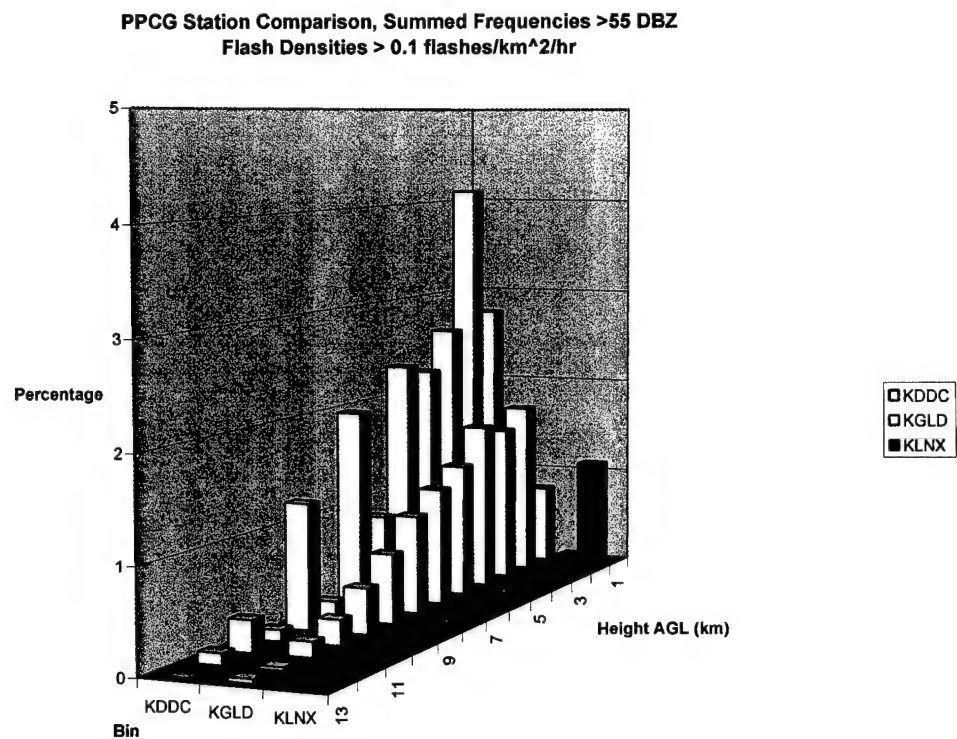
a)

b)

Figure 4.17: Dodge City frequency distribution of storms with flash densities of > 0.1 flashes $km^{-2} hr^{-1}$ for a) Positive storms and b) Negative storms

a)

PPCG Station Comparison, Summed Frequencies >55 DBZ
Flash Densities > 0.1 flashes/km^2/hr

b)

PNCG Station Comparison, Summed Frequencies >55 DBZ
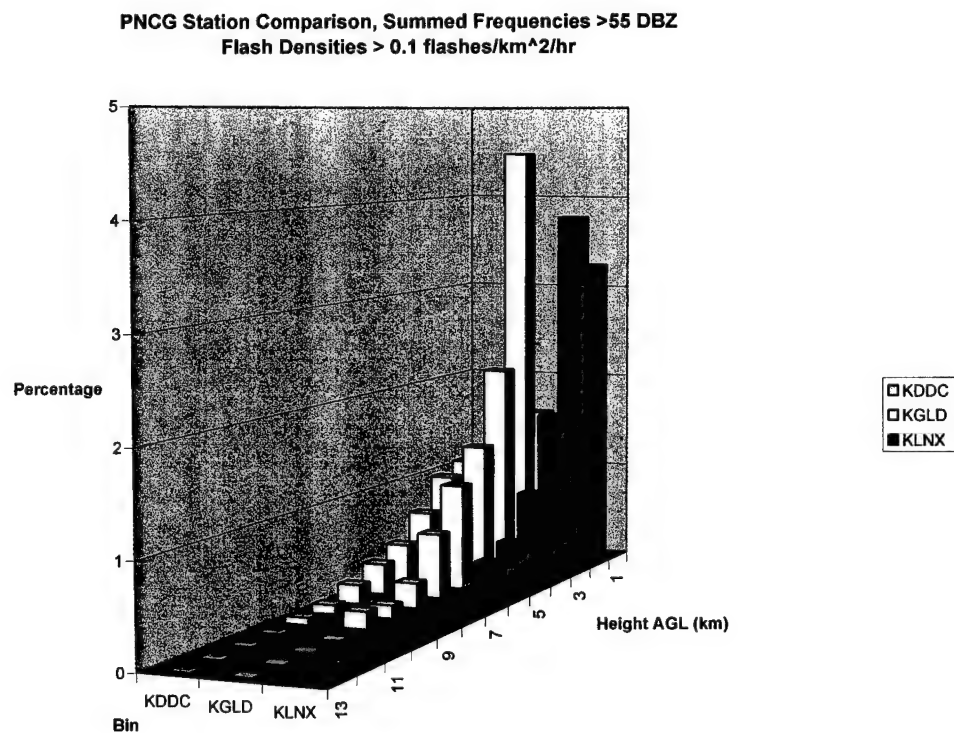**Flash Densities > 0.1 flashes/km^2/hr**

Figure 4.18: Latitudinal comparison of High Plains stations, Dodge City, Goodland, KS, and North Platte, NE for a) Positive storms and b) Negative storms.

4.4 Storm Scale Analysis

4.4.1 Introduction

One advantage to our analysis method discussed in Section 4.1 is that it can be applied to individual storms. This section examines three separate storms, a supercell, and two mesoscale convective systems (MCS) in order to shed light on the hypothesis presented at the end of Section 4.3. These storm reflectivity profiles will support our conclusion from the previous section. All three cases were from upper plains location in Kansas and Nebraska, two taken from Goodland, KS and one from North Platte, NE. This section will show the utility of this method on storm scale analysis. Since we are now looking at individual storms, we will refer to positive and negative *grid boxes* in our discussion. As such, we will be able to infer differences in reflectivity profiles between life cycle phases.

4.4.2 Jun 29, 2000 Supercell, Goodland, KS

The 29 Jun case was the highlight of the STEPS campaign. This right moving supercell lasted for over four hours and produced a tornado and golfball size hail. Figures 4.19-4.21 show the storm structure and movement, with ten minute CG lightning locations overlaid. Throughout its life, the storm produced predominately positive CG lightning. In its early stages however, this storm produced very little CG lightning, though the reflectivities indicate vigorous convection (Fig 4.19-4.21). This storm generated so little negative CG lightning, we could not calculate meaningful distributions for any negative flash densities above 0.01 flashes km^{-2} hr^{-1}. It is important to note that

the storm was producing copious intracloud flash rates during this period (P. R. Khreibel, personal communication).

The frequency distributions for this case are striking. Figure 4.22a shows a significant percentage of reflectivities above 55 dBZ in the portions of the storm that were producing positive flash densities greater than 0.1 flashes km^{-2} hr^{-1}. This distribution shows this storm produced reflectivities greater than 55 dBZ above 13 km. In fact, below 7 km, nearly a third of the pixels were above 55 dBZ. On a storm scale, this suggests *the highest flash densities were located in and around the storm core*. Figures 4.19-4.21 confirms this and also indicates that the 29 June supercell was not horizontally extensive. Figures 4.22b and 4.23a show weaker, yet still vigorous reflectivities associated with lesser positive flash densities. From Figure 4.23b (those grids with the lowest flash densities), we see a distinct reflectivity maximum aloft. The maximum is well defined in the mid levels, near 7 km. Figure 4.23a also shows evidence of this maximum from the bimodal structure of the 55 dBZ reflectivity bin, with a peak near 7 km. Notably, Fig. 23b shows a higher incidence of reflectivities between 65-70 dBZ in the upper levels, above 6 km, than do the grids with higher flash densities (Figs. 4.22 and 4.23a). This figure suggests that *the periods when the supercell was producing very low positive CG rates occurred during its developmental stage, when large particles, likely hail, were suspended aloft by strong updrafts*. Conversely, Fig 4.24 shows the low negative flash density grids. We see no elevated reflectivities, rather we see maximum of reflectivities above 55 dBZ at low levels. We might infer that these low negative signatures occur in the dissipating phase of the storm, when the cloud is raining out.

4.4.3 Jun 29, 2000 MCS, North Platte, NE

This case is from the same day and approximately the same time as the supercell case above. This MCS formed a convective line stretching northeast from the Colorado, Nebraska, Kansas border intersection. It was along this line, to the southwest that the supercell formed. As such, we are able to compare differences between a relatively compact supercell against an extensive MCS under similar conditions. This storm also produced a tornado and greater than 1 in. hail, but it produced predominately negative cloud-to-ground lightning.

Figures 4.25-4.27 show the reflectivity profiles for this MCS. This storm did not produce clusters of cloud-to-ground lightning so that flash densities remained below 0.1 flashes km^{-2} hr^{-1}. Examination of Figures 4.25-4.27 demonstrates significant differences between the supercell and the MCS. These figures show the frequency distribution for positive and negative grids with flash densities between 0.03-0.1, 0.01-0.03, and 0.0-0.01 flashes km^{-2} hr^{-1}, respectively. Figure 4.25a displays an elevated reflectivity maximum which implies precipitation sized particles were suspended aloft and not falling out. This upper maximum is revealed in positive grids and provides further evidence that positive CGs tend to be associated with developing convection. This conclusion will require additional study and will be a recommendation for further research. We see a much weaker reflectivity distribution in general and find that the strongest reflectivities are found in Fig 4.26a, those grids with positive flash densities between 0.01-0.03 flashes km^{-2} hr^{-1}. The reflectivities here represent the strongest phase of the storm, but they are associated with low flash densities. This supports our hypothesis as it suggests CG

strikes are not going to ground near the storm core. Likewise, the highest flash density grids (Fig. 4.25) provide evidence that the strikes are going to ground away from the storm's convective center.

4.4.4 22 Jun 2000 MCS, Goodland, KS

Another well organized MCS, this case developed along the Colorado-Kansas border and produced a predominance of positive CGs. Hail greater than 1 inch in diameter (also experienced by the author) was reported with these cells along with surface winds up to 30 m/s. A brief, weak tornado was reported around 1800 MST.

Figures 4.28-4.31 show the reflectivity profiles for the 22 Jun MCS. Figures 4.28 and 4.29 show the positive grids for each of the flash densities studied. Figure 4.28a shows CGs are not going to ground below the core. The highest reflectivities sampled are indicative of the storm core and are captured in Figures 4.28b and 4.29a. These observations also support our conclusion from Section 4.3, that convective systems with extensive stratiform regions can channel lightning flashes to ground away from the convective center, where the majority of the flashes are likely to originate. Figures 4.29b-4.31 are generally weaker on average and have reflectivity maximums in the low levels suggesting they are occurring in precipitating grids.

4.4.5 Discussion

Though we have only examined three individual storms, their profiles support our hypothesis that charged stratiform regions within a convective system possibly strongly influence the location of CG flashes. The tightly contained supercell produced vigorous

convection, and lightning discharges preferentially struck ground very near the convective core. MCSs on the other hand, have a greater horizontal extent and can produce complex charge structures within the system. Charged regions throughout the system can provide favorable paths for lightning discharges to occur. This situation will limit our analysis. Our data show that negative CG lightning grids tend to have reflectivities with low level maximums and suggest that negative CGs are more likely to occur in or around rain shafts. Our findings also indicate that developing convection tends to be associated with positive strikes compared to negative flashes.
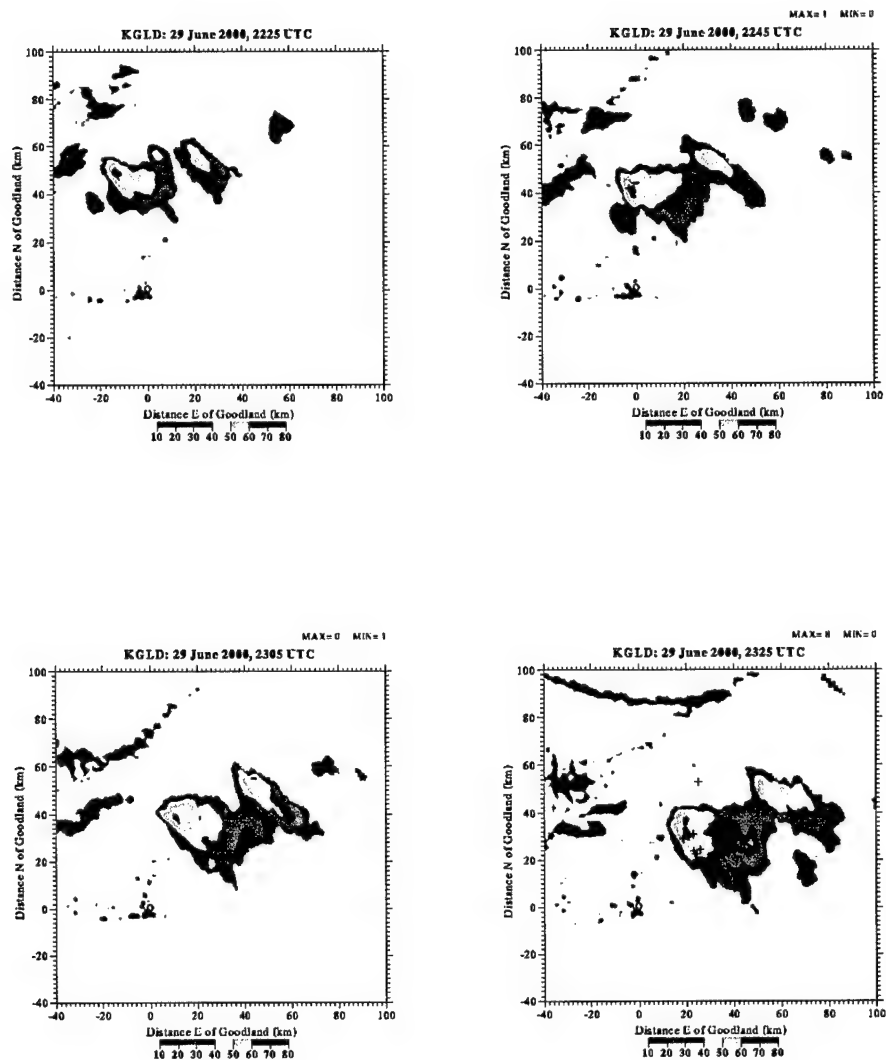
Figure 4.19: 29 Jun 2000 (2225-2325 UTC) time series of reflectivities with cloud-to-ground lightning flashes overlaid; "+" indicates a positive CG, "-" represents a negative flash. "MAX" ("MIN") indicates the number of positive (negative) CGs over the ten minute period.
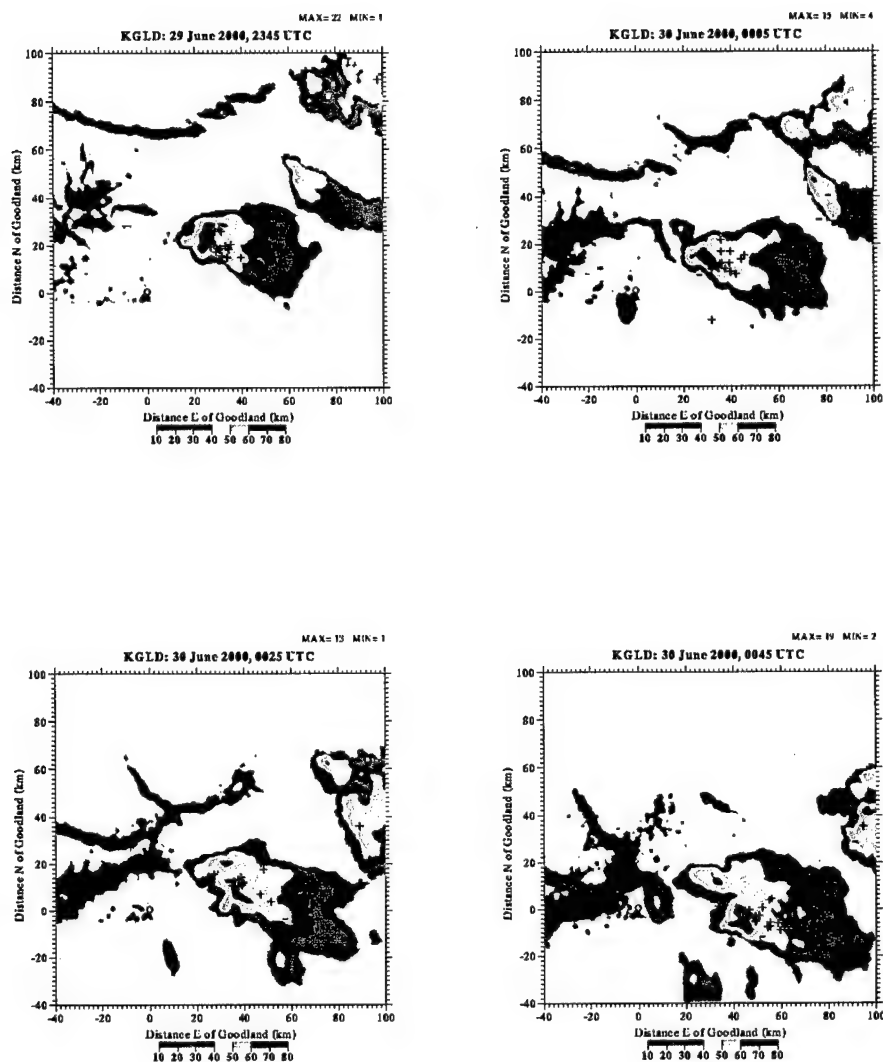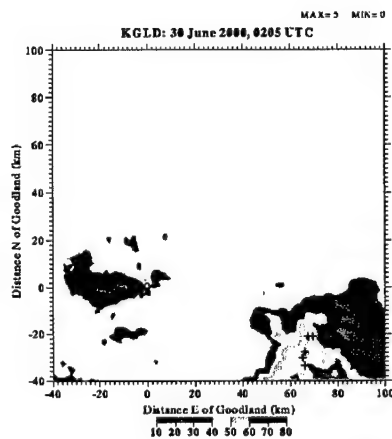
Figure 4.20: 29 Jun 2000 (2345-0045 UTC) time series of reflectivities with cloud-to-ground lightning flashes overlaid; "+" indicates a positive CG, "-" represents a negative flash. "MAX" ("MIN") indicates the number of positive (negative) CGs over the ten minute period.
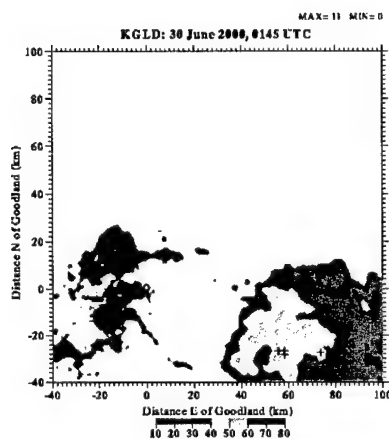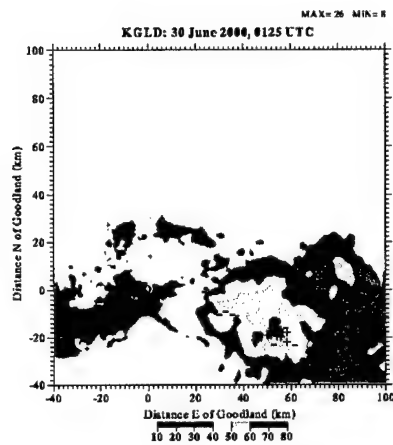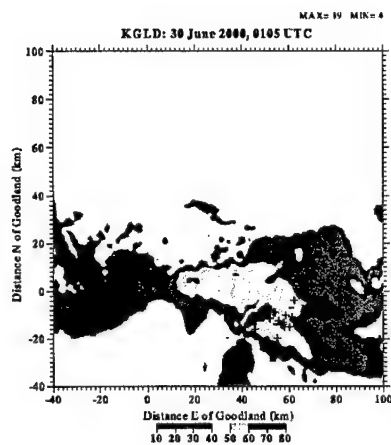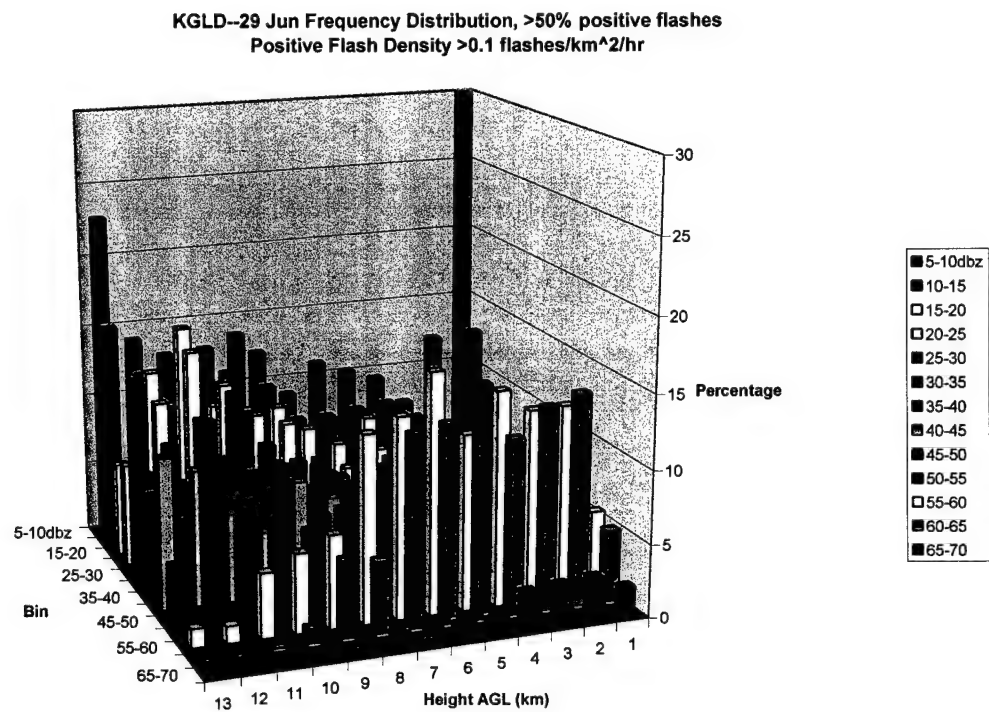
Figure 4.21: 29 Jun 2000 (0105-0205 UTC) time series of reflectivities with cloud-to-ground lightning flashes overlaid; "+" indicates a positive CG, "-" represents a negative flash. "MAX" ("MIN") indicates the number of positive (negative) CGs over the ten minute period.
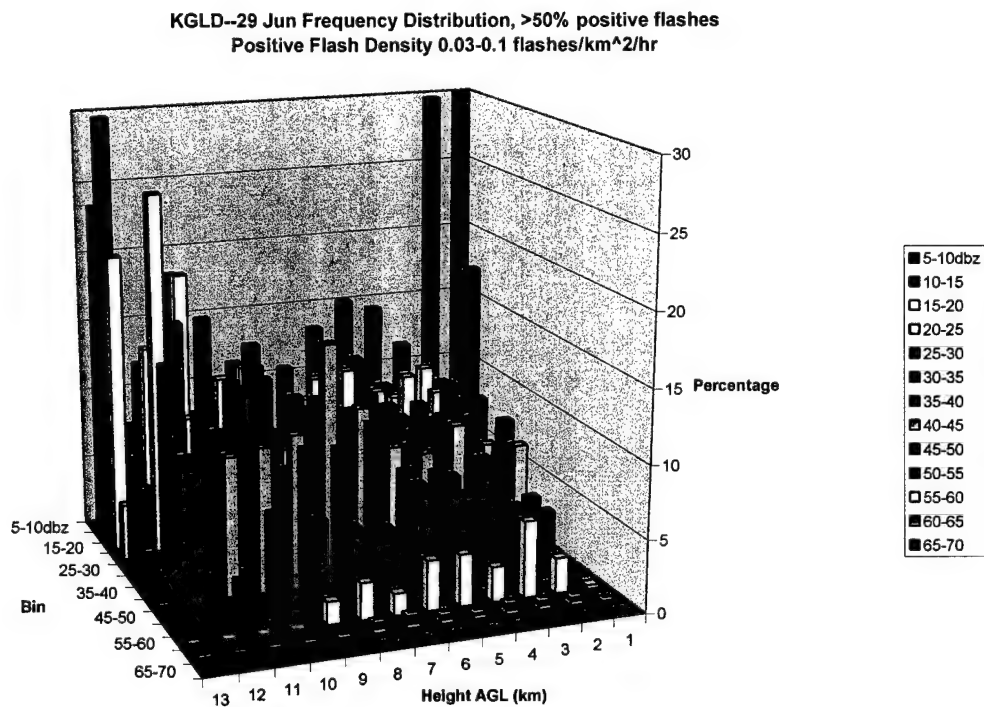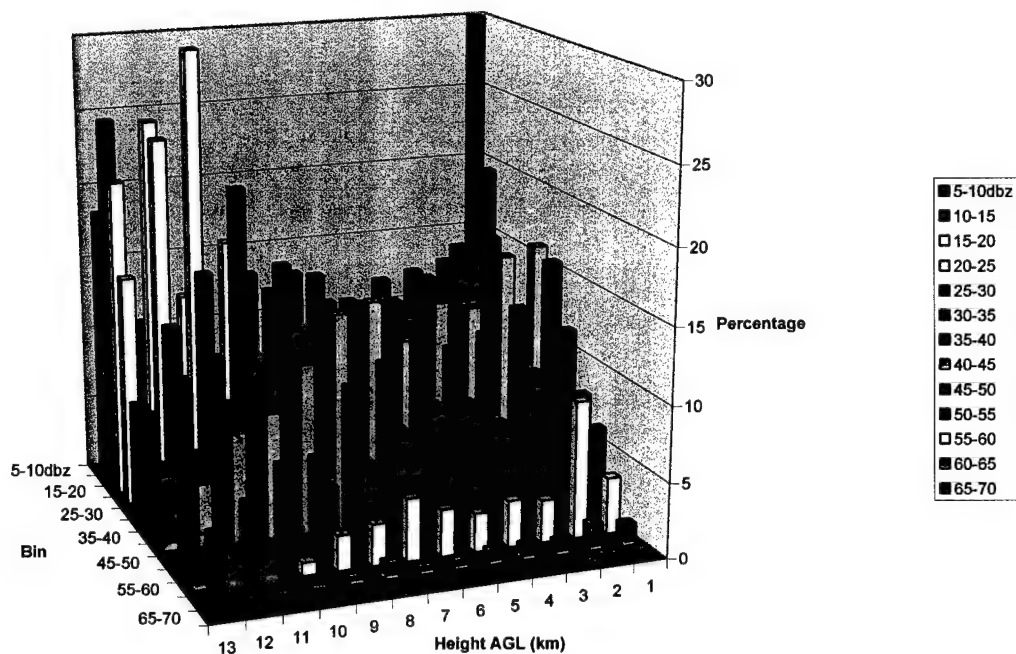
a)

Figure 4.22: 29 Jun supercell frequency distribution for positive flash densities a) > 0.1 flashes km^{-2} hr^{-1} and b) 0.03-0.1 flashes km^{-2} hr^{-1}.

a)

KGLD--29 Jun Frequency Distribution, >50% positive flashes
Positive Flash Density, 0.01-0.03 flashes/km^2/hr

b)

KGLD--29 Jun Frequency Distribution, >50% positive flashes
Positive Flash Density 0.0-0.01 flashes/km^2/hr
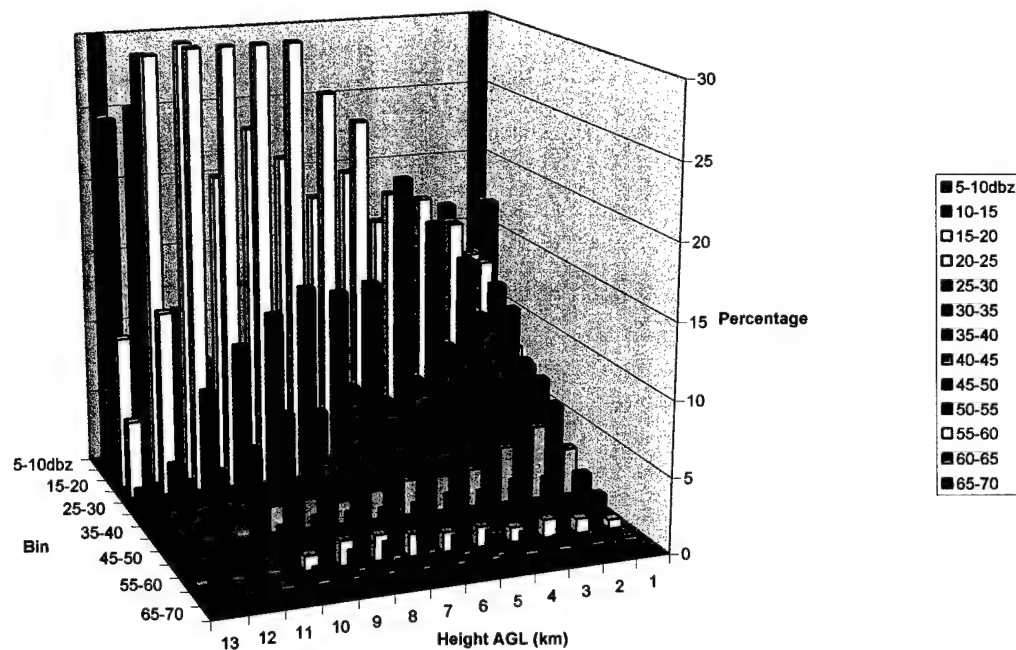
Figure 4.23: 29 Jun supercell frequency distribution for positive flash densities a) 0.01-0.03 flashes km^{-2} hr^{-1} and b) 0.0-0.01 flashes km^{-2} hr^{-1}.

KGLD--29 Jun Frequency Distribution, >50% Negative flashes
Negative Flash Density 0.0-0.01 flashes/km^2/hr
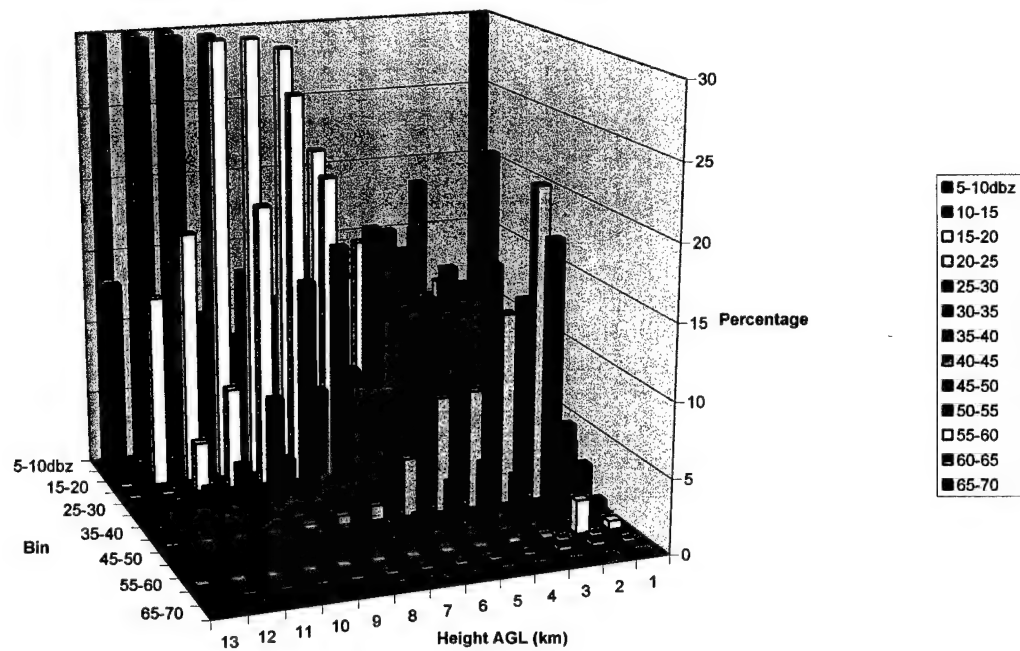
Figure 4.24: 29 Jun supercell frequency distribution for negative flash densities between 0.01-0.03 flashes km^{-2} hr^{-1}.

a)
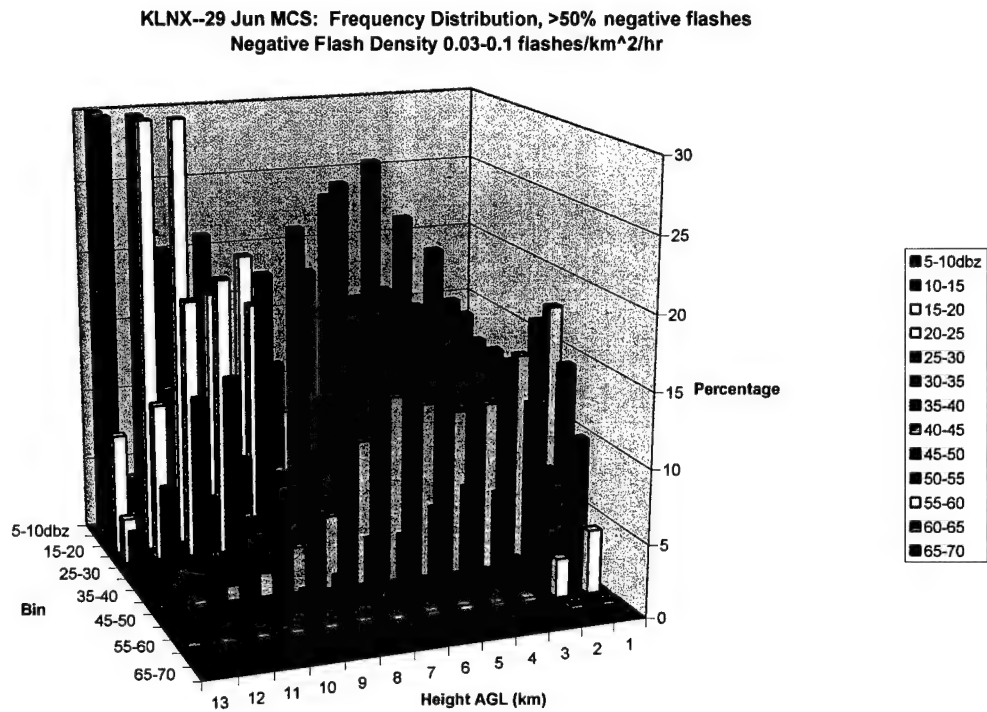
b)

Figure 4.25: 29 Jun MCS frequency distribution for positive flash densities between 0.03-0.1 flashes km^{-2} hr^{-1} for a) positive grids and b) negative grids.

79

a)

KLNX--29 Jun MCS: Frequency Distribution, >50% positive flashes
Positive Flash Density 0.01-0.03 flashes/km^2/hr

b)

KLNX--29 Jun MCS: Frequency Distribution, >50% negative flashes
Negative Flash Density 0.01-0.03 flashes/km^2/hr

Figure 4.26: 29 Jun MCS frequency distribution for positive flash densities between 0.01-0.03 flashes km^{-2} hr^{-1} for a) positive grids and b) negative grids.

80

a)

KLNX--29 Jun MCS: Frequency Distribution, >50% positive flashes
Positive Flash Density 0.0-0.01 flashes/km^2/hr

b)
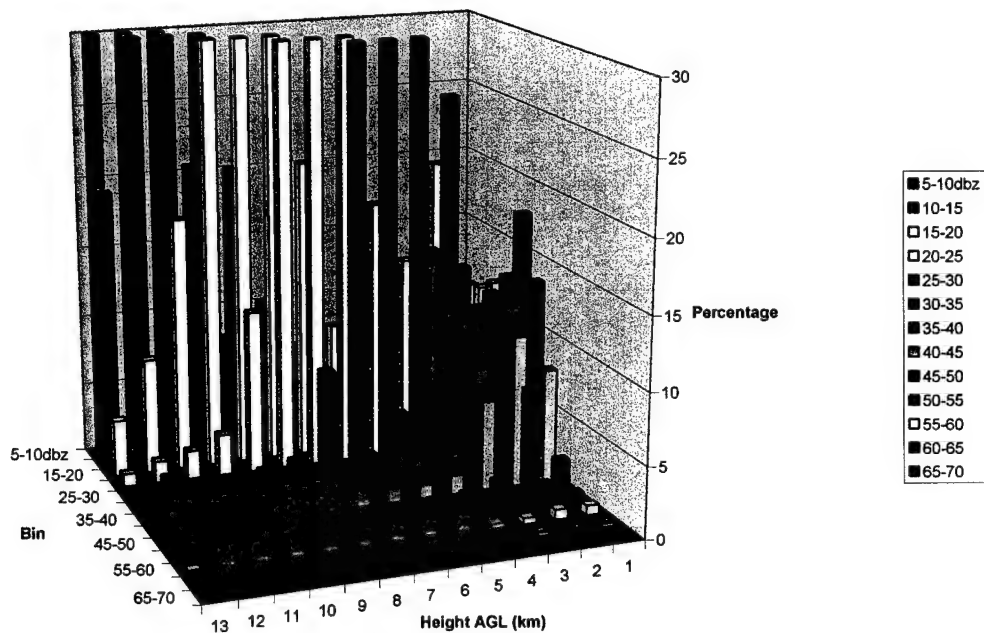
KLNX--29 Jun MCS: Frequency Distribution, >50% negative flashes
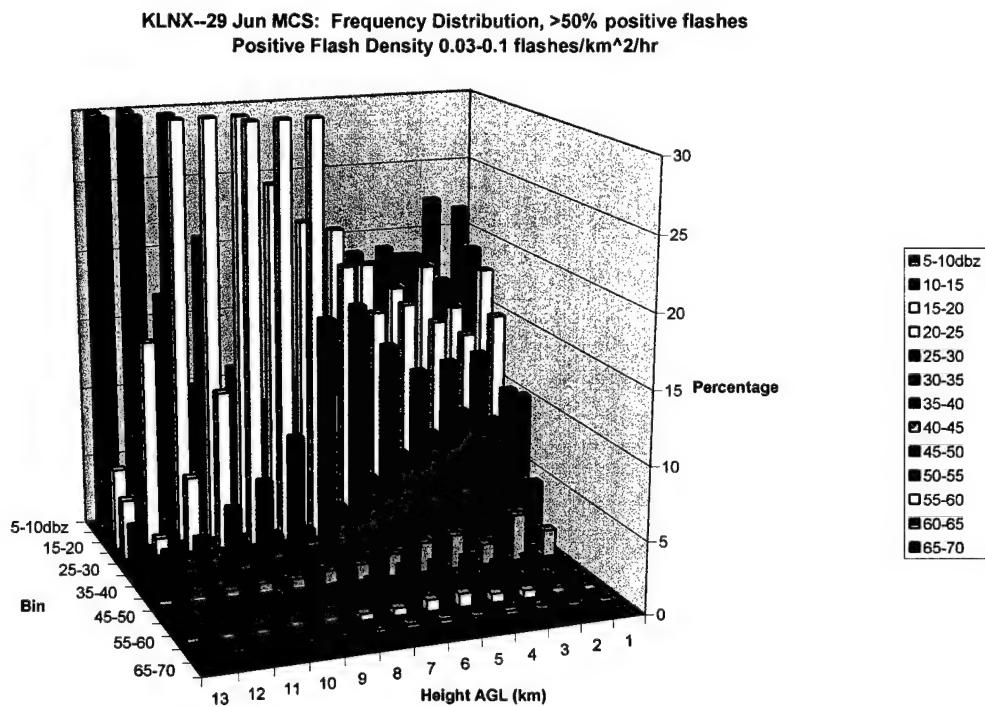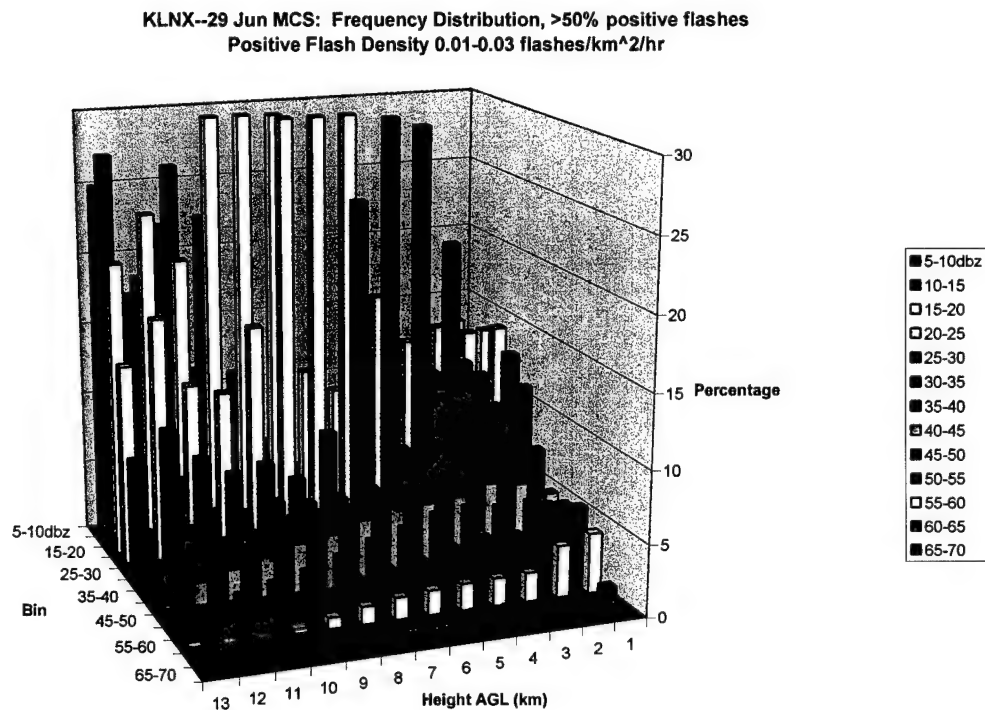**Negative Flash Density 0.0-0.01 flashes/km^2/hr**

Figure 4.27: 29 Jun MCS frequency distribution for positive flash densities between 0.0-0.01 flashes km^{-2} hr^{-1} for a) positive grids and b) negative grids.
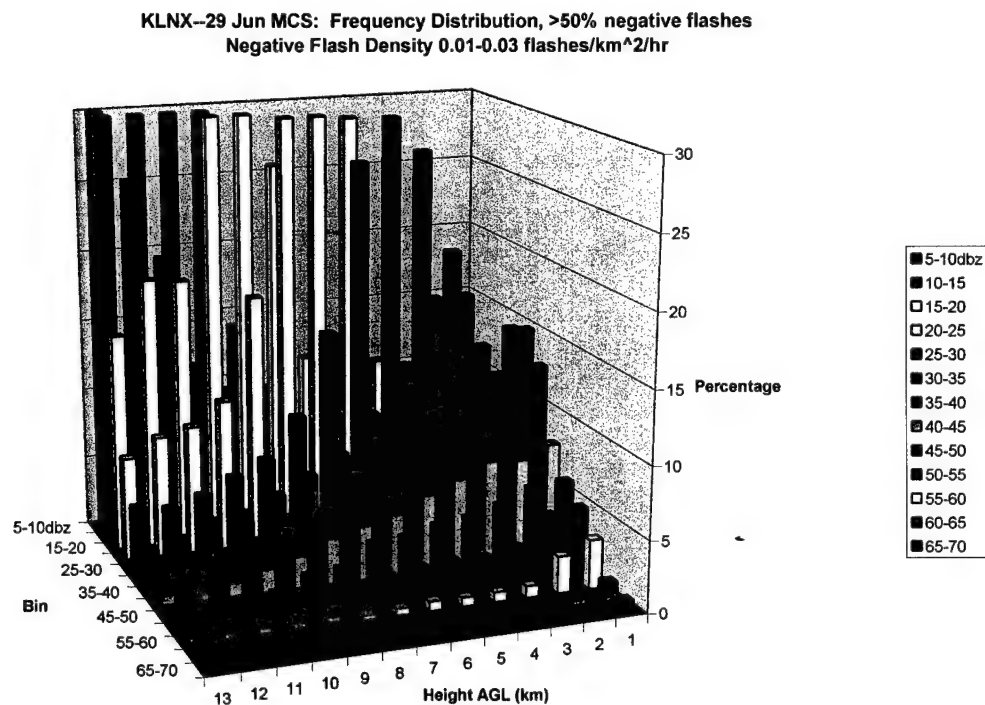
81

a)

KGLD--22 Jun MCS, Frequency Distribution, >50% positive flashes
Positive Flash Density >0.1 flashes/km^2/hr

b)

KGLD--22 Jun Frequency Distribution, >50% positive flashes
Positive Flash Density 0.03-0.1 flashes/km^2/hr
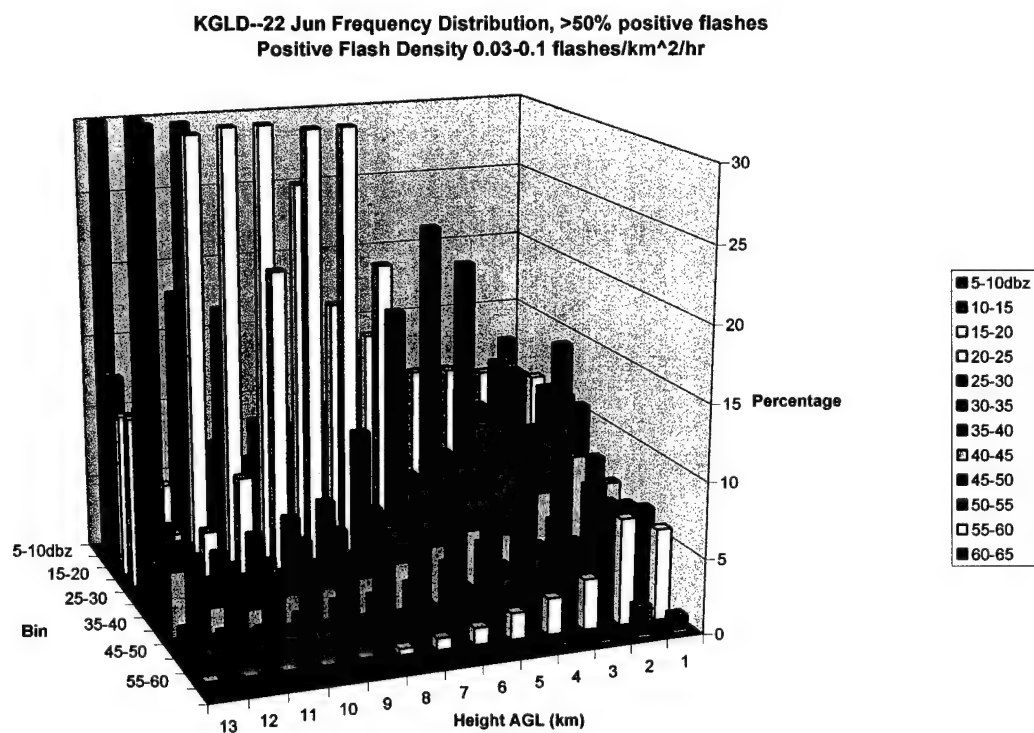
Figure 4.28: 22 Jun MCS frequency distribution for positive flash densities a) > 0.1 flashes km^{-2} hr^{-1} and b) 0.03-0.1 flashes km^{-2} hr^{-1}.

a)

KGLD--22 Jun Frequency Distribution, >50% positive flashes
Positive Flash Density 0.01-0.03 flashes/km^2/hr

b)

KGLD--22 Jun Frequency Distribution, >50% positive flashes
Positive Flash Density 0.0-0.01 flashes/km^2/hr
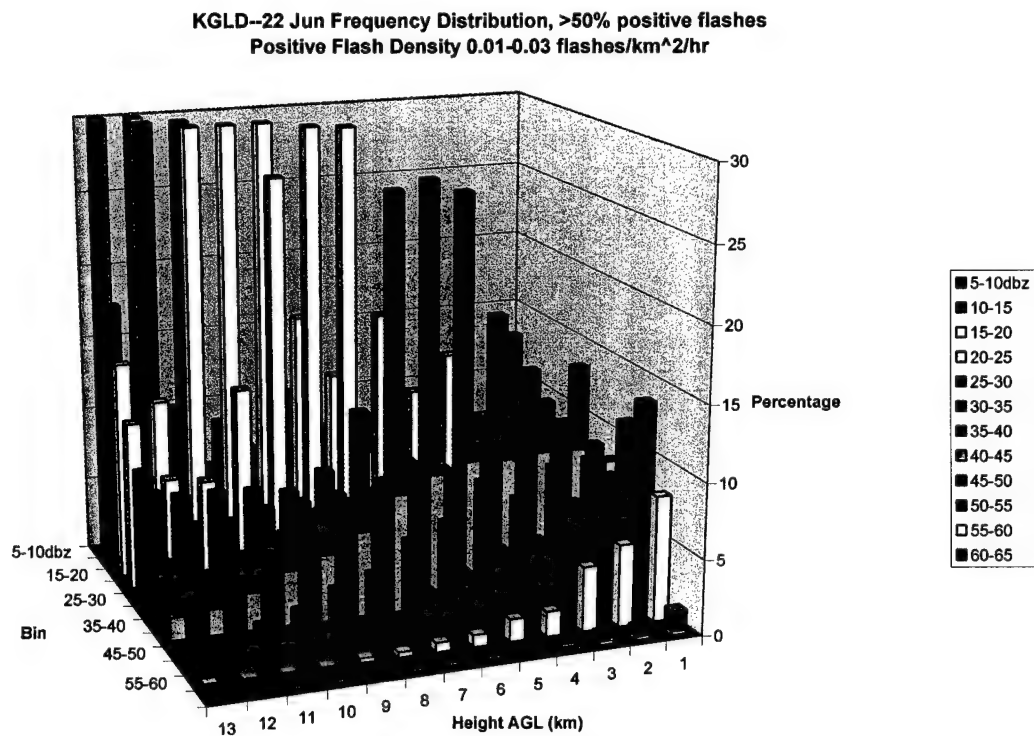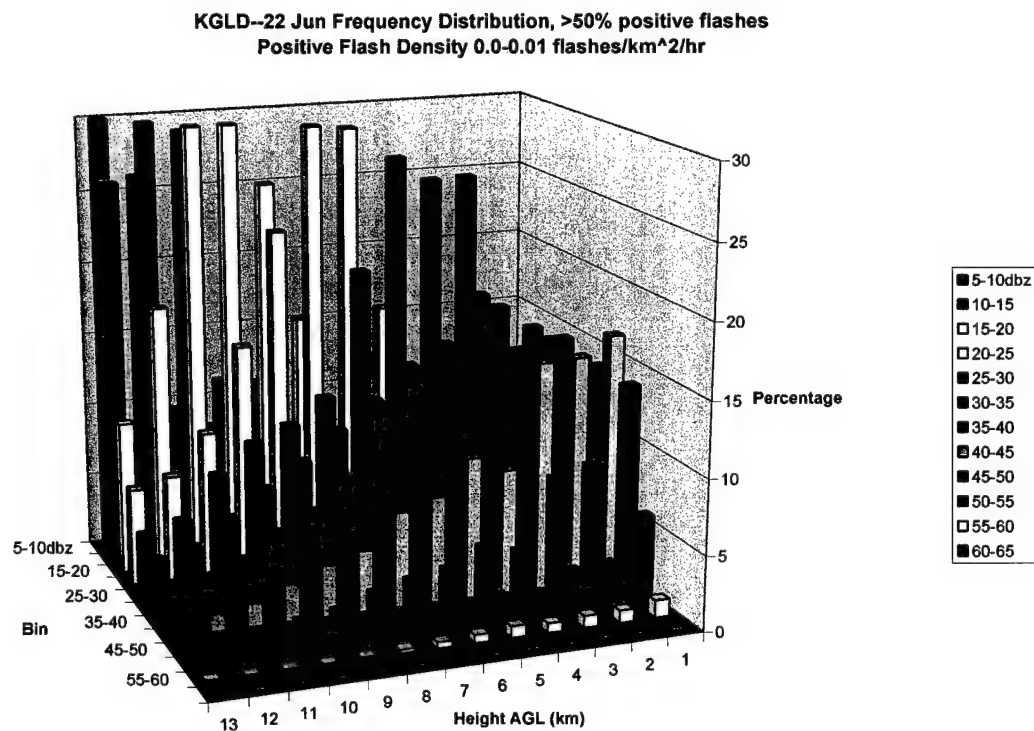
Figure 4.29: 22 Jun MCS frequency distribution for positive flash densities a) 0.01-0.03 flashes km^{-2} hr^{-1} and b) 0.0-0.01 flashes km^{-2} hr^{-1}.

a)

KGLD--22 Jun Frequency Distribution, >50% negative flashes
Negative Flash Density 0.03-0.1 flashes/km^2/hr

b)

KGLD--22 Jun Frequency Distribution, >50% negative flashes
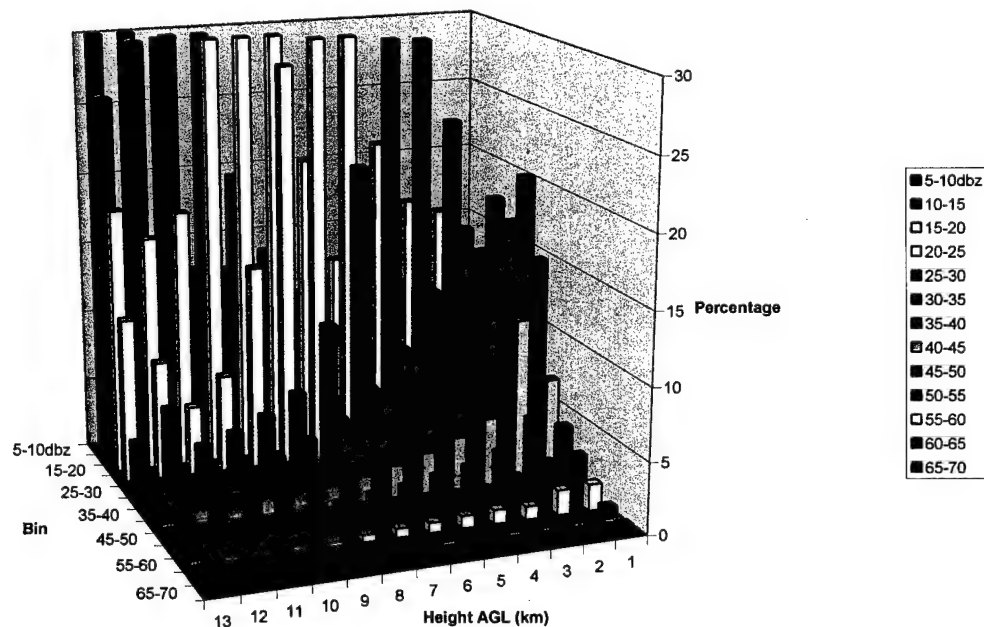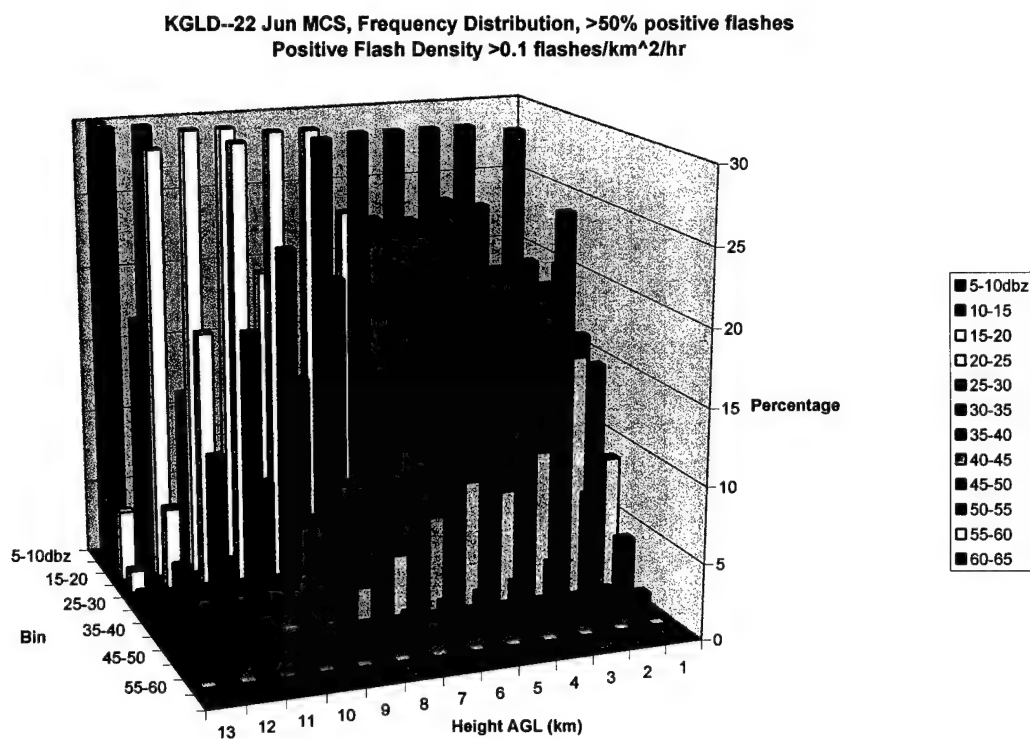**Negative Flash Density 0.01-0.03 flashes/km^2/hr**
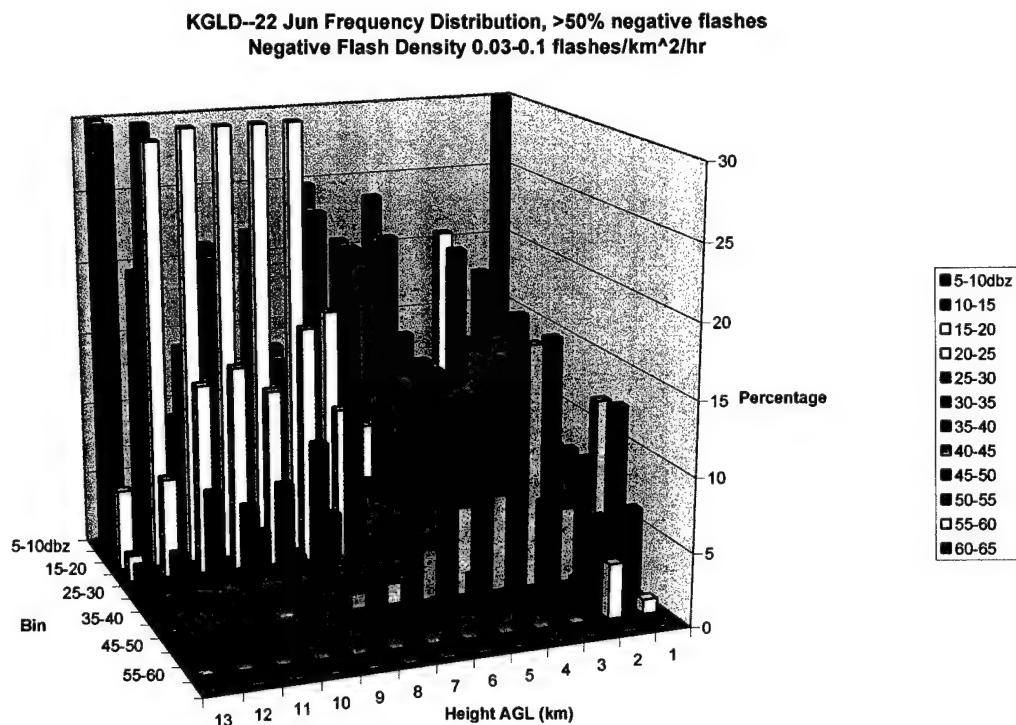
Figure 4.30: 22 Jun MCS frequency distribution for negative flash densities a) 0.03-0.1 flashes km^{-2} hr^{-1} and b) 0.01-0.03 flashes km^{-2} hr^{-1}.
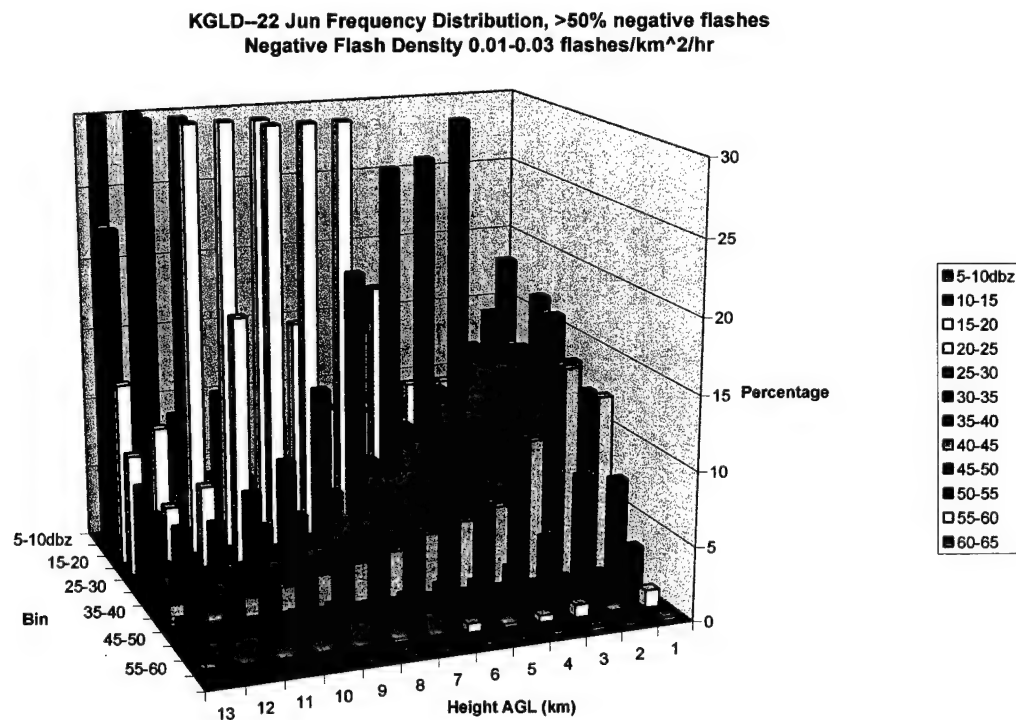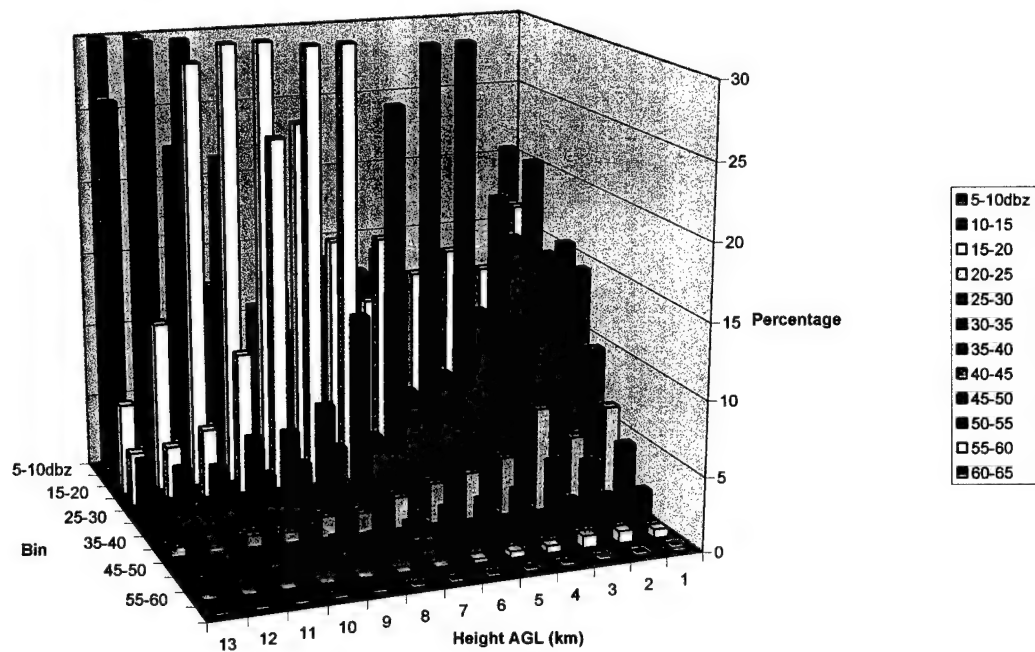
Figure 4.31: 22 Jun MCS frequency distribution for negative flash densities a) 0.0-0.01 flashes km^{-2} hr^{-1} and b) 0.0-0.01 flashes km^{-2} hr^{-1}.

4.5 Low CG Storms

4.5.1 Introduction (Method)

In this section we try to build upon the knowledge that there are a number of robust storms that produce very little CG lightning. Lang (2001) showed some intense storms can produce very little cloud-to-ground lightning. He suggested that low CG storms may be similar to positive CG storms in that they too may forewarn of severe weather. By thresholding our data we isolated vigorous, low CG storms. For consistency we use essentially the same method as we have described in Chapter 3. In this case however, we only considered low CG storms, with flash densities less than 0.03 flashes $km^{-2} hr^{-1}$ (less than 9 CGs in a half hour). First those grids were isolated and then checked for reflectivities above 55 dBZ at 3 km (or higher) in the vertical. An operational rule of thumb for hail relates 55 dBZ reflectivity returns to the presence of hail within the cloud, and we can infer the presence of graupel size or larger particles and at least moderate non-inductive charging within the cloud. With 55 dBZ as a minimum threshold, we can presume vigorous convection and keep the sample population high (and the statistical distribution robust). By doing this we effectively eliminate storms that are simply weak and producing very little total lightning. And we have isolated storms that are fairly energetic--they have fairly strong reflectivities--and yet produce very little cloud-to-ground lightning. The end state is a strongly convective storm, assumed electrically active, that is producing intra-cloud lightning but very little cloud-to-ground lightning.

We would hope to find some clues from the reflectivity profiles into the microphysical workings of these storms. As we found in Section 4.4 there are instances of elevated reflectivity maximums in positive, low flash density storms. In those cases

we can infer large particles suspended aloft with little surface precipitation. We might expect a similar result here, which we now examine.

4.5.2 Discussion

By analyzing all of the low CG storms in our study, we were able to quantify how frequently these storms produce robust reflectivities. There was a marked difference between the Front Range stations and the plains stations. We found that out of all of the Front Range storms that produced less than nine CGs in a half hour, only 5.5% contained reflectivities above 55 dBZ above 2 km. Conversely, from the plains stations, we find that 23% of the low CG storms meet these conditions. These results suggest a difference in storm morphology, life cycle, or both.

Reflectivity distributions were produced for each station. Each profile, regardless of polarity, looks very similar to Figure 4.32. This figure was selected as representative of the group of distributions. There was very little variability among these profiles. The overall structure of Figure 4.32 shows a low level maximum, between 1-2 km, and indicates the largest particles are generally in these levels and suggests precipitating particles. From this figure as well as the comparable profiles (not shown) from the other radar sites, we can infer that *the vast majority of low CG storms (with reflectivities above 55 dBZ) are those that are in their dissipating stage.*

However figure 4.32 does show that there is a maximum at 7 km for reflectivities between 65-70 dBZ. As we have previously suggested, this is an indication of very strong updrafts suspending hail aloft and is typical of developing thunderstorms. This signature though is weakly defined, so we must assume that the vast majority of these

cases occur in the dissipating phase of a storms life cycle and these cases overwhelm the

distribution. Thus, these results are mixed; there are signs that low CG conditions exist

in electrically active storms during the growth phase, but more frequently occur during a

storm's dissipating phase. This might be an interesting topic for future research. If we

could isolate a storm's different phases, we might shed light on these low CG storms.

KLNX: Frequency Distribution, >50% positive flashes
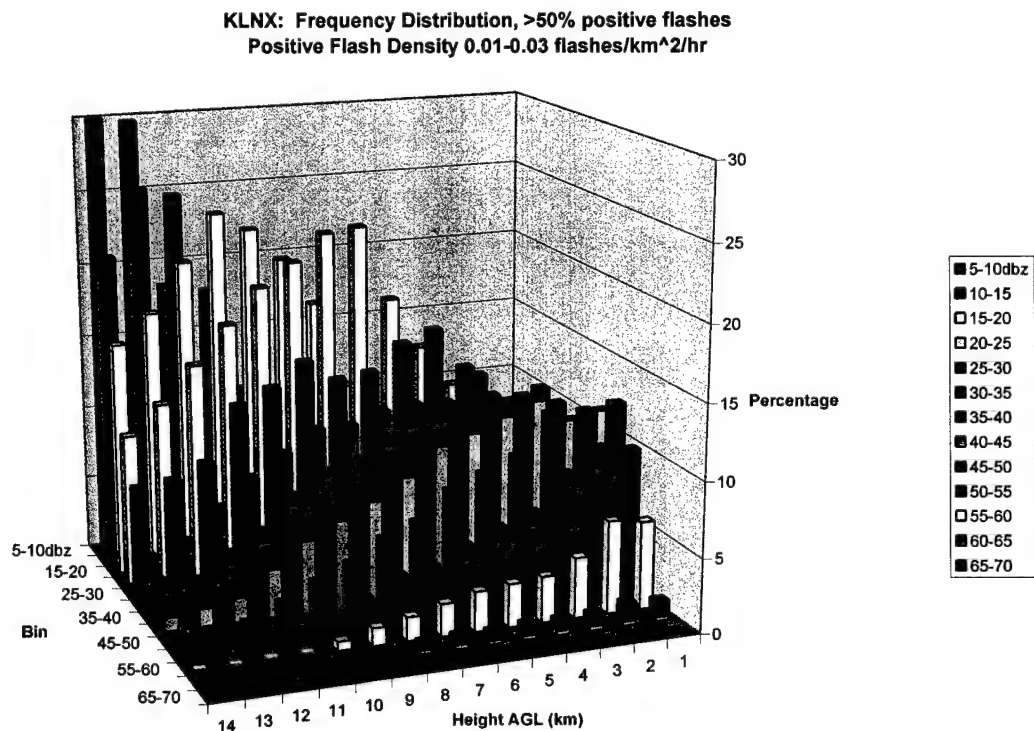**Positive Flash Density 0.01-0.03 flashes/km^2/hr**

Figure 4.32: North Platte frequency distribution for low CG storms. Storms that did not contain reflectivities above 55 dBZ were excluded. This figure is representative of low CG storms from all stations in our study.

CHAPTER FIVE

CONCLUSIONS AND RECOMMENDATIONS FOR FURTHER RESEARCH

5.1 Conclusions

This thesis presents and analysis of lightning producing storms over the High Plains during the summer of 2000 as part of the Severe Thunderstorm Electrification and Precipitation Study (STEPS) field campaign. WSR-88D NEXRAD and National Lightning Detection Network (NLDN) data sets were used to produce statistical radar reflectivity distributions based on cloud-to-ground lightning flash densities. Comparisons were made based on flash polarity, geographical location and storm type. Our goal was to improve our understanding of the relationship between radar reflectivity and cloud-to-ground lightning and to increase the knowledge base as to why some storms produce a high percentage of positive CG lightning. With these goals in mind, we have arrived at the following conclusions:

1. In Section 4.2 we found that there were systematic differences between positive and negative lightning producing storms. *Statistically, for high flash densities, (above 0.1 flashes km^{-2} hr^{-1}) the relative frequency of reflectivities between 55-70 dBZ is five times higher from positive storms than from negative storms.*

2. Also in Section 4.2 we noted evidence that *low flash density storms (less than three CGs in thirty minutes), are more likely to contain upper level reflectivity maximums if the*

CGs are positive. This result suggests that positive CGs are favored when a storm contains strong updrafts and contains large particles suspended aloft. These conditions are generally associated with developing convection, prior to the onset of heavy precipitation.

3. We made regional comparisons in Section 4.3 and found that *over the plains (between 36.8°-43.0° N and 99.6°-106.1° W), strong positive storms were favored to the south and decreased with increasing latitude.* We concluded that Mesoscale Convective Systems (MCS) were favored to the north and hypothesized that *MCS-type systems produce cloud-to-ground lightning that statistically tends to reach ground away from the storms' convective cores.* This had the effect of distributing the number of CG flashes over a large area and reduced the apparent number of high flash density storms.

4. By analyzing individual storms in Section 4.4, we provided further evidence that MCS tend to distribute cloud-to-ground lightning over a larger area, whereas convective storms without extensive stratiform regions (supercells) tend to concentrate their CGs over a smaller area. We found that in the supercell we analyzed, *the highest flash densities were located in and around the storm core.*

5. Also in Section 4.4 we found further evidence to support conclusion #2, above—*when the supercell was producing very low positive CG rates, large particles, likely hail, were suspended aloft, indicating the storm was in its development stage.*

6. In Section 4.5 we calculated the frequency of occurrence of "strong" storms—those with greater than 55 dBZ radar reflectivities—that produce low flash densities and found that only 5.5 % of low flash density storms over the Front Range meet these conditions whereas 23 % of storms over the plains stations met the criteria. Based on the reflectivity

profiles, we concluded *the vast majority of low CG storms (with reflectivities above 55 dBZ) are storms in their dissipating stages.*

5.2 Recommendations for Further Research

Since the installation of the NLDN, we have been able to study when and where lightning occurs in a climatological sense. This research represents one of the first attempts to take the next step and statistically relate lightning information to the physics of storms. Certainly more research is need in this area, and specific recommendations are listed below. The next phase of research envisioned for the next decade might be to conduct a similar analysis with polarimetric radar information, possibly combined with three-dimensional interferometric lightning data. Doing so would allow us to examine microphysical parameters within thunderstorms and relate them to the sources of lightning discharges. However, these data are not produced on a large scale, and statistical distributions such as those produced in this research will not be possible until the use of these instruments becomes more widespread.

Based on our results and lessons learned we recommend the following areas for further research:

1. Though we analyzed over 1 terabyte of data, we suggest that a larger data set would provide greater statistical reliability. As our data set was divided into smaller subsets, some frequency distributions became unreliable and had to be eliminated from our analysis. Additional years of warm season data would improve the statistical accuracy of the distribution and would eliminate any annual variation.

2. Separating convective and stratiform regions and repeating this analysis might provide greater insight into the apparent differences in reflectivity profiles and suggest

91

mechanisms which produce cloud-to-ground lightning strikes between these two storm types. Automation of this process however, poses problems. The coarseness of the radar data limits our ability to distinguish storm types with current algorithms.

3. Likewise, isolating different storm life cycle phases and then analyzing the statistical distribution would increase our understanding of lightning production.

4. This analysis could be repeated with polarimetric radar variables, which might provide great insight into storm microphysics in a statistical sense.

5. Including total storm lightning, not just cloud-to-ground lightning, would provide a mechanism to further test the elevated dipole hypothesis.

6. This analysis could be repeated for different geographical locations in order to better determine regional differences in lightning production.

References

Baker, M. B., and J.G. Dash, 1994: Mechanism of charge transfer between colliding ice particles in thunderstorms. *J. Geophys. Res.*, **99**, 10,621-26.

Branick, M. L., and C. A. Doswell III, 1992: An observation of the relationship between supercell structure and lightning ground strike polarity. *Wea and Forecasting*, **7**, 143-149.

Buechler, D. S., S. J. Goodman, and M. E. Weber, 1988: Cloud-to-ground lightning activity in microburst producing storms. Preprints, 15th Conf. on Severe Local Storms, Amer. Meteor. Soc., Baltimore, MD, 496-500.

Carey, L. D., S. A. Rutledge, and B. A. Zajac, 1997: An investigation of the relationship between severe storm reports and positive cloud-to-ground lightning. Eos, Trans., AGU, **78**, Fall Meeting Suppl., No. 46.

Carey, L. D. and S. A. Rutledge, 1998: Electrical and multiparameter radar observations of a severe hailstorm. *J. Geophys. Res.*, **103**, 13979-14000.

Carey, L. D., S. A. Rutledge, and W. A. Petersen, 2001: The relationship between severe storm reports and cloud-to-ground lightning polarity in the contiguous United States from 1989-1998. Submitted to *Mon. Wea. Rev.* July 2001.

Changnon, S. A., 1977: The climatology of hail in North America. In *Hail: A Review of Hail Science and Hail Suppression. Meteor. Monogr.*, **38**, G.B. Foote and C.A. Knight, Eds., Amer. Meteor. Soc., Boston, Mass., 107-128.

Changnon, S. A., 1992: Temporal and spatial relations between hail and lightning. *J. Appl Meteor.*, **31**, 587-604.

Cressman, G. P., 1959: An operational objective analysis system. *Mon. Wea. Rev.*, **87**, 367-374.

Cummins, K. L., M. J. Murphy, E. A. Bardo, W. L. Hiscox, R. B. Pyle, and A. E. Pier, 1998: A combined TOA/MDF technology upgrade of the U. S. National Lightning Detection Network. *J. Geophys. Res.*, **103**, 9035-9044.

Curran, E. B., and W. D. Rust, 1992: Positive ground flashes produced by low-precipitation thunderstorms in Oklahoma on 26 April 1984. *Mon. Wea. Rev.*, **120**, 544-553.

Doviak, R. J. and D. S. Zrnic, 1993: *Doppler Radar and Weather Observations*, 2nd Ed., Academic Press, San Diego, California, 562 pp.

Elster, J., and H. Geitel, 1913: Zur influenzheorie der Niederschlangselek-trizitat. *Phys. Z.*, **14**, 1287.

Gauthier, M. L., and S. A. Rutledge, 1999: Multiparameter investigation of significant lightning producing storms in Northeastern Colorado. Master's Thesis, Colorado State University, 164 pp.

Global Atmospherics Inc., 2000: http:// www.glatmos.com/nldn/nldn.html

Illingworth, A. J., and J. Latham, 1977: Calculations of electric field structure and charge distributions in thunderstorms. *Q. J. R. Meteorol. Soc.*, **103**, 281-295.

Jayaratne, E. R., C. P. R. Saunders, and J. Hallet, 1983: Laboratory studies of the charging of soft hail during ice crystal interactions. *Q. J. R. Meteorol. Soc.*, **109**, 609-630.

Keith, W. D., and C. P. R. Saunders, 1989: Charge transfer during multiple large ice crystal interactions with a riming target. *J. Geophys. Res.*, **94**, 13,103-13,106.

Krehbiel, P. R., 1986: The electrical structure of thunderstorms, in *The Earth's Electrical Environment*, Washington D. C., National Academy Press, 90-113.

Lang, T. J. 1997: Relationship between storm structure and lightning activity in Colorado convection observed during STERAO-A. Master's Thesis, Colorado State University, 167 pp.

Lang, T. J., S. A. Rutledge, J. E. Dye, M. Venticinque, P. Laroche, and E. Defer, 2000: Anomalously low negative cloud-to-ground lightning flash rates in intense convective storms observed during STERAO-A. *Mon. Wea. Rev.*, **128**, 160-173.

Lang, T. J., 2000: Dissertation on the relationships between convective storm kinematics, microphysics, and lightning. Doctoral Dissertation, Colorado State University, 238 pp.

MacGorman, D. R., and W. L. Taylor, 1989a: Positive cloud-to-ground lightning detection by direction-finder network. *J. Geophys. Res.*, **94**, 13,313-13,318.

MacGorman, D. R., D. W. Burgess, V. Mazur, W. D. Rust, W. L. Taylor, and B. C. Johnson, 1989b: Lightning rates relative to tornadic storm evolution on 22 May 1981. *J. Atoms. Sci.*, **46**, 221-250.

MacGorman, D. R., and K. E. Nielsen, 1991: Cloud-to-ground lightning in a tornadic storm in 8 May 1996. *Mon. Wea. Rev.*, **119**, 1557-1574.

MacGorman, D. R. and D. W. Burgess, 1994: Positive cloud-to-ground lightning in tornadic storms and hailstorms. *Mon. Wea. Rev.*, **122**, 1671-1697.

MacGorman, D. R., and W. D. Rust, 1998: *The Electrical Nature of Storms.* Oxford University Press, 422 pp.

Mohr, C. G., L. J. Miller, R. L. Vaughn, and H. W. Frank, 1986: The merger of mesoscale datasets into a common Cartesian format for efficient and systematic analysis. *J. Atoms. Oceanic Technol.*, **3**, 143-161.

Orville, R. E., 1991: Lightning ground flash density in the contiguous United States— 1989. *Mon. Wea. Rev.*, **119**, 573-577.

Orville, R. E., 1994: Cloud-to-ground lightning flash characteristics in the contiguous United States: 1989-1991. *J. Geophys. Res.*, **99**, 10833-10841.

Orville, R. E., and A. C. Silver, 1997: Lightning ground flash density in the contiguous United States: 1992-1995. *Mon. Wea. Rev.*, **125**, 631-638.

Orville, R. E. and G. R. Huffines, 2001: Cloud-to-ground lightning in the United States: NLDN Results in the first decade, 1989-1998. *Mon. Wea. Rev.*, **129**, 1179-1193.

Perez, A. H., R. E. Orville, and L. J. Wicker, 1995: Characteristics of cloud-to-ground lightning associated with violent tornado producing supercells. Preprints, 9th Conf on Applied Climatology, Amer. Meteor. Soc., Dallas, TX, 409-413.

Petersen, W. A., 1992: Cloud-to-ground lightning in tropical mesoscale convective systems. M. S. thesis, Colorado State University, Fort Collins, 225 pp.

Petersen, W. A., and S. A. Rutledge, 2001: Regional variability in tropical convection: observations from TRMM. *J. Climate*, in press.

Prentice, S. A., and D. Mackerras, 1977: Ratio of cloud-to-ground lightning flashes in thunderstorms. *J. Appl Met.*, **16**, 545-550.

Price, C., and D. Rind, 1993: What determines the cloud-to-ground lightning fraction in thunderstorms? *Geophys. Res. Lett*, **20**, 463-466.

Reap, R. M., 1986: Evaluation of cloud-to-ground lightning data from the Western United States for the 1983-84 summer seasons. *J. Climate Appl. Meteor.*, **25**, 785-799.

Reap, R. M., and D. R. MacGorman, 1989: cloud-to-ground lightning: Climatological characteristics and relationships to model fields, radar observations, and severe local storms. *Mon. Wea. Rev.*, **117**, 518-535.

Rutledge, S. A., and D. R. MacGorman, 1988: Cloud-to-ground lightning activity in the 10-11 Jun 1985 mesoscale convective system observed during the Oklahoma-Kansas PRE_STORM project. *Mon. Wea. Rev.*, **116**, 1393-1408.

Rutledge, S. A., C. Lu, and D. R. MacGorman, 1990: Positive cloud-to-ground lightning in mesoscale convective systems. *J. Atoms. Sci.*, **47**, 2085-2100.

Ryan, J. J. 1999: Relationship between lightning flash rates and radar observations from Colorado and Australia. Master's Thesis, Colorado State University, 134pp.

Saunders, C. P. R., W. D. Keith, and R. P. Mitzeva, 1991: The effect of liquid water on thunderstorm charging. *J. Geophys. Res.*, **96**, 11,007-11017.

Schuur, T. J., and S. A. Rutledge, 2000: Electrification of stratification regions in mesoscale convective systems. Part I: An observational comparison of symmetric and asymmetric MCSs. *J. Atoms. Sci.*, **57**, 1961-1982.

STEPS science proposal, 2000:
http://www.mmm.ucar.edu/pdas/stepsscience.html#Program

Stolzenburg, M., W. D. Rust, and T. C. Marshall, 1998a: Electrical structure in thunderstorm convective regions. Part I: Mesoscale convective systems. *J. Geophys. Res.*, **103**, 14059-14078.

Stolzenburg, M., W. D. Rust, and T. C. Marshall, 1998b: Electrical structure in thunderstorm convective regions. Part III: Synthesis. *J. Geophys. Res.*, **103**, 14097-14108.

Stolzenburg, M., 1994: Observations of high ground flash densities of positive lightning in summertime thunderstorms. *Mon. Wea. Rev.*, **122**, 1740-1750.

Takahashi, T., 1978: Riming electrification as a charge generation mechanism in thunderstorms. *J. Atoms. Sci.*, **35**, 1536-1548.

Vonnegut, B., 1963: Some facts and speculations concerning the origin and role of thunderstorm electricity. *Meteor. Monogr.*, **5**, 224-241.

Williams, E. R., 1989: The tripole structure of thunderstorms. *J. Geophys. Res.*, **94**, 13,151-13,167.

Workman, E. J., and S. E. Reynolds, 1949: Electrical activity as related to thunderstorm cell growth, *Bull. Amer. Meteor. Soc.*, **30**, No. 4, 142-144.

Yuter, S. E., and R. A. Houze Jr., 1995: Three-dimensional kinematic and microphysical evolution of Florida cumulonimbus. Part II: Frequency distributions of vertical velocity, reflectivity, and differential reflectivity. *Mon. Wea. Rev.*, **123**, 1941-1963.

Zajac, B. A., 1998: Climatological characteristics of cloud-to-ground lightning activity in the contiguous United States, M. S. Thesis, Colorado State University, 119 pp.

Zajac, B. A., and S. A. Rutledge, 2001: Cloud-to-ground lightning activity in the contiguous United States from 1995-1999. *Mon. Wea. Rev.*, **129**, 999-1019.